Johann Heinrich von Thünen-Institut

Landbauforschung
vTI Agriculture and Forestry Research

Sonderheft 319
Special Issue

Detailed documentation of the PLATIN (PLant-ATmosphere INteraction) model

Ludger Grünhage and Hans-Dieter Haenel

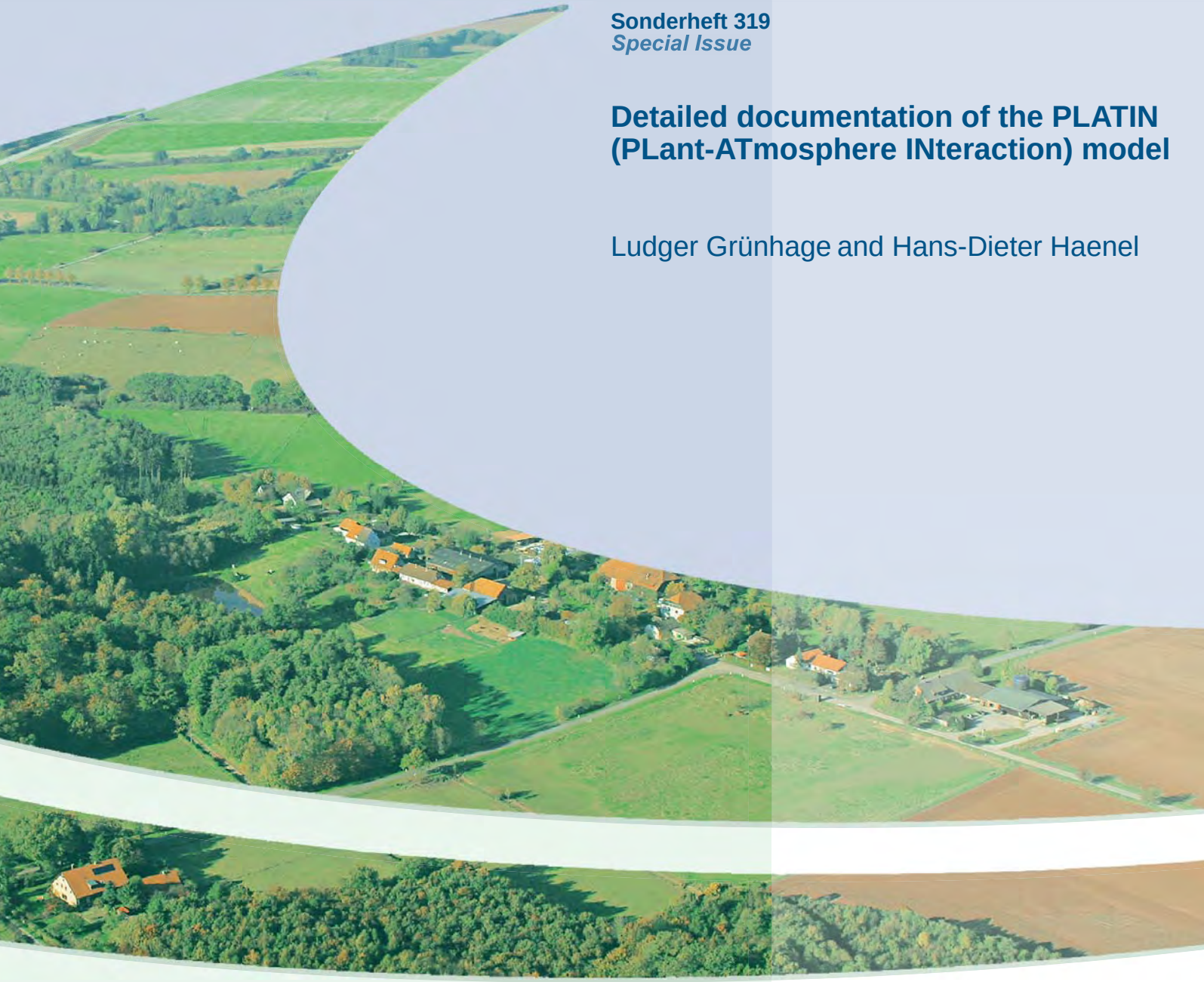

Bundesministerium für Ernährung, Landwirtschaft und Verbraucherschutz

Bibliografische Information der Deutschen Bibliothek

Die Deutsche Bibliothek verzeichnet diese Publikation in der Deutschen Nationalbibliografie; detaillierte bibliografische Daten sind im Internet über http://www.dnb.ddb.de abrufbar.

2008

Landbauforschung
vTI Agriculture and Forestry Research

Johann Heinrich von Thünen-Institut

Bundesforschungsinstitut für
Ländliche Räume, Wald und Fischerei (vTI)

Bundesallee 50, 38116 Braunschweig,
Germany

Die Verantwortung für die Inhalte liegt bei den Verfassern.

landbauforschung@vti.bund.de
www.vti.bund.de

Preis / Price 10 €

ISSN 0376-0723
ISBN 978-3-86576-044-9

Johann Heinrich
von Thünen-Institut

Landbauforschung
vTI Agriculture and Forestry Research

Sonderheft 319
Special Issue

Detailed documentation of the PLATIN (PLant-ATmosphere INteraction) model

Ludger Grünhage[1] and Hans-Dieter Haenel[2]

[1]Institute for Plant Ecology, Justus-Liebig-University, Heinrich-Buff-Ring 26-32, D-35392 Gießen, Germany

[2] Institute of Agricultural Climate Research, Johann Heinrich von Thünen-Institut, Federal Research Institute for Rural Arear, Forestry and Fisheries, Bundesallee 50, D-38116 Braunschweig, Germany

Index of contents

Detailed documentation of the PLATIN (PLant-ATmosphere INteraction) model

Ludger Grünhage [1] *and Hans-Dieter Haenel* [2]

Abstract

The exchange of energy and matter between phytosphere and near-surface atmosphere is a complex process controlled by a number of influence factors. These not only comprise the state of the air above and within the plant canopy (temperature, humidity, flow velocity, gas or particle concentration in the air) and the air's transport capability, but also several physical, physiological, and chemical properties of the vegetation (plant architecture, vertically varying capability to receive or emit energy and gases, water budget, chemical reactions).

Modelling the underlying processes requires a more or less extensive reduction of their complexity. The degree of simplification depends on what is to be modelled and on the availability of data to operate the model. The SVAT model PLATIN (PLant-ATmosphere-INteraction) presented here belongs to the category of models to be used for practical purposes e.g. in agriculture (the need for irrigation, among other things) or to establish dose-response functions in ecotoxicology. Like numerous other SVAT models PLATIN is based on the *big-leaf* concept which replaces the vertical resolution of sources and sinks within the plant stand (including the soil surface beneath) by the idea of a single *big leaf* with overall properties equivalent to those of the complete plant/soil-surface system.

The core module of PLATIN is based on the canopy energy budget and calculates the exchange of sensible and latent heat between phytosphere and near-surface atmosphere. Coupled to this the exchange of trace gases and fine-particle constituents is quantified. The vertical transport between an above-canopy reference height, for which air properties and concentrations of matter must be known, and the sinks and/or sources of the plant/soil-surface system is modelled using three resistances: the turbulent atmospheric transport resistance between reference height and the level of momentum sink; the quasi-laminar resistance between momentum-sink level and the surface of the *big leaf* to account for the differences between momentum transfer and transport of energy and matter; canopy resistance which in turn is modelled using a number of further resistances arranged in series and in parallel. In general, the resistance values depend on the type of entity transported (momentum, heat, gaseous species, particles).

PLATIN calculates numerous detailed results which agree quite well with measurements, demonstrating good model performance. In order to improve the treatment of the influence of the vertical light distribution within the canopy as well as to provide an additional way to validate the model, PLATIN was extended by a submodule to estimate the stomatal uptake of trace gases (e.g. ozone) by the two different categories of sunlit and shaded leaves. This is achieved by extending the *big-leaf* concept by subdividing the *big-leaf* into a sunlit and a shaded fraction. One of the results obtained by this submodule is the stomatal conductance for sunlit leaves normalized by the leaf area index. This stomatal conductance represents an interface to measurements of trace gas exchange on leaf level.

[1] Institute for Plant Ecology, Justus-Liebig-University, Heinrich-Buff-Ring 26-32, D-35392 Gießen, Germany

[2] Institute of Agricultural Climate Research, Johann Heinrich von Thunen Institute, Federal Research Institute for Rural Areas, Forestry and Fisheries, Bundesallee 50, D-38116 Braunschweig, Germany

Detaillierte Dokumentation des SVAT-Modells PLATIN (PLant-ATmosphere INteraction)

Zusammenfassung

Der Austausch von Energie und gasförmigen Luftbeimengungen zwischen Phytosphäre und bodennaher Atmosphäre ist ein komplexer Prozess, der durch eine Vielzahl von Faktoren bestimmt wird. Diese umfassen nicht nur den Zustand der Luft oberhalb und innerhalb des Pflanzenbestandes (Temperatur, Feuchte, Gaskonzentration, Strömungsgeschwindigkeit) und ihr Transportvermögen, sondern auch eine Reihe von physikalischen, physiologischen und chemischen Eigenschaften der Vegetation (Bestandesarchitektur, vertikal differenzierte Fähigkeit zur Aufnahme und Abgabe von Energie und Gasen, Wasserversorgung, chemische Reaktionen).

Die Modellierung dieser Zusammenhänge erfordert eine mehr oder minder weit reichende Reduktion der Komplexität. Der Grad der Vereinfachung richtet sich nach der Zielsetzung und der Verfügbarkeit von Daten zum Betrieb des Modells. Praxisorientierte SVAT-Modelle, wie das hier vorgestellte PLATIN (PLant-ATmosphere-INteraction), werden zur Beantwortung z. B. von Fragen aus dem landwirtschaftlichen Bereich (u. A. Bewässerungsbedarf) oder der Erstellung von Dosis-Wirkung-Beziehungen in der Ökotoxikologie benötigt. Wie zahlreiche andere SVAT-Modelle beruht auch PLATIN auf dem *big-leaf*-Konzept. Dieses ersetzt die vertikale Differenzierung des Bestandes bezüglich der Quellen- und Senkenverteilung sowie der Transportmechanismen durch die Modellvorstellung eines einzigen "großen Blattes", dessen Eigenschaften effektiv denjenigen des gesamten Bestandes und des darunter liegenden Bodens entsprechen.

Das Kernmodul von PLATIN berechnet den Austausch von fühlbarer und latenter Wärme zwischen Phytosphäre und bodennaher Atmosphäre unter Berücksichtigung des Energiehaushaltes des Pflanzenbestandes. In Wechselwirkung damit wird der Austausch von Spurengasen und Schwebstaubinhaltsstoffen quantifiziert. Der Transport zwischen einer Referenzhöhe oberhalb des Bestandes, für die alle relevanten Atmosphäreneigenschaften und Stoffkonzentrationen bekannt sein müssen, und den Senken bzw. Quellen des Systems Pflanze/Boden wird im Wesentlichen mit Hilfe dreier Widerstände modelliert: atmosphärischer Transportwiderstand zwischen Referenzhöhe und Senkeniveau für Impuls; quasi-laminarer Widerstand zwischen Impulssenkenniveau und *big-leaf*-Oberfläche zur Berücksichtigung der Unterschiede zwischen Impulstransport einerseits und Energie- und Stofftransporten andererseits; Bestandeswiderstand, der wiederum mit Hilfe verschiedener in Serie und parallel angeordneter Einzelwiderstände modelliert wird. Die Werte der Widerstände sind i. d. R. abhängig von der Art der transportierten Größe (Impuls, Wärme, Gas-Spezies, Partikel) und stehen zum Teil in Rückkoppelung mit den sich ergebenden Transportdichten.

PLATIN berechnet eine Vielzahl von Detailergebnissen, deren weitgehende Übereinstimmung mit Messungen für die Güte des Modells spricht. Zur Verbesserung der Beschreibung des Einflusses der Lichtverteilung im Pflanzenbestand auf den Energie- und Stoffaustausch sowie zur Erweiterung der Möglichkeit zur Validierung wurde PLATIN um ein Sub-Modul ergänzt, das die Abschätzung der für sonnenbeschienene und abgeschattete Blätter unterschiedlichen stomatären Aufnahme von Spurengasen (z.B. Ozon) erlaubt. Für diesen speziellen Zweck wird das *big-leaf*-Konzept mit einer Aufteilung des Pflanzenbestandes in besonnte und abgeschattete Anteile unterlegt. Das Sub-Modul liefert als Ergebnis u. A. den auf eine Blattflächeneinheit normierten stomatären Leitwert für besonnte Bestandespartien, eine Größe, die als direkte Schnittstelle zu Messungen des Spurengasaustausches auf Blattebene dienen kann.

1 Introduction

Classical air pollution problems caused by very high concentrations of sulphur dioxide (SO_2) and London-type smog have decreased to acceptable levels in most parts of Europe. Nevertheless, there are still a number of potential ecological threats such as acidification and eutrophication of terrestrial and aquatic ecosystems, increased tropospheric ozone (O_3) concentrations and stratospheric ozone depletion, as well as greenhouse effects and human health problems caused by suspended particulate matter. Reactive atmospheric nitrogen species contribute to all these phenomena (cf. Dämmgen and Sutton, 2001; Erisman et al., 1998; Graedel and Crutzen, 1995).

During the 1970s it was recognised that transboundary air pollution has ecological as well as economic consequences e.g. for the forest and fish industries (UNECE, 2004). As a consequence, the countries of the UNECE (UN Economic Commission for Europe) developed a legal, organisational and scientific framework to deal with these problems. In 1979 the UNECE Convention on Long-Range Transboundary Air Pollution (LRTAP) was signed; it entered into force in 1983 (UNECE, 1979). In this context, the so called multi-pollutant multi-effect or Gothenburg protocol (UNECE, 1999) requires the quantification - or at least estimation - of fluxes of atmospheric reactive nitrogen and sulphur species as well as of ozone and particulate matter between the ecosystems under consideration and the atmosphere near the ground.

Ideally, fluxes should be measured continuously and in an area-covering manner. Of course, this is not feasible. Another problem is that for some air constituents the toxicologically relevant flux is only a part of the total flux. Therefore modelling of fluxes has become a useful tool. Measurement and modelling techniques separate into two main categories, according to the type of species under consideration and their deposition properties: gases and fine particles (0.002 µm < d_p < 2.5 µm, with d_p the aerodynamic diameter of particles) on the one hand and coarse particles ($d_p \geq 2.5$ µm; Finlayson-Pitts and Pitts, 1986; Gallagher et al., 1997) on the other hand. 'Particles' in this context may be solid or liquid (including rain and cloud drops). In general, fluxes of inert gases or fine particles are governed by turbulent diffusion in the atmosphere, by molecular diffusion within the (quasi-laminar) boundary layer adjacent to plant and soil surfaces, and by chemical reactions at the surfaces. In case of reactive gases or fine particles, also chemical reactions in the air have to be taken into account. Fluxes of very large particles (d_p > 100 µm) are predominantly controlled by gravitational forces whereas fluxes of smaller particles (d_p < 100 µm) are a result of diffusive, gravitational and inertial effects (interception, including impaction and turbulent inertial effects), depending on particle size and density (cf. Slinn 1982, Grünhage et al. 1998). Figure 1 shows a separation of air constituents with respect to their deposition properties (particle size and mass, state). Overviews on monitoring and modelling of biosphere/atmosphere exchange of gases, fine and coarse particles as well as of wet deposition are given in Dämmgen et al. (1997), Grünhage et al. (2000), Krupa (2002), Dämmgen et al. (2005) and Erisman et al. (2005).

Modelling of biosphere/atmosphere exchange of gases and fine-particle constituents also depends on the resolution in space and time needed. Whereas local scale Soil-Vegetation-Atmosphere-Transfer (SVAT) models rely on the detailed description of the canopy energy balance of the ecosystem under consideration, regional or national scale models make use of simplifying and integrating assumptions and make use of typical deposition velocities rather than site-specific driving forces (cf. Erisman et al., 2005). At the European scale, flux estimates are based on large-scale modelled meteorology and concentration fields; ecosystem properties are replaced by those of a vegetation type (cf. Grünhage et al., 2004). Necessarily, the complexity of details and processes considered in flux modelling decreases with increasing scale in space in time. This means that those generalized approaches must be carefully calibrated by well validated local scale models.

SVAT models serve two purposes: (1) In agricultural and forest meteorology they are used to calculate water dynamics e.g. to predict irrigation; (2) in the context of the ecotoxicology of air constituents they are needed to derive dose-response relationships (cf. Dämmgen and Grünhage, 1998).

Any perturbation on plant or ecosystem level is a function of the absorbed dose, i.e. the integral of the absorbed flux density $F_{c,\,absorbed}$ over time (cumulative flux density). In the context of acidification and

eutrophication of terrestrial ecosystems, $F_{c,\ absorbed}$ is the overall input of acidifying or eutrophying species into the system as a whole ($F_{c,\ absorbed} = F_{c,\ total}$). On the other hand, for SO_2 or for O_3 (in particular as phytotoxic agents), $F_{c,\ absorbed}$ is only a part of the total flux: the total flux $F_{c,\ total}$ must then be partitioned into fluxes (1) absorbed by the plant through the stomata and the cuticle ($F_{c,\ stom\ \&\ cut}$), and (2) deposited on external plant surfaces and the soil ($F_{c,\ non\text{-}stomatal}$; combined non-stomatal deposition). Studies show that penetration through the cuticle can be neglected in comparison to stomatal uptake (cf. literature cited in Grünhage et al., 2000). For ammonia (NH_3) bi-directional fluxes have to be taken into account, because, dependent on the nitrogen status of the respective system, deposition or emission situations can occur.

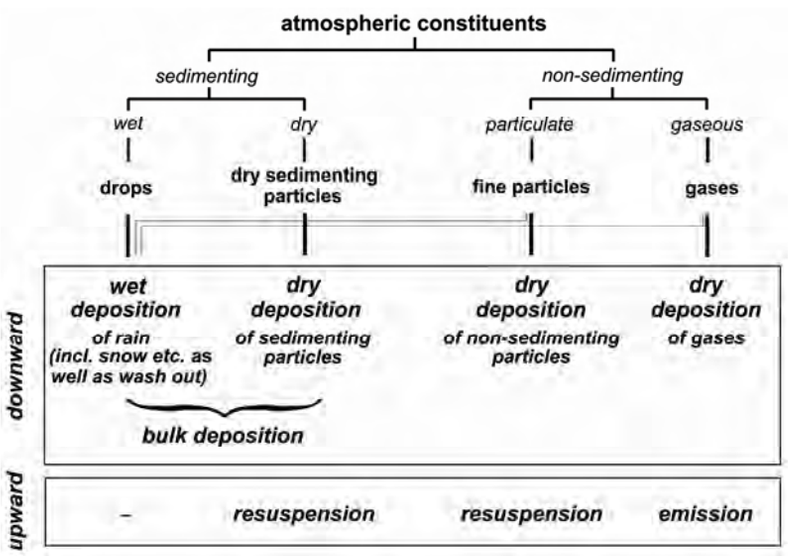

Fig. 1
Conceptual separation of atmospheric constituents with respect to their deposition properties (particle size and mass, state; Grünhage et al., 1993, modified)

Non-stomatal deposition of phytotoxic gases (O_3, SO_2) is toxicologically almost irrelevant under ambient conditions in Europe but nevertheless a considerable part of the total flux (Grünhage et al., 1998; Fowler et al., 2001; Gerosa et al., 2003, 2004). Modelling of stomatal behaviour is crucial for the establishment of dose-response relationships (cf. Dämmgen et al., 1997; Grünhage et al., 2004; Tuovinen et al., 2004). As illustrated by Grünhage et al. (2003), any parameterization of stomatal behaviour in SVAT models for this purpose has to be validated at least via measurements of canopy level water vapour exchange.

This paper, which is a contribution to the European BIAFLUX joint programme (Biosphere Atmosphere Exchange of Pollutants; http://www.accent-network.org), presents the documentation of an extended version of the *big leaf* SVAT model PLATIN (PLant-ATmosphere INteraction) published by Grünhage and Haenel (1997) for the estimation of the exchange of latent and sensible heat, trace gases and fine-particle constituents between the plant/soil system and the atmosphere near the ground. Already the former PLATIN model had been published (in a simplified version) as an EXCEL version (named WINDEP for Worksheet-INtegrated Deposition Estimation Programme, cf. Grünhage and Haenel, 2000) in order to allow users to easily reflect model structure and equations and to adapt the model to their own requirements. In the EXCEL version of the extended PLATIN model, the equations presented in this paper are cited in the Excel spreadsheets with their original equation numbers. The new PLATIN model will be available as 'PLATIN for Excel' via download from:

http://www.uni-giessen.de/cms/ukl-en/PLATIN

PLATIN consists of several modules, as is illustrated in Figure 2. The core module solves the canopy energy balance while simultaneously providing all the resistances also relevant for trace gas exchange. The description of the underlying processes is given in Chapter 2 with special aspects more detailed in the Appendices C, E, and F. As the functioning of the core module is essential for the entire performance of PLATIN, a short subsection at the end of Chapter 2 provides an overview-like comparison of measured and modelled latent and sensible heat fluxes above a semi-natural grassland in 2004 at the Linden field site (for details see Grünhage et al., 1996; Jäger et al., 2003).

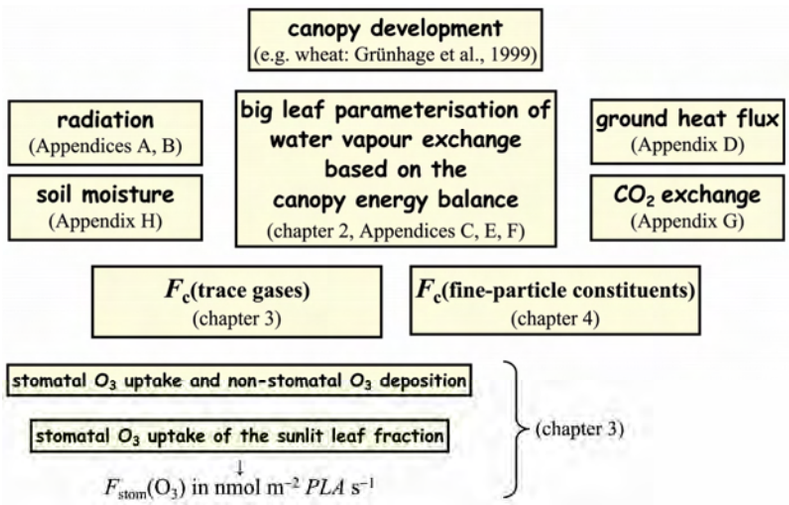

Fig. 2
Modular structure of the PLant-ATmosphere INteraction (PLATIN) model

The solution of the energy balance requires auxiliary modules (radiation, soil moisture, ground heat flux, and CO_2 exchange) being described in the respective Appendices (A, B, H, D, and G). Modelling canopy development is understood as another auxiliary module, which, however, is treated elsewhere (e.g. for wheat in Grünhage et al., 1999).

Chapters 3 and 4 will present the modules quantifying biosphere/atmosphere exchange of O_3, SO_2, NH_3, nitric oxide (NO), nitrogen dioxide (NO_2), nitrous acid (HNO_2) and nitric acid (HNO_3) as well as of ammonium (NH_4), nitrate (NO_3) and sulphate (SO_4) in fine particles. Chemical sinks and/or sources between reference height and canopy surface are not taken into account. For a discussion see Grünhage et al. (2000). A special submodule described in Chapter 3 estimates the stomatal O_3 uptake of the sunlit leaf fraction yielding the leaf area-related stomatal conductance for sunlit parts of the plant stand and thus providing an interface to measurements on gas exchange on leaf level.

A comparison of measured and modelled flux densities of trace gases will be published elsewhere.

2 Biosphere/atmosphere exchange of latent and sensible heat

Vertical flux densities of energy are part of the typical entities governing structure and function of ecotopes (Dämmgen et al., 1997). Energy fluxes must be known to establish the biosphere's energy budget, which, along with the budget of matter, is essential for the understanding of ecosystem behaviour. However, while energy fluxes between the near-surface atmosphere and the biosphere can be measured, it is far more difficult to derive the energy balance of the biosphere from measurements. Thus, a common approach has become to model the biosphere system. In general, this modelling is

one-dimensional, i.e. based on the assumption that all properties be functions of height z only. A short description of model scheme principles is given in Grünhage et al. (2000).

The one-dimensional PLant-ATmosphere INteraction model (PLATIN) is based on the *big leaf* concept which assumes that the vertical distribution of sources and/or sinks of a scalar (sensible heat, latent heat, ozone or another trace gas) can be represented by a single source and/or sink at the *big leaf* surface located at the conceptual height $z = d + z_{0scalar}$. It is convenient to assume that the roughness length for gaseous species e.g. z_{0H2O} equals the roughness length for sensible heat z_{0h}.

The core module of PLATIN deals with the solution of the canopy energy balance defined for the *big leaf* surface by

$$R_{net} = H + \lambda E + G \qquad (1)$$

with	R_{net}	net radiation balance [W·m^{-2}]
	H	turbulent vertical flux density of sensible heat [W·m^{-2}]
	λE	turbulent vertical flux density of latent heat [W·m^{-2}]
	G	ground heat flux density [W·m^{-2}]

Net radiation balance R_{net} [W·m^{-2}] is preferably provided by measurements. Otherwise it can be estimated in parts or completely as discussed in Appendix A. The same holds for the ground heat flux density G [W·m^{-2}] the approximation of which is described in Appendix D.

The calculation of the fluxes of sensible and latent heat, H and λE, (and of gas fluxes) is based on Ohm's law making use of a resistance network as illustrated in Figure 3.

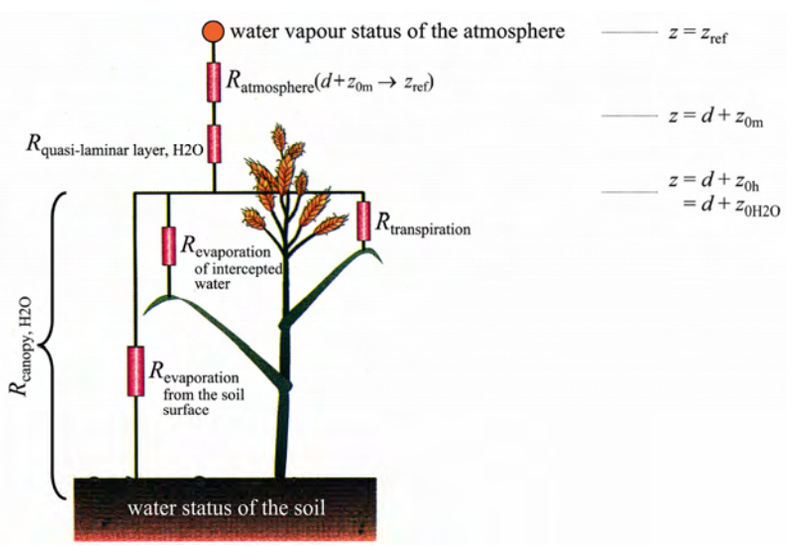

Fig. 3
A resistance analogue for water vapour (modified from PORG, 1997)

There are three major resistance components (which will be discussed in more detail in subsequent chapters):

(1) the atmospheric resistance $R_{atmosphere}(d+z_{0m}, z_{ref})$ [s·m^{-1}], representing the atmospheric transport properties between the conceptual height of the momentum sink near the *big leaf* surface $z = d + z_{0m}$ and a reference height z_{ref} above the canopy, where d is the displacement height and z_{0m} is the roughness length for momentum.
(Atmospheric turbulence is driven both by mechanical and thermal forces. The latter intensifies the mechanically induced turbulence within periods of atmospheric heating during daylight hours

(unstable atmospheric stratification), whereas it weakens mechanically induced turbulence during cooling periods especially in the night (stable atmospheric stratification). Atmospheric transport by molecular diffusion can be neglected under turbulent conditions. Therefore $R_{atmosphere}$ can be approximated by $R_{atmosphere} \cong R_{ah}$, where R_{ah} is the turbulent atmospheric resistance for sensible heat transfer including a correction for non-neutral atmospheric stability conditions.);

(2) the quasi-laminar layer resistance $R_{quasi\text{-}laminar\ layer}$ or R_b [s·m^{-1}] between momentum sink height $z = d + z_{0m}$ and the conceptual sink/source height for sensible heat and trace gases (including H_2O) at $z = d + z_{0h}$; and

(3) the bulk canopy or surface resistance R_{canopy} or R_c [s·m^{-1}], describing the influence of the plant/soil system on the vertical exchange of trace gases (including H_2O).

2.1 Turbulent atmospheric resistance

According to the Monin-Obukhov theory (Monin and Obukhov, 1954), the turbulent atmospheric resistance R_{ah} between two heights z_1 and z_2 ($z_1 < z_2$) can be expressed by

$$R_{ah}(z_1, z_2) = \frac{\ln\left(\frac{z_2 - d}{z_1 - d}\right) - \Psi_h\left(\frac{z_2 - d}{L}\right) + \Psi_h\left(\frac{z_1 - d}{L}\right)}{\kappa \cdot u_*} \qquad (2)$$

with	z_1	e.g. momentum sink height $d+z_{0m}$ [m]
	z_2	e.g. reference height $z_{ref,\,T}$ for actual air temperature t_a [°C] or reference height $z_{ref,\,A}$ for a trace gas or fine-particle constituent
and	L	Monin-Obukhov length [m]
	κ	dimensionless von Kármán constant (κ = 0.41; cf. Dyer, 1974)
	u_*	friction velocity [m·s^{-1}]
	Ψ_h	atmospheric stability function for sensible heat

For vegetation like wheat or forests the displacement height and the roughness length are usually approximated by $d = 0.67 \cdot h$ and $z_{0m} = 0.13 \cdot h$, respectively, with h the canopy height (Brutsaert, 1984). A parameterization of canopy height h for spring and winter wheat as a function of phenological development is given in Grünhage et al. (1999).

Calculation of energy balance time series for growing agricultural crops requires also the definition of the roughness length for bare agricultural soil. There is no unique value for all types of soils and their possible surface states. Table 2.2 in Oke (1978) gives a range of 0.001 – 0.01 m (along with displacement height d = 0 m).

The roughness length for sensible heat z_{0h} is smaller than z_{0m}. According to Figure 4.24 in Brutsaert (1984) a typical value of $\ln(z_{0m}/z_{0h})$ is 2 for grass and corn so that we assume a value of 2 to be representative also for agricultural crops. For forests $\ln(z_{0h}/z_{0m}) = 1$ seems to be an acceptable value. Note that we use $\ln(z_{0m}/z_{0h}) = 2$ also for bare soil.

Eq. (2) is based on Monin-Obukhov theory. Strictly, this theory is valid only above the roughness sublayer which may range up to 2 or 2.5 times the vegetation height over tall and very rough canopies. For discussion see e.g. Cellier and Brunet (1992). Except for maize it seems tolerable to use eq. (2) for agricultural crops without further correction, because the height of the roughness sublayer is generally smaller than the typical agrometeorological reference height of 2 m (for e.g. air temperature measurements). Over forests, however, most often the reference height is located within or at least at the upper boundary of the roughness sublayer. For this case, PLATIN makes use of a modified resistance equation (see e.g. Sellers et al., 1986):

$$R_{\text{ah, forests}}(z_1, z_2) = \frac{R_{\text{ah}}(z_1, z_2)}{2} \tag{3}$$

The friction velocity is given by:

$$u_* = \frac{\kappa \cdot u(z_{\text{ref}})}{\ln\left(\frac{z_{\text{ref, u}} - d}{z_{0\text{m}}}\right) - \Psi_{\text{m}}\left(\frac{z_{\text{ref, u}} - d}{L}\right) + \Psi_{\text{m}}\left(\frac{z_{0\text{m}}}{L}\right)} \tag{4}$$

with $u(z_{\text{ref}})$ horizontal wind velocity at reference height $z_{\text{ref, u}}$ [m·s^{-1}]
Ψ_{m} atmospheric stability function for momentum

The Monin-Obukhov length L (Monin and Obukhov, 1954) is defined as:

$$\begin{aligned} L &= -\rho_{\text{moist air}} \cdot c_{\text{p, moist air}} \cdot \frac{\overline{\overline{\theta}} \cdot u_*^{\,3}}{\kappa \cdot g \cdot H} \\ &\approx -\rho_{\text{moist air}} \cdot c_{\text{p, moist air}} \cdot \frac{\theta(z_{\text{ref}}) \cdot u_*^{\,3}}{\kappa \cdot g \cdot H} \end{aligned} \tag{5}$$

with $\overline{\overline{\theta}}$ average potential temperature of the air layer under consideration [K]
g gravitational acceleration (g = 9.81 m·s^{-2})
$\rho_{\text{moist air}}$ density of moist air [kg·m^{-3}] at absolute temperature T [$T = t_{\text{a}}$ + 273.15 K] with t_{a} the actual air temperature (°C) measured at reference height $z_{\text{ref, T}}$ (see Appendix F, eq. (F7))
$c_{\text{p, moist air}}$ specific heat of moist air at a constant pressure [m^2·s^{-2}·K^{-1}] (see Appendix F, eq. (F9))

It is sufficient to approximate the layer-average potential temperature by the potential temperature at reference height, $\theta(z_{\text{ref}})$, which is estimated from the actual air temperature $T(z_{\text{ref}})$ according to (cf. Stull, 1988):

$$\theta(z_{\text{ref}}) = T(z_{\text{ref}}) + (z_{\text{ref}} \cdot \Gamma_{\text{d}}) \tag{6}$$

with Γ_{d} dry adiabatic lapse rate [Γ_{d} = – 9.76 K·km^{-1}]

The atmospheric stability functions for momentum Ψ_{m} and sensible heat Ψ_{h} are given in Appendix C.

As u_* and H implicitly depend on L, L must be calculated iteratively. For this purpose a so-called neutral value is defined: $L_{\text{neutral}} = 10^{20}$ m. (In reality L should approach plus or minus infinity under neutral atmospheric stability conditions. However, from the mathematical point of view it is sufficient to use a very high positive value of L as is done with L_{neutral}.) Iteration starts with $L = L_{\text{neutral}}$. In the rather rare case that iteration does not converge L is finally reset to L_{neutral}. This may be incorrect to some extent but is estimated to be more effective than to drop the complete evaluation of the current data set (which would interrupt the calculation of storage terms like the interception reservoir or the soil water content). Of course the neutral value $L = L_{\text{neutral}}$ also applies in situations where $H = 0$.

2.2 Quasi-laminar layer resistance for sensible heat and water vapour

The quasi-laminar layer resistance for water vapour $R_{\text{b, H2O}}$ is estimated according to the approach by Hicks et al (1987) taking into account the empirical results for permeable rough canopies described by Brutsaert (1984); for details see Grünhage et al. (2000):

$$R_{\mathrm{b,\,H2O}} = R_{\mathrm{b,\,heat}} \cdot \left(\frac{\mathrm{Sc_{H2O}}}{\mathrm{Pr}}\right)^{\frac{2}{3}} = \frac{\ln\left(\frac{z_{0\mathrm{m}}}{z_{0\mathrm{h}}}\right) - \Psi_{\mathrm{h}}\left(\frac{z_{0\mathrm{m}}}{L}\right) + \Psi_{\mathrm{h}}\left(\frac{z_{0\mathrm{h}}}{L}\right)}{\kappa \cdot u_*} \cdot \left(\frac{\mathrm{Sc_{H2O}}}{\mathrm{Pr}}\right)^{\frac{2}{3}} \tag{7}$$

with
- $R_{\mathrm{b,\,heat}}$ quasi-laminar layer resistance for sensible heat
- $\mathrm{Sc_{H2O}}$ Schmidt number for water vapour (the ratio of the kinematic viscosity of dry air and the molecular diffusivity of the respective trace gas)
- Pr Prandtl number (the ratio of the kinematic viscosity of dry air and the molecular diffusivity of heat)

For water vapour, $(\mathrm{Sc/Pr})^{2/3}$ is 0.90 (cf. Table 2, Chapter 3).

2.3 Bulk canopy resistance for water vapour

The bulk canopy resistance $R_{\mathrm{c,\,H2O}}$ is a composite resistance describing stomatal and cuticular transpiration and evaporation. $R_{\mathrm{c,\,H2O}}$ can be approximated by a weighted combination of soil resistance R_{soil}, bulk stomatal resistance $R_{\mathrm{c,\,stom}}$ and bulk cuticle resistance $R_{\mathrm{c,\,cut}}$ known for a fully developed canopy (without senescent leaves) under optimum conditions for maximal transpiration. The weights depend on the actual canopy development stage taking into account the transition from a dense canopy (one-sided leaf area index $LAI = LAI_{\mathrm{max}}$ [$\mathrm{m^2 \cdot m^{-2}}$]) to a sparse canopy:

$$\frac{1}{R_{\mathrm{c,\,H2O}}} = \left[(1-\beta^*)\cdot\left(\frac{1}{R_{\mathrm{c,\,stom,\,H2O}}} + \frac{1}{R_{\mathrm{c,\,cut,\,H2O}}}\right) + \frac{\beta}{R_{\mathrm{soil,\,H2O}}}\right] \tag{8}$$

In order to keep as close as possible to the single-leaf representation of the biosphere in PLATIN, eq. (8) makes use of a weighted R_{soil} (cf. Grünhage et al., 2000) instead of an additional in-canopy scalar transport resistance, where the coefficient β must be unity for bare soil and approaches zero for a fully developed dense canopy. If all leaves could contribute to the energy and water exchange between canopy and atmosphere, the weight of the reciprocal sum of $R_{\mathrm{c,\,stom,\,H2O}}$ and bulk cuticle resistance $R_{\mathrm{c,\,cut,\,H2O}}$ would be $(1 - \beta)$. However, as only non-senescent leaves are relevant, a modified weight $(1 - \beta^*)$ is introduced.

Grünhage and Haenel (1997) presented a plausible ad-hoc approach to estimate $(1 - \beta^*)$ and β. It was based on the fact that the vertical distribution of incoming radiation energy within the canopy is one of the main limiting factors for the total canopy energy and water budget. Grünhage and Haenel (1997) simply assumed the available radiation energy to decrease exponentially with increasing distance from the top of the canopy and introduced a vegetation-type specific coefficient c_{LAI} to describe the attenuation effect. They defined:

$$1-\beta^* = 1 - \mathrm{e}^{-c_{\mathrm{LAI}} \cdot LAI_{\mathrm{non\text{-}senescent}}} \tag{9}$$

and

$$\beta = \mathrm{e}^{-c_{\mathrm{LAI}} \cdot LAI_{\mathrm{total}}} \tag{10}$$

The expression $(1 - \beta^*)$ may be interpreted as the fraction of radiation intercepted by non-senescent (green) leaves which is given by $LAI_{\mathrm{non\text{-}senescent}}$ (= one-sided leaf area index of non-senescent leaves; = projected leaf area *PLA* according to UNECE (2004, 2007)). The weight β estimates the fraction of radiation reaching the ground depending on one-sided total leaf area index LAI_{total} (= non-senescent plus senescent leaves). For spring and winter wheat a parameterization to calculate LAI_{total} and $LAI_{\mathrm{non\text{-}senescent}}$ as a function of phenological stages is given in Grünhage et al. (1999).

As radiation distribution within the canopy is (at least) a function of the solar elevation angle ϕ and of leaf angle distribution, the same should hold for c_{LAI}. However, Grünhage and Haenel (1997) made successfully use of a constant value for c_{LAI}, only dependent on vegetation type. This constant value may be interpreted as an effective mean value. Coefficients averaged over all solar elevations are summarized for different vegetation types e.g. in Monteith and Unsworth (1990). For most vegetation types c_{LAI} is in the range of 0.3 to 0.6 (Ross, 1981). This includes $c_{LAI} \approx 0.4$ for crops as described by Ritchie (1972) as well as 0.5 for spring wheat (Choudhury et al., 1987) and a maritime pine canopy (Granier and Lousteau, 1994). On the other hand, for canopies with predominantly horizontally arranged leaves (e.g. cabbage, clover) c_{LAI} approaches 1.8 as can be deduced from Monteith (1965).

PLATIN for Excel now incorporates a canopy radiation submodel (see Appendix B), which allows to calculate the vertical radiation energy distribution and related entities within the canopy. Therefore, the parameterizations of the weights $(1 - \beta^*)$ and β, i.e. eqs. (9) and (10) had to be reconsidered in so far, as it could be possible and reasonable to replace the externally given coefficient c_{LAI} by an entity calculated by the canopy radiation model. However, as radiation distribution is only a predictor for the weights $(1 - \beta^*)$ and β, care had to be taken when adopting results from the new radiation model.

The canopy radiation model allows to calculate an attenuation coefficient k_b similar to c_{LAI}, but dependent on solar height:

$$k_b = \frac{k_{b,90°}}{\sin \phi} \tag{11}$$

with $k_{b,90°}$ k_b value for solar elevations of 90°

According to eq. (13) in Sellers (1985), $k_{b,90°}$ is 0.5 for spherically arranged leaves, 0.27 for vertical and 1.23 for horizontal leaves. However, there is no use to replace c_{LAI} in (10) by k_b according to (11), because (11) is valid only for daylight hours while the weight β is needed also during night. Therefore it was decided to replace c_{LAI} in the calculation of β by $k_{b,max}$ rather than k_b:

$$\beta = e^{-k_{b,max} \cdot SAI} \tag{12}$$

with SAI total surface area of the vegetation [$m^2 \cdot m^{-2}$]

and

$$k_{b,max} = \frac{k_{b,90°}}{\sin \phi_{max}} \tag{13}$$

where ϕ_{max} solar elevation at 12 h TST (true solar time)

A minor adjustment is the formal replacement of LAI_{total} in eq. (10) by SAI, the total surface area of the vegetation. SAI is set equal to LAI_{total} + 1 for forests (Tuovinen et al., 2004) and to LAI_{total} for short vegetation (crops, grassland).

The advantage of eq. (12) over (10) is that the annual course of solar height is now accounted for. The switch from c_{LAI} to $k_{b,max}$ does not change the results significantly.

Stomatal behaviour of the plants strongly depends on irradiance absorption. This means that, when simulating stomata-related processes, the fraction of radiation intercepted by the non-senescent leaves should be taken into account explicitly within the parameterization of $(1 - \beta^*)$. With entities calculated by the canopy radiation submodel, $(1 - \beta^*)$ has been redefined for the current PLATIN version as follows:

$$1 - \beta^* = \frac{I_{c,sunlit} + I_{c,shaded}}{PAR} \tag{14}$$

with $I_{c,\,sunlit}$ irradiance absorbed by the sunlit fraction of non-senescent leaves of the canopy [µmol·m^{-2}·s^{-1}]

$I_{c,\,shaded}$ irradiance absorbed by the shaded fraction of non-senescent leaves of the canopy [µmol·m^{-2}·s^{-1}]

PAR photosynthetically active radiation measured above the canopy [µmol·m^{-2}·s^{-1}]

Eq. (14) is needed as base for other calculations like the fractioning of the total ozone stomatal uptake into stomatal uptake by the sunlit and shaded leaf fraction of the canopy during daylight hours. Clearly, eq. (14) is meaningless during night time. But as the nocturnal stomatal uptake is of inferior importance, β^* can then simply be replaced by β according to eq. (12), but calculated with the non-senescent *LAI*.

Soil resistance for water vapour

$R_{soil,\,H2O}$ is a complex function of vertical soil water distribution. An important feature of evaporation from bare soil is a fast reduction due to the drying of the uppermost soil layer after rainfall. Therefore, $R_{soil,\,H2O}$ is parameterized in the following manner:

(a) For a fully wet soil, $R_{soil,\,H2O}$ equals $R_{soil,\,H2O,\,min}$ (= 100 s·m^{-1}).

(b) For daylight hours (i.e. time intervals with global radiation $S_t \geq 50$ W·m^{-2}), $R_{soil,\,H2O}$ is increased by a given fraction of $R_{soil,\,H2O,\,min}$ if there is no precipitation:

$$(R_{soil,H2O})_n = (R_{soil,H2O})_{n-1} + RX \cdot R_{soil,H2O,min} \quad (15)$$

where n is the index of the data set under consideration and n−1 denotes the previous data set. RX is chosen to be 0.05 for half-hourly data sets and 0.1 for hourly data sets. $R_{soil,\,H2O}$ is bound by the upper limit of 4000 s·m^{-1}, the choice of which is based on the results of Daamen and Simmonds (1996).

(c) At night $R_{soil,\,H2O}$ stays constant at the value calculated for the last late-afternoon daylight hour, i.e. $(R_{soil,\,H2O})_n = (R_{soil,\,H2O})_{n-1}$.

(d) At any time interval with precipitation not reaching the ground, $R_{soil,\,H2O}$ stays constant at the value calculated before, i.e. $(R_{soil,\,H2O})_n = (R_{soil,\,H2O})_{n-1}$.

(e) At any time interval with precipitation and/or dew reaching the ground, $R_{soil,\,H2O}$ is decreased by a fraction RY = $a_{soil} \cdot W_{in}$ of $R_{soil,\,H2O,\,min}$:

$$(R_{soil,H2O})_n = (R_{soil,H2O})_{n-1} - a_{soil} \cdot W_{in} \cdot R_{soil,H2O,min} \quad (16)$$

with W_{in} amount of precipitation and/or dew reaching the ground (water input) [mm]

For short vegetation (crops, grassland), the empirical constant a_{soil} is set to 10 mm^{-1} for half-hourly and 20 mm^{-1} for hourly data sets.

The amount of precipitation and/or dew reaching the ground depends on the interception reservoir capacity of the canopy. In PLATIN, this capacity INT_{max} [mm] is assumed to be proportional to total *LAI*:

$$INT_{max} = b_{INT} \cdot LAI_{total} \quad (17)$$

The constant b_{INT} is chosen as 0.2 mm according to Dickinson (1984), neglecting the fact that leaves become able to intercept more precipitation during senescence (cf. Braden, 1995).

The interception reservoir is filled by precipitation *Precip* and dew and depleted by evaporation. Dew formation and depletion of the reservoir is estimated due to potential evapotranspiration rate E_{pot} [mm]

applying the Penman-Monteith approach (see Chapter 2.4) with $R_{c,\,H2O}$ = 0 s·m^{-1} assuming neutral atmospheric stratification. The interception *INT* [mm] is parameterized according to

$$INT_n = Precip_n + INT_{n-1} - E_{pot,\,n} \tag{18}$$

with $0 \le INT_n \le INT_{max}$. The precipitation and dew reaching the ground W_{in} is than given by:

$$W_{in,\,n} = Precip_n + (INT_{n-1} - E_{pot,\,n}) - INT_{max} \tag{19}$$

with $W_{in} \ge 0$ mm.

For forests, the coefficients RX and a_{soil} have not yet been properly adjusted. As a plausible working model, applicable to forests in Central Europe with generally non-drying soil, $R_{soil,\,H2O}$ can be set to $R_{soil,\,H2O,\,min}$.

Note: $R_{c,\,H2O}$ is set to zero if the interception reservoir is not empty. Comparisons of modelled evapotranspiration rates with measured fluxes show that setting $R_{c,\,H2O}$ to zero overestimates the real fluxes. Therefore, interception is not taken into account in latent heat flux modelling at present (see Chapter 2.4).

Bulk cuticle resistance for water vapour

Investigations of cuticular permeability of water vapour and other trace gases show that penetration through the cuticle can be neglected in comparison to stomatal exchange (Kerstiens and Lendzian, 1989a, b; Lendzian and Kerstiens, 1991; Kerstiens et al., 1992). According to the aforementioned authors $R_{cut,\,H2O}$ on leaf basis is 9·10^4 s·m^{-1} (cf. Table 3, Chapter 3.1). According to Grünhage et al. (1999) resistances derived on leaf basis are upscaled to canopy level taking into account the PLATIN formulation of canopy architecture and radiation distribution within the canopy. Similar to the minimum value of the bulk stomatal resistance $R_{c,\,stom,\,min,\,H2O}$, which is representative for a fully developed canopy (without senescent leaves) under optimum conditions for maximal transpiration, upscaling from leaf to canopy level is performed applying $k_{b,max}$ at maximum solar elevation of the year (summer solstice):

$$R_{canopy} = R_{leaf,\,literature} \cdot \left(1 - e^{-k_{b,max,\,summer\,solstice} \cdot LAI_{leaf,\,literature}}\right) \tag{20}$$

Bulk stomatal resistance for water vapour

The gas transfer through the stomata is by molecular diffusion. An inverse dependence of stomatal resistance on molecular diffusivity is generally accepted. In PLATIN, the dependence of stomatal resistance on radiation, temperature and the water budgets of atmosphere and soil as well as on modifying influence of time of day, phenology, ozone and CO_2 is described according to the Jarvis-Stewart approach (Jarvis, 1976; Stewart, 1988):

$$R_{c,\,stom,\,H2O} = \left[\frac{1}{R_{c,\,stom,\,min,\,H2O}} \cdot f_1(S_t) \cdot f_2(t_a) \cdot f_{3/4}(VPD, SM) \cdot f_5(\text{time}) \cdot f_6(\text{PHEN}) \cdot f_7(O_3) \cdot f_8(CO_2)\right]^{-1} \tag{21}$$

or

$$R_{\mathrm{c,\,stom,\,H2O}} = \left[\frac{1}{R_{\mathrm{c,\,stom,\,min,\,H2O}}} \cdot f_1(S_\mathrm{t}) \cdot f_2(t_\mathrm{a}) \cdot f_3(VPD) \cdot f_4(SM) \cdot f_5(\mathrm{time}) \cdot f_6(\mathrm{PHEN}) \cdot f_7(\mathrm{O_3}) \cdot f_8(\mathrm{CO_2}) \right]^{-1} \quad (22)$$

where $R_{\mathrm{c,\,stom,\,min,\,H2O}}$ represents the minimum value of the stomatal resistance for water vapour of the respective ecosystem. Functions $f_1(S_\mathrm{t})$, $f_2(t_\mathrm{a})$, $f_3(VPD)$ and $f_4(SM)$ account for the effects of solar radiation S_t [W·m^{-2}], air temperature t_a [°C], water vapour pressure deficit of the atmosphere *VPD* [hPa] and soil moisture *SM* [m^3·m^{-3}] on stomatal aperture ($0 \le f_\mathrm{i} \le 1$). While eq. (22) is based on a multiplicative dependence of stomatal resistance on *VPD* and *SM* in PLATIN, a combined function $f_{3/4}(VPD, SM)$ is preferred for biological reasons. A combined function $f_{3/4}(VPD, SM)$ reflects the observation that increasing soil moisture deficits strongly influence stomatal closure due to *VPD*. It is recommended to use measured soil moisture content *SM* for $f_{3/4}(VPD, SM)$ or $f_4(SM)$. If no *SM* data are available they must be simulated by a soil water model, a simple one is described in Appendix H. With f_5(time) a time-dependent impact on stomatal resistance can be taken into account (cf. Körner, 1994). f_6(PHEN) and $f_7(\mathrm{O_3})$ represent the influence of phenology and ozone on stomatal resistance: both senescence due to natural ageing and premature senescence induced by ozone are limiting factors for stomatal aperture. The Jarvis-Stewart functions used are described in Appendix E. For $S_\mathrm{t} = 0$, $R_{\mathrm{c,\,stom,\,H2O}}$ is set to 20000 s·m^{-1}. Under ambient conditions with elevated CO_2 the influence of elevated CO_2 on stomatal aperture must be taken into account by an additional Jarvis-Stewart function $f_8(\mathrm{CO_2})$.

2.4 Latent and sensible heat flux densities

It is straightforward to formulate *H* and λE as analogs of Ohm's law and to use them to operate a SVAT model like PLATIN. However, for PLATIN another way has been chosen. Inserting the resulting resistance-based formula for *H* in eq. (1) and solving for λE yields the well-known Penman-Monteith equation (Monteith, 1965):

$$\lambda E = \frac{s_\mathrm{c} \cdot (R_\mathrm{net} - G) + \rho_{\mathrm{moist\,air}} \cdot c_{\mathrm{p,\,moist\,air}} \cdot \dfrac{VPD}{R_\mathrm{ah}(d + z_{0\mathrm{m}}, z_{\mathrm{ref,\,T}}) + R_{\mathrm{b,\,heat}}}}{s_\mathrm{c} + \gamma \cdot \dfrac{R_\mathrm{ah}(d + z_{0\mathrm{m}}, z_{\mathrm{ref,\,T}}) + R_{\mathrm{b,\,H2O}} + R_{\mathrm{c,\,H2O}}}{R_\mathrm{ah}(d + z_{0\mathrm{m}}, z_{\mathrm{ref,\,T}}) + R_{\mathrm{b,\,heat}}}} \quad (23)$$

with γ psychrometric constant (= 0.655 hPa·K^{-1})
VPD water vapour pressure deficit of the atmosphere [hPa] (see Appendix F, eq. (F1))

and

$$s_\mathrm{c} = \frac{e_\mathrm{sat}(T_\mathrm{s}) - e_\mathrm{sat}(T(z_\mathrm{ref}))}{T_\mathrm{s} - T(z_\mathrm{ref})} \quad (24)$$

with e_sat saturation water vapour pressure of the atmosphere [hPa] (see Appendix F, eqs. (F2) and (F3))
and T_s absolute canopy surface temperature at conceptual height $z = d + z_{0\mathrm{h}}$ [K]

Once R_net, *G*, and λE are known (λE according to eq. (23)), their values are inserted into eq. (1) to obtain the sensible heat flux *H* as residual. This procedure exactly yields the same results as if both λE and *H* had been estimated by the simple Ohm's-law formulation. In any case the solution of the energy balance can be achieved only iteratively, because the real unknown in eq. (1) is the surface temperature T_s which is involved in a non-linear way in the set of equations described above to solve eq. (1).

However, the method used in PLATIN offers the option to get rid of iterations by replacing eq. (24) by the slope of water vapour saturation pressure at reference-height air temperature (see eqs. (F5) or (F6) in Appendix F). This is the way the Penman-Monteith equation is often used as a kind of stand-alone model to estimate evapotranspiration, because it yields results only slightly different from eq. (23), cf. discussion in McArthur (1990). Another advantage of the method used in PLATIN is that any kind of λE estimate can be entered instead of eq. (23). This may be of interest e.g. in the case that measured values of λE are available and shall be tested within the modelling frame, or that not all relevant data are available to use eq. (23) so that a less data-demanding approach must be taken to obtain λE. However, as far as not mentioned otherwise, PLATIN for Excel makes use only of eq. (23).

The surface temperature T_s is related to potential canopy surface temperature θ_s [K]

$$\theta_s = \theta(z_{\mathrm{ref,T}}) + \frac{H \cdot \left(R_{\mathrm{ah}}(d + z_{0\mathrm{m}}, z_{\mathrm{ref,T}}) + R_{\mathrm{b,heat}}\right)}{\rho_{\mathrm{moist\,air}} \cdot c_{\mathrm{p,\,moist\,air}}} \tag{25}$$

by eq. (6). As eq. (25) is part of the set of model equations needed to solve iteratively the energy balance (eq. (1)), a starting value of θ_s is needed which is assigned the value of the air temperature at reference height minus 0.1 K.

According to the conceptual structure of PLATIN, total latent heat flux density λE can be split up into the contribution by the vegetation $\lambda E_{\mathrm{transpiration}}$ and the one coming from the soil $\lambda E_{\mathrm{evaporation}}$ as given in eqs. (26) and (27):

$$\lambda E_{\mathrm{transpiration}} = \frac{\lambda E}{1 + \frac{\beta}{1-\beta^*} \cdot \frac{R_{\mathrm{c,stom,H2O}} \cdot R_{\mathrm{c,cut,H2O}}}{R_{\mathrm{soil,H2O}} \cdot \left(R_{\mathrm{c,stom,H2O}} + R_{\mathrm{c,cut,H2O}}\right)}} \tag{26}$$

$$\lambda E_{\mathrm{evaporation}} = \lambda E - \lambda E_{\mathrm{transpiration}} \tag{27}$$

With the latent heat of water vaporisation

$$\lambda \cong (2.501 - 0.00237 \cdot t_a) \cdot 10^6 \ \mathrm{J \cdot kg^{-1}} \tag{28}$$

the actual evapotranspiration E [mm, l·m^{-2}] can be computed for the time interval t_1 to t_2:

$$E = \int_{t_1}^{t_2} \frac{\lambda E}{\lambda} \cdot \mathrm{d}t \tag{29}$$

The water vapour flux density $F_c(H_2O)$ [g·m^{-2}·s^{-1}] is:

$$F_c(\mathrm{H_2O}) = \frac{\lambda E}{\lambda \cdot 10^{-3}} \tag{30}$$

2.5 Comparison of measured and modelled latent and sensible heat flux densities

At the Linden grassland site, friction velocity, latent heat, as well as sensible heat are measured using the eddy covariance method by means of a Solent R3 research ultrasonic anemometer (Gill Instruments Ltd, Hampshire, UK) in combination with a LI-7500 open path CO_2/H_2O gas analyzer (Li-COR Environmental, Lincoln, Nebraska, USA). To guarantee data sets of high accuracy several corrections and quality tests are applied (WPL correction, Schotanus/Liu correction, coordinate rotation, footprint analysis, test to check the fulfilment of stationarity and of well developed turbulence conditions; cf. Grünhage and Gerosa, 2008).

Model adjustment is based on data sets for which the energy balance residual is less then 30 W·m^{-2}. A description how to estimate displacement height d, roughness length for momentum z_{0m} and bulk canopy resistance for water vapour $R_{c,\,H2O}$ can be found in Appendices I and J.

Figure 4 clearly illustrates that PLATIN is able to simulate measured fluxes adequately.

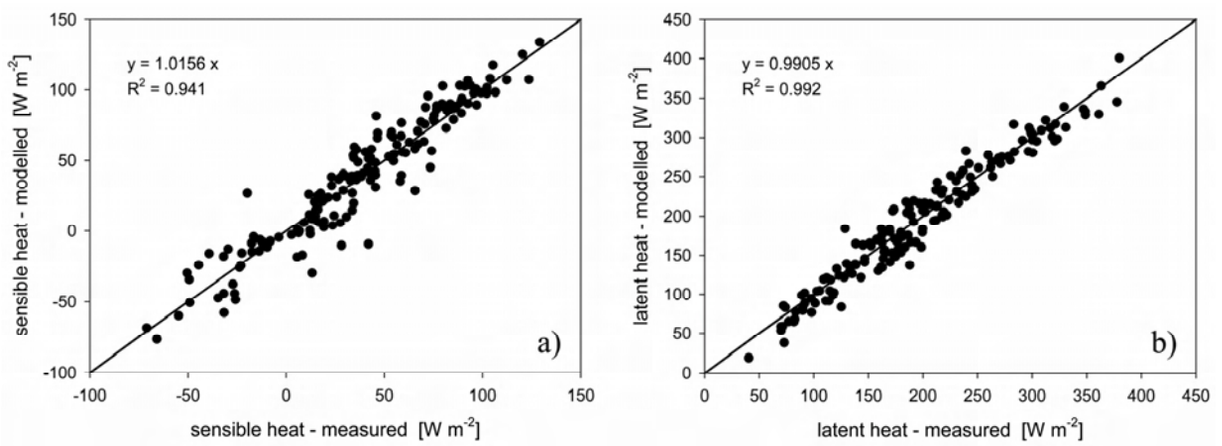

Fig. 4
Comparison of measured and modelled sensible heat (a) and latent heat (b) for June 2004 during daylight hours

3 Biosphere/atmosphere exchange of trace gases

The exchange of trace gas species A, F_c(A), between the phytosphere and the atmosphere near the surface can be modelled by:

$$F_c(\mathrm{A}) = -\frac{\rho_A(z_{ref,\,A}) - \rho_A(d+z_{0m})}{R_{ah}(d+z_{0m}, z_{ref,\,A})} \tag{31}$$

$$= -\frac{\rho_A(z_{ref,\,A}) - \rho_A(d+z_{0c})}{R_{ah}(d+z_{0m}, z_{ref,\,A}) + R_{b,\,A}} \tag{32}$$

$$= -\frac{\rho_A(z_{ref,\,A}) - \rho_{A,\,comp}}{R_{ah}(d+z_{0m}, z_{ref,\,A}) + R_{b,\,A} + R_{c,\,A}} \tag{33}$$

with

F_c(A)	total vertical atmosphere-canopy flux of trace gas A [µg·m^{-2}·s^{-1}]
$\rho_A(z_{ref})$	measured concentration (potential) of trace gas A at height $z = z_{ref,\,A}$ [µg·m^{-3}]
$\rho_A(d+z_{0m})$	concentration of trace gas A at the conceptual height $z = d+z_{0m}$ [µg·m^{-3}]
$\rho_A(d+z_{0c})$	concentration of trace gas A at the conceptual height $z = d+z_{0c} = d+z_{0h}$ [µg·m^{-3}]
$\rho_{A,\,comp}$	canopy compensation concentration of trace gas A [µg·m^{-3}]

The respective resistance scheme is shown in Figure 5. It is based on the assumption that chemical sinks and/or sources between reference height and canopy surface can be neglected. Under this assumption it is allowed to adopt the turbulent atmospheric resistance R_{ah} calculated after eq. (2), and the quasi-laminar layer resistance $R_{b,\,A}$ calculated after eq. (7) taking into account the respective $(Sc_A/Pr)^{2/3}$ (cf. Table 2; see Chapter 3.1).

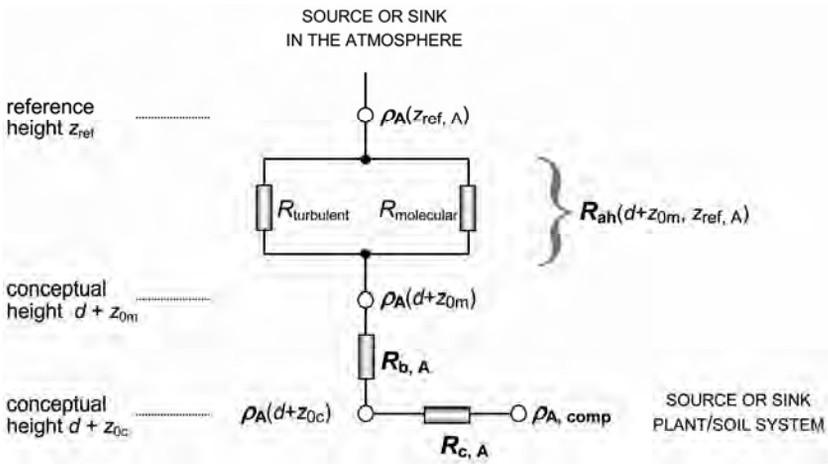

Fig. 5
Resistance analogue of trace gas exchange between the atmospheric surface layer and terrestrial ecosystems as used for the *big leaf* concept (Grünhage et al., 2000; modified)

The so-called canopy compensation concentration $\rho_{A, comp}$ is an effective concentration. It is defined by eq. (33) and represents, along with the bulk canopy resistance $R_{c, A}$ (see eq. (34)) a more complex network as depicted in Figure 6.

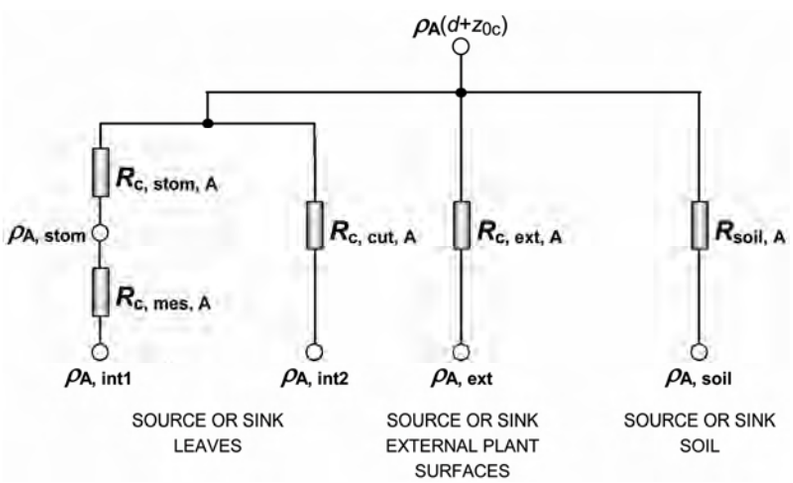

Fig. 6
Resistance analogue of trace gas exchange between the conceptual height $z = d+z_{0c}$ and the plant soil system

If a plant/soil system can be considered a perfect sink as is usually assumed for the exchange of O_3, SO_2, NO_2 and HNO_3, one can set $\rho_{A, int1} = \rho_{A, int2} = \rho_{A, ext} = \rho_{A, soil} = 0$ which leads to $\rho_{A, comp} = 0$. For NH_3 (and HONO) the scheme must allow for bi-directional fluxes which means that, in general, all the aforementioned concentrations are different from zero and have to be parameterized (for more details see Chapter 3.4).

The bulk canopy resistance $R_{c, A}$ represents a combination of resistances (Figure 6) characterizing the fluxes through the leaf stomata ($R_{c, stom, A}$), into or out the mesophyll tissue ($R_{c, mes, A}$), through the cuticle of the leaves ($R_{c, cut, A}$), to or from external plant surfaces ($R_{c, ext, A}$), and down to or up from the soil surface ($R_{soil, A}$):

$$\frac{1}{R_{\mathrm{c,A}}} = \left(\frac{1-\beta^*}{R_{\mathrm{c,stom,A}} + R_{\mathrm{c,mes,A}}} + \frac{1-\beta^*}{R_{\mathrm{c,cut,A}}} \right) + \frac{1-\beta}{R_{\mathrm{c,ext,A}}} + \frac{\beta}{R_{\mathrm{soil,A}}} \tag{34}$$

Parameters β^* and β account for the phenological stage of the canopy on vertical exchange of gaseous species between the plant/soil system and the atmosphere near the ground (see Chapter 2.3).

Nitric acid is a special case, because bulk canopy resistance $R_{\mathrm{c,HNO3}}$ is effectively zero in normal conditions. For numerical reasons a minimum value of $R_{\mathrm{c,HNO3}}$ of 1 s·m^{-1} is enforced. Considering a low-temperature resistance R_{low} at sub-zero air temperatures t_{a} [°C] according to Wesely (1989)

$$R_{\mathrm{low}} = 1000 \cdot \exp(-t_{\mathrm{a}} - 4) \ \mathrm{s \cdot m^{-1}} \tag{35}$$

results in:

$$R_{\mathrm{c,HNO3}} = \max(1\,\mathrm{s \cdot m^{-1}}, R_{\mathrm{low}}) \tag{36}$$

Note: According to Wesely (1989) R_{low} is added to $R_{\mathrm{c,ext}}$ and R_{soil} for all gases mentioned below with exception of sulphur dioxide. For the resistance of snow-covered surfaces we refer to the approximations given by Erisman et al. (1994).

3.1 Bulk stomatal, mesophyll and cuticular resistances for trace gases

The bulk stomatal resistance for a gaseous species A is related to that of water vapour by the ratio the respective molecular diffusivities *D* (cf. Table 2):

$$R_{\mathrm{c,stom,A}} = R_{\mathrm{c,stom,H2O}} \cdot \frac{D_{\mathrm{H2O}}}{D_{\mathrm{A}}} \tag{37}$$

According to Wesely (1989), the canopy mesophyll resistance for any trace gas is given by:

$$R_{\mathrm{c,mes,A}} = \left(\frac{H_{\mathrm{A}}^*}{3000} + 100 \cdot f_{0,\mathrm{A}} \right)^{-1} \tag{38}$$

with H_{A}^* effective Henry's Law value (cf. Table 3)
$f_{0,\mathrm{A}}$ chemical reactivity factor (cf. Table 3)

This formulation allows for two parallel pathways to the sink: one dominant for a primarily water soluble species like SO_2, and the other one for a primarily chemically reactive species like O_3. The value 3000 was derived from considerations of carbon dioxide uptake by vegetation (for details see Wesely, 1989). There is experimental evidence that $R_{\mathrm{c,mes,NO2}}$ calculated according to eq. (38) is much too small for conifer species as reviewed by Ganzeveld and Lelieveld (1995). They approximated the mesophyll resistance for NO_2 by:

$$\text{conifers}: \quad R_{\mathrm{c,mes,NO2}} = 0.5 \cdot R_{\mathrm{c,stom,NO2}} \tag{39}$$

As mentioned above, the cuticular resistances for trace gases published in the literature are given on leaf basis (cf. Table 3) and must therefore be upscaled to canopy level by eq. (20).

3.2 Bulk external plant surface resistance for trace gases

Permeation through cuticles excluded, the amount of deposition on external plant surfaces depends on, for example, the wetness of the surface, the pH of the wetted surface or the surface temperature (e.g. Wesely, 1989; Erisman et al., 1994; Fowler et al., 2001; Zhang et al., 2002; Massman, 2004; Altimir et al., 2004, 2006).

Table 2
Diffusivities in air (Benner et al., 1988; Grünhage and Haenel, 1997; Massman, 1998) and related values

Species 'A'	Grünhage and Haenel (1997)	Massman (1998)	Benner et al. (1988)	used in PLATIN
	D_A [10^{-6} $m^2 \cdot s^{-1}$] [a)] reference air temperature T_0 = 273.15 K; reference air pressure p_0 = 1013.25 hPa			
H_2O (water vapour)	21.9 ± 0.4	21.78		21.9
CO_2 (carbon dioxide)	13.7 ± 0.4	13.81		13.7
SO_2 (sulphur dioxide)	10.7	10.89		10.7
O_3 (ozone)	14.5	14.44		14.5
NH_3 (ammonia)	20.3 ± 0.7	19.78		20.0
NO (nitric oxide)	18.0	18.02		18.0
NO_2 (nitrogen dioxide)	14.2	13.61		13.9
HNO_3 (nitric acid)			9.1	9.1
HNO_2 (nitrous acid)			8.7	8.7
[a)] $D_A(T, p) = D_A \cdot [(T \cdot T_0^{-1})^{1.81}] \cdot (p_0 \cdot p^{-1})$				
	Sc_A (= $\nu \cdot D_A^{-1}$)	$(Sc_A \cdot Pr^{-1})^{2/3}$		$D_{H2O} \cdot D_A^{-1}$
H_2O (water vapour)	0.61	0.90		1
CO_2 (carbon dioxide)	0.97	1.23		1.60
SO_2 (sulphur dioxide)	1.24	1.45		2.05
O_3 (ozone)	0.92	1.19		1.51
NH_3 (ammonia)	0.67	0.96		1.10
NO (nitric oxide)	0.74	1.03		1.22
NO_2 (nitrogen dioxide)	0.96	1.22		1.58
HNO_3 (nitric acid)	1.46	1.62		2.41
HNO_2 (nitrous acid)	1.53	1.67		2.52
kinematic viscosity of dry air ν = $13.3 \cdot 10^{-6}$ $m^2 \cdot s^{-1}$ Prandtl number Pr = 0.71				

In general, three qualitative "surface wetness states" can be distinguished: wet, partially wet, dry. Based on plausible reasoning or on data from the literature, PLATIN assumes external plant surfaces to be wet if at least one of the following conditions applies:

- precipitation *Precip* > 0 mm
- relative interception reservoir charge $INT_n \cdot INT_{max}^{-1} \geq 0.2$
- relative humidity *rH* > 90 % (according to Erisman et al., 1993)

The Unified EMEP model (Simpson et al., 2003) does not explicitly use a wet state, but extends the state of partial wetness gradually up to 100 % *rH.* However, this does not meet e.g. observations of plant surfaces still wet after precipitation events while air humidity has already fallen below 100 %. This discrepancy resolves when taking into account that the Unified EMEP model is to calculate surface resistances on a horizontal scale much greater than that of local SVAT models like PLATIN. On such

great horizontal scales completely wet surfaces are not likely to exist. Nevertheless, the concept of a gradual approach from dry to wet and vice versa has often been reported in literature also for local considerations, and it will explicitly be introduced in PLATIN where it has not yet been defined before (see below in context with eqs. (46) to (49)). When not defined otherwise, PLATIN also adopts the upper humidity threshold for the surface state "dry" as given by EMEP (Simpson et al., 2003): *rH* = 85 % for forests and *rH* = 75 % for other canopies. These provisional thresholds are based upon results of wetness measurements presented by Klemm et al. (2002).

Table 3
Effective Henry's Law values H_A* for water with nearby neutral pH and chemical reactivity factors $f_{0,A}$ (Wesely, 1989) as well as bulk mesophyll resistance $R_{c,mes,A}$ and leaf cuticular resistance $R_{leaf,cut,A}$

	H_A* [M atm^{-1}]	$f_{0,A}$	$R_{c,mes,A}$ [s·m^{-1}]	$R_{leaf,cut,A}$ [s·m^{-1}]
H_2O (water vapour)	---	---	---	$9\cdot10^4$
CO_2 (carbon dioxide)	4.4	0	682	$1\cdot10^7$
SO_2 (sulphur dioxide)	$1\cdot10^5$	0	0.03	$2\cdot10^6$
O_3 (ozone)	0.01	1	0.01	$3\cdot10^7$
NH_3 (ammonia)	$2\cdot10^4$	0	0.15	$3\cdot10^6$
NO (nitric oxide)	$2\cdot10^{-3}$	0	$1.5\cdot10^{-6}$	$8\cdot10^7$
NO_2 (nitrogen dioxide)	0.01	0.1	0.10	$2\cdot10^6$
HNO_3 (nitric acid)	$1\cdot10^{14}$	0	$3\cdot10^{-11}$	$1\cdot10^5$
HNO_2 (nitrous acid)	$1\cdot10^5$	0.1	0.02	$2\cdot10^6$ *)

*) HNO_2 is treated as NO_2

The external plant surfaces resistance for ammonia $R_{c,ext,NH3}$ depends on relative air humidity *rH*, surface temperature, and the molar "acidity ratio" of SO_2 and NH_3 concentration. An approximation of $R_{c,ext,NH3}$ taking into account all these three factors can be found in Simpson et al. (2003). While surface temperature could be provided by PLATIN, SO_2 concentrations may not always be available. Thus PLATIN keeps to the less data demanding approach given by Sutton and Fowler (1993) which is based on *rH* only:

$$R_{c,ext,NH3} = 2 \cdot \exp\left(\frac{100 - rH}{12}\right) \quad (40)$$

Evidently, there is no need to distinguish between different surface wetness states.

The external plant surfaces resistance for sulphur dioxide $R_{c,ext,SO2}$ depends on rain events, relative humidity *rH* and air temperature t_a and is parameterized according to Erisman et al. (1994):

if external plant surfaces are wet: $R_{c,ext,SO2} = 1 \text{ s}\cdot\text{m}^{-1}$ (41)

if $t_a > -1$ °C and *rH* > 81.3 %: $R_{c,ext,SO2} = 0.58\cdot10^{12}\cdot\exp(-0.278\cdot rH) \text{ s}\cdot\text{m}^{-1}$ (42)

if $t_a > -1$ °C and *rH* ≤ 81.3 %: $R_{c,ext,SO2} = 25000\cdot\exp(-0.0693\cdot rH) \text{ s}\cdot\text{m}^{-1}$ (43)

if -5 °C < $t_a \le -1$ °C: $R_{c,ext,SO2} = 200 \text{ s}\cdot\text{m}^{-1}$ (44)

if $t_a \le -5$ °C: $R_{c,ext,SO2} = 500 \text{ s}\cdot\text{m}^{-1}$ (45)

Similar to $R_{c,\,ext,\,NH3}$, there is no need to distinguish between different surface wetness states.

Note: This parameterization does not take into account the control of $R_{c,\,ext,\,SO2}$ by the NH_3 levels in the air (cf. Simpson et al., 2003). Here again, PLATIN makes use of the less data demanding approach.

Often, for ozone as well as for all other trace gas species, constant external plant surface resistances are defined separately for wet and dry surface conditions. For dry surface conditions $R_{c,\,ext,\,dry,\,O3}$ is estimated by

$$R_{c,\,ext,\,dry,\,O3} = 2000 \cdot \left(1 - e^{-k_{b,\,max,\,summer\,solstice}}\right) \; s \cdot m^{-1} \tag{46}$$

For $k_{b,max,summer\,solstice}$ see Chapter 2.3, context of eq. (20). The leaf-level resistance $R_{leaf,\,ext,\,dry,\,O3}$ of 2000 $s \cdot m^{-1}$ is adopted from Gao et al. (1993). For other gases than NH_3, SO_2 and O_3 $R_{c,\,ext,\,dry,\,A}$ is computed according to Wesely (1989):

$$R_{c,\,ext,\,dry,\,A} = \frac{R_{c,\,ext,\,dry,\,O3}}{(10^{-5} \cdot H_A^{*}) + f_{0,\,A}} \tag{47}$$

As described in the PLATIN version published by Grünhage and Haenel (1997), the "wet" resistance for O_3 is calculated by

$$R_{c,\,ext,\,wet,\,O3} = \left(\frac{1}{1000} + \frac{1}{3 \cdot R_{c,\,ext,\,dry,\,O3}}\right)^{-1} \tag{48}$$

while for all gases other than NH_3, SO_2 and O_3 the resistance is estimated from:

$$R_{c,\,ext,\,wet,\,A} = \left(\frac{1}{3 \cdot R_{c,\,ext,\,dry,\,A}} + \frac{H_A^{*}}{10^{7}} + \frac{f_{0,\,A}}{3 \cdot R_{c,\,ext,\,dry,\,O3}}\right)^{-1} \tag{49}$$

While not reported explicitly in the literature, a gradual shifting between "dry" and "wet" resistances as given by eqs. (46) to (49) seems plausible and is incorporated in PLATIN according to the scheme described in Simpson et al. (2003). It is based on the definition of a so-called humidity factor F_{rH}

$$F_{rH} = \begin{cases} 0 & \text{for} \quad rH \le rH_{dry} \\ \dfrac{rH - rH_{dry}}{rH_{wet} - rH_{dry}} & \text{for} \quad rH_{dry} < rH \le rH_{wet} \\ 1 & \text{for} \quad rH_{wet} < rH \end{cases} \tag{50}$$

where, as mentioned above, rH_{wet} = 90 % while rH_{dry} = 85 % for forests and rH_{dry} = 75 % for other canopies. With F_{rH} the resulting external-surface resistance for species A (including O_3, but not NH_3 and SO_2) reads:

$$\frac{1}{R_{c,\,ext,\,A}} = F_{rH} \cdot \frac{1}{R_{c,\,ext,\,wet,\,A}} + (1 - F_{rH}) \cdot \frac{1}{R_{c,\,ext,\,dry,\,A}} \tag{51}$$

Note: For O_3, relations (46) and (48) represent only a first estimate. As illustrated by Fowler et al. (2001), the external plant surface resistance for O_3 decreases as global radiation S_t and therefore surface temperature increase:

$$R_{c,\,non\text{-}stomatal,\,dry,\,O3} = -129.9 \cdot \ln(S_t) + 989.1 \tag{52}$$

This reduction of $R_{c,\ non\text{-}stomatal,\ dry,\ O3}$, observed over moorland vegetation at solar radiation fluxes above 100 $W \cdot m^{-2}$ in southern Scotland, is regarded as evidence of thermal decomposition of O_3 at the leaf surfaces. In the context of O_3 exchange modelling, future research has to focus on the derivation of parameterizations of the non-stomatal O_3 resistance.

3.3 Soil resistance for trace gases

The deposition rates of trace gases on soil surfaces depend on their water solubility as well as on their reactivity. The soil surface resistance for any gaseous species $R_{soil,\ dry,\ A}$ is computed as

$$R_{\mathrm{soil,\,dry,\,A}} = \left(\frac{H_{\mathrm{A}}^{*}}{10^{5} \cdot R_{\mathrm{soil,\,dry,\,SO2}}} + \frac{f_{0,\,\mathrm{A}}}{R_{\mathrm{soil,\,dry,\,O3}}} \right)^{-1} \tag{53}$$

according to Wesely (1989), where $R_{soil,\ dry,\ SO2}$ is set to 500 $s \cdot m^{-1}$ and $R_{soil,\ dry,\ O3}$ at 200 $s \cdot m^{-1}$ (Gao et al., 1993). Soil surface resistance under wet conditions (i.e. when $R_{soil} = R_{soil,\ min}$) depends on whether ozone or another species is concerned. It is calculated the same way as for external plant surfaces, i.e. according to eqs. (48) and (49). For the resistance of snow covered surfaces the approximations described in Erisman et al. (1994) can be used. In agreement with the observations for $R_{soil,\ O3}$ summarized in Figure 3 in Massman (2004), the parameterization given above results in a soil resistance which is higher for wet conditions than for dry conditions.

3.4 Special treatment of NH_3

The estimation of NH_3 fluxes over vegetated land deserves special attention, because, in contrast to e.g. O_3 and SO_2, NH_3 fluxes over vegetated land are bi-directional, i.e. the net flux can combine simultaneously occurring deposition and emission. In addition, different parts of the plants and also the soil may serve as sources or sinks. Nemitz et al. (2000) found the siliques of oilseed rape to emit NH_3 while the leaves definitely act as a sink and the decomposing leaf litter at the ground again was identified to be a NH_3 source.

Another issue is the effect of fertilization. With mineral fertilization, arable fields are likely to be net sinks for reactive nitrogen, while application of slurry turns them into net sources (U. Dämmgen, von Thunen Institute, Braunschweig, personal communication). NH_3 may be released directly from the fertilizer due to thermal decomposition: $NH_4^+ + HCO_3^- \rightarrow NH_3 + H_2O + CO_2$. Urea decomposes at the surface partly due to enzymatic clearage. N from fertilizer, which passes through root and stem into the leaves, increases the concentration of ammonium in the apoplast (see below), leading to NH_3 emission from the leaves.

Another point is that emission and deposition rates depend to some degree on the results of preceding physical and chemical processes.

These issues have to be considered by modelling of NH_3 fluxes between the atmosphere and vegetated surfaces. In order to account for a vertical distribution of sources and sinks within the canopy and on the ground, multi-layer resistance models are likely to be the appropriate choice as pointed out by Nemitz et al. (2000). Dynamic effects can be included, in principle, by introducing capacitors into the model's resistance network as was done by Sutton et al. (1998). More difficult is the treatment of slurry and mineral fertilizer application which, at the time being, no mechanistic modelling approach is available for. Therefore it is recommended (U. Dämmgen, von Thunen Institute, Braunschweig, personal communication) for the first seven days after slurry or mineral fertilizer application not to use a SVAT model like PLATIN but to estimate the cumulative NH_3 emissions from emission factors according to EMEP/CORINAIR (2007).

At the present state of development, PLATIN is a steady-state single-layer model which cannot cope with the multi-layer and dynamic requirements formulated above. However, PLATIN could be extended in future by introducing new branches into the resistance network depicted in Figure 6 to account for additional NH_3 sinks or sources like the oilseed rape siliques or a litter layer beneath the canopy. Also, the introduction of capacitors (the charge or discharge of which requires knowledge about the respective conditions during past times) would not impose any problems. This can be seen from the fact that PLATIN can already be driven with a rain interception reservoir, cf. Chapter 2.3, which in effect is nothing else than a capacitor (with respect to evaporation fluxes). As soon as a mathematical description is available for NH_3 flux resulting from fertilizing, it can be integrated in the PLATIN resistance network if the node can be identified where this flux is entering the network.

Nevertheless, already the present state of PLATIN represents an important tool to approach an overall nitrogen balance of vegetated surfaces. The base to estimate NH_3 atmosphere-canopy exchange is eq. (32) which requires knowledge of NH_3 concentration $\rho_{NH3}(d+z_{0c})$ at the conceptual position $z = d + z_{0c}$ of the *big leaf* surface for gaseous fluxes. The concentration at this level has been called canopy "compensation point" by Sutton and Fowler (1993), but is rather to be considered the "net potential for NH_3 emission from the canopy" (cf. Sutton et al., 1998). According to Figure 5 the following equation for $\rho_{NH3}(d+z_{0c})$ results:

$$\rho_{NH3}(d+z_{0c}) = \frac{\dfrac{\rho_{NH3}(z_{ref,NH3})}{R_{ah}(d+z_{0m}, z_{ref,NH3})+R_{b,NH3}} + (1-\beta^*)\cdot\left(\dfrac{\rho_{NH3,stom}}{R_{c,stom,NH3}}+\dfrac{\rho_{NH3,int2}}{R_{c,cut,NH3}}\right)+(1-\beta)\cdot\dfrac{\rho_{NH3,ext}}{R_{c,ext,NH3}}+\beta\cdot\dfrac{\rho_{NH3,soil}}{R_{c,soil,NH3}}}{\dfrac{1}{R_{ah}(d+z_{0m}, z_{ref,NH3})+R_{b,NH3}}+\dfrac{(1-\beta^*)}{R_{c,stom,NH3}}+\dfrac{(1-\beta^*)}{R_{c,cut,NH3}}+\dfrac{(1-\beta)}{R_{c,ext,NH3}}+\dfrac{\beta}{R_{soil,NH3}}} \quad (54)$$

with $\rho_{NH3,\,stom}$ ammonia concentration in the sub-stomatal cavities [µg·m^{-3}]

Because exchange of gaseous species through the plant's cuticle is of minor importance (cf. Chapter 2.3, Table 3) in the present PLATIN version, penetration of NH_3 through the plant's cuticle is neglected by completely dropping the respective flow branch from the resistance scheme. Additionally, emissions from external plant surfaces and from the soil beneath the canopy are disregarded by assigning zero value to $\rho_{A,\,ext}$ and $\rho_{A,\,soil}$. With these simplifications eq. (54) modifies to[1]:

$$\rho_{NH3}(d+z_{0c}) = \frac{\dfrac{\rho_{NH3}(z_{ref,\,NH3})}{R_{ah}(d+z_{0m}, z_{ref,\,NH3})+R_{b,\,NH3}} + (1-\beta^*)\cdot\dfrac{\rho_{NH3,\,stom}}{R_{c,\,stom,\,NH3}}}{\dfrac{1}{R_{ah}(d+z_{0m}, z_{ref,\,NH3})+R_{b,\,NH3}}+\dfrac{(1-\beta^*)}{R_{c,\,stom,\,NH3}}+\dfrac{(1-\beta)}{R_{c,\,ext,\,NH3}}+\dfrac{\beta}{R_{soil,NH3}}} \quad (55)$$

Note: $R_{c,\,ext,\,NH3}$ and $R_{soil,\,NH3}$ are parameterized as described in Chapters 3.2 and 3.3.

In order to apply eq. (55) it is necessary to calculate $\rho_{NH3,\,stom}$. According to Sutton et al. (1994) the NH_3 gas phase concentration in the sub-stomatal cavities of the canopy $\rho_{NH3,\,stom}$ is related to the plant's nitrogen status and pH in the apoplast by the Henry and dissociation equilibria for NH_3 and NH_4^+ (cf. Flechard and Fowler, 1998):

[1] Schaaf and Meesenburg (2005) who also used PLATIN present an equation which is quite similar to (55) but physically inadequate, because it neglects the important influence of canopy architecture represented by the factors $(1-\beta^*)$, $(1-\beta)$, and β. Schaaf and Meesenburg (2005) name $\rho_{NH3}(d+z_{0c})$ the canopy compensation point, which may have been the reason for, or the outcome of, their Figures 5.1 and 5.2 which are contradictory regarding just the position of this compensation point within the resistance network. (Their Figure 5.2 identifies $\rho_{A,\,stom}$ with $\rho_{A,\,int1}$ in our Figure 5). In addition, the equation for $R_{c,A}$ given in Schaaf and Meesenburg (2005, chapter 5.1.5) does not agree with their Figure 5.2 which does not display the unique potential at the model surface implicitly invoked by the respective equation. Schaaf and Meesenburg (2005) write they used an extended PLATIN version. It must be noted that all model features they describe had previously been introduced in PLATIN or related model versions by the authors of PLATIN, Grünhage and Haenel. Nevertheless, the latter are not responsible for possible errors in description and application of PLATIN by Schaaf and Meesenburg (2005).

$$\rho_{\mathrm{NH3,stom}} = a_{\mathrm{NH3}} \cdot \frac{10^{\,15.43 - \frac{4507.08}{T_s}}}{T_s} \cdot \Gamma \tag{56}$$

where Γ vegetation type-specific ratio of ammonium to protons in the apoplast [mol·mol^{-1}]
T_s surface absolute temperature of the canopy [K]
a_{NH3} dimension adaptation factor (= 1 µg·m^{-3}·K)

The vegetation type-specific ratio of ammonium to protons in the apoplast Γ represents a modelling concept rather than a measurable entity. However, Nemitz et al. (2001) determined Γ experimentally. As described by Flechard et al. (1999), Γ values published for growing arable crops are mostly in the rage of 250 – 4000 mol·mol^{-1}. Estimates for moorland vegetation are substantially lower: 80 – 3000 mol·mol^{-1}. The authors describe a value of 180 mol·mol^{-1} for a moorland in southern Scotland. Sorteberg and Hov (1996) quote $\Gamma \approx$ 950 mol·mol^{-1} for crops and grassland and $\Gamma \approx$ 320 mol·mol^{-1} for other vegetated surfaces. For a semi-natural ungrazed short grassland Γ approximates 1000 mol·mol^{-1} (Spindler et al., 2001). Nemitz et al. (2001) indicate a value of 2000 mol·mol^{-1} for oilseed rape canopy. For the extremely eutrophied Speulder forest in the Netherlands a value of 8500 mol·mol^{-1} is adequate (according to private communication of J.W. Erisman, ECN Petten, and E. Nemitz, CEH Edinburgh, as quoted in Schaaf and Meesenburg, 2005). Accordingly the following default values of Γ are recommended for use in PLATIN:

- extremely eutrophicated ecosystems: $\Gamma \approx$ 8500 mol·mol^{-1}
- intensively managed grassland and arable crops: $\Gamma \approx$ 2000 mol·mol^{-1}
- extensively managed grassland and forest: $\Gamma \approx$ 1000 mol·mol^{-1}
- N-limited ecosystems: $\Gamma \approx$ 300 mol·mol^{-1}

3.5 Partitioning of total atmosphere-canopy flux

In case of deposition, the resistance network (Figures 5, 6) allows to partition the total atmosphere-canopy flux $F_{c,\,total}(A)$ into (1) fluxes absorbed by the plant through the stomata and the cuticle $F_{c,\,stom\,\&\,cut} = F_{c,\,stom}(A) + F_{c,\,cut}(A)$, and (2) fluxes down to external plant surfaces $F_{c,\,ext}(A)$ and the soil beneath the canopy $F_{soil}(A)$. Studies show that penetration of gases through the cuticle $F_{c,\,cut}(A)$ can be neglected in comparison to stomatal uptake $F_{c,\,stom}(A)$ (cf. Chapter 2.3).

Combining $F_{c,\,ext}$ and F_{soil} to $F_{c,\,non\text{-}stomatal}$ and neglecting cuticular fluxes (i.e. approximating $F_{c,\,stom\,\&\,cut} \approx F_{c,\,stom}$) one obtains:

$$F_{c,\,total}(A) = F_{c,\,stom\,\&\,cut}(A) + F_{c,\,ext}(A) + F_{soil}(A) \cong F_{c,\,stom}(A) + F_{c,\,non\text{-}stomatal}(A) \tag{57}$$

The integral of $F_{c,\,stom\,\&\,cut} \cong F_{c,\,stomatal}$ over time t is the ***p**ollutant **a**bsorbed **d**ose*, $PAD(A)$ [µg·m^{-2}] (Fowler and Cape, 1982):

$$PAD(A) = \int_{t_1}^{t_2} \left| F_{c,\,stom\,\&\,cut}(A) \right| \cdot \mathrm{d}t \cong \int_{t_1}^{t_2} \left| F_{c,\,stom}(A) \right| \cdot \mathrm{d}t \tag{58}$$

For O_3 the integral of $F_{c,\,stom\,\&\,cut} \cong F_{c,\,stom}$ over time t is called *accumulated stomatal flux of ozone, AF_{st}* (UNECE, 2004, 2007).

Applying concentration- or flux-based critical levels of O_3 (UNECE, 2004, 2007) or the maximum-permissible O_3 concentration concept (Grünhage et al., 2001) requires O_3 concentration measured at reference height above the canopy $\rho_{O3}(z_{ref})$ to be transformed to concentration at the upper surface of the laminar boundary layer of the uppermost sunlit leaves. According to the single-leaf concept, PLATIN

disposes only of one single canopy-representative laminar boundary layer the surface of which is located at $d + z_{0m}$. The concentration at this height is calculated from:

$$\rho_{O3}(d + z_{0m}) = \rho_{O3}(z_{ref,O3}) + \left[F_{c,total}(O_3) \cdot R_{ah}(d + z_{0m}, z_{ref,O3})\right] \quad (59)$$

This is contrasted by the UNECE (2004, 2007) approach that the concentration at the upper surface of the laminar boundary layer of the sunlit upper canopy leaves be represented by the O_3 concentration at the top of the canopy $z = h$. Within the M-O framework, this concentration is given by:

$$\rho_{O3}(h) = \rho_{O3}(z_{ref,O3}) + \left[F_{c,total}(O_3) \cdot R_{ah}(h, z_{ref,O3})\right] \quad (60)$$

Besides the fact that the effective upper surface of all the laminar boundary layers existing within the canopy is probably represented better by $d + z_{0m}$ than by h, application of eq. (60) is prone to proper definition of h. Does h e.g. represent the maximum or the average height of canopy elements above ground? Due to numerous irregularities in canopy architecture as well as wind-driven bending of the upper parts of a canopy it may be difficult to find a robust estimate of canopy height. Therefore it seems worthwhile to demonstrate the differences in stomatal uptake calculated according to eq. (61; see below) with O_3 concentrations from eq. (60) for varying h. This is done exemplarily using the daylight-hour data sets from June 2004 at Linden. Except for h, all data needed to evaluate eq. (60) were determined by precedent PLATIN runs using the aforementioned data sets.

In order to obtain a reasonable measure for h, we inverted the usual relations between displacement height and roughness length for momentum on one hand and the canopy height on the other hand, which allows to calculate h from given displacement height d and roughness length z_{0m} by $h = (d + z_{0m}) \cdot 0.8^{-1}$ according to Brutsaert (1984). In order to reveal the influence of the differing heights in eqs. (59) and (60), the stomatal uptake as calculated with O_3 concentrations from eq. (60) has then been normalised by the one obtained with O_3 concentrations from eq. (59). As stomatal uptake is proportional to O_3 concentration, this ratio of stomatal uptake turns out to be identical to the ratio of the respective O_3 concentrations. This concentration ratio is displayed in Figure 7.

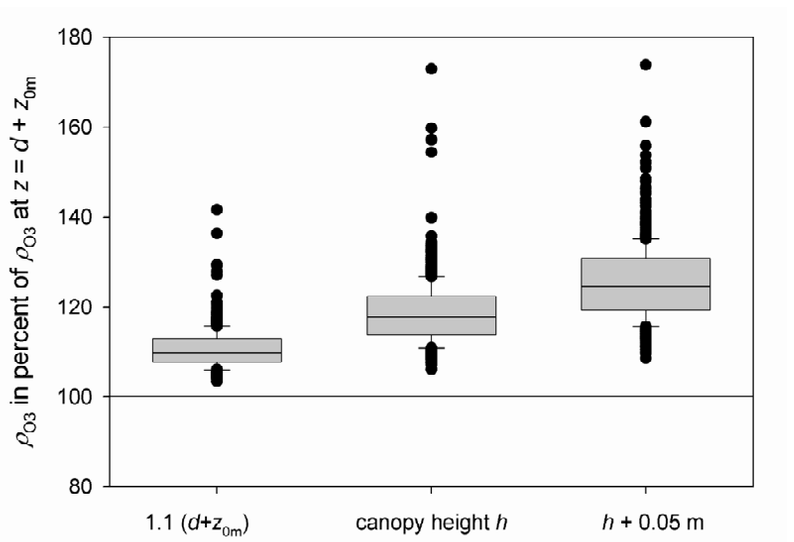

Fig. 7
Box-and-whisker plot of O_3 concentrations at $z = (d + z_{0m}) \cdot 1.1$, $z = h$ and $z = h + 0.05$ m in percent of O_3 concentrations at $z = d + z_{0m}$ during daylight hours in June 2004

Estimating stomatal uptake from h rather than $d + z_{0m}$ generally leads to overestimation of stomatal uptake which may not be negligible. This overestimation clearly depends on how much h differs from

$d + z_{0m}$, which is demonstrated by varying h by plus 5 and $d + z_{0m}$ by a factor of 1.1. (Diminishing h, on the other hand, would mean to approach $d + z_{0m}$ and therefore reduce overestimation. However, h should never reach $d + z_{0m}$, because then h would not be representative for canopy height any longer.)

Even if a stomatal uptake approach as given by UNECE (2004, 2007) could be combined with guidance how to properly estimate canopy height h, the problem still remains that h is not the best measure of the effective height of the canopy's laminar boundary layer. Therefore we recommend to calculate stomatal uptake by a model like PLATIN which is calibrated by a number of water and energy balance quantities and which, therefore, is much less sensitive to the correct estimation of canopy height.

Because stomatal uptake of O_3, $F_{c,\,stom}(O_3)$ is the toxicologically effective share of $F_{c,\,total}(O_3)$, flux-effect relationships should be based on that component which is given by:

$$F_{c,\,stom}(O_3) = -\frac{\rho_{O3}(z_{ref,\,O3})}{R_{ah} + R_{b,\,O3} + \frac{R_{c,\,stom+mes,\,O3}}{1-\beta^*} + \left([R_{ah} + R_{b,\,O3}] \cdot \frac{R_{c,\,stom+mes,\,O3}}{1-\beta^*} \cdot \left[\frac{1-\beta^*}{R_{c,\,cut,\,O3}} + \frac{1-\beta}{R_{c,\,ext,\,O3}} + \frac{\beta}{R_{soil,\,O3}} \right] \right)} \quad (61)$$

with $$R_{ah} = R_{ah}(d + z_{0m}, z_{ref,\,O3})$$

$$R_{c,\,stom+mes,\,O3} = R_{c,\,stom,\,O3} + R_{c,\,mes,\,O3} \quad (62)$$

The flux of O_3 through the cuticle $F_{c,\,cut}(O_3)$, which normally can be neglected, can be derived from eq. (63),

$$F_{c,\,cut}(O_3) = -\frac{\rho_{O3}(z_{ref,\,O3})}{R_{ah} + R_{b,\,O3} + \frac{R_{c,\,cut,\,O3}}{1-\beta^*} + \left([R_{ah} + R_{b,\,O3}] \cdot \frac{R_{c,\,cut,\,O3}}{1-\beta^*} \cdot \left[\frac{1-\beta^*}{R_{c,\,stom+mes,\,O3}} + \frac{1-\beta}{R_{c,\,ext,\,O3}} + \frac{\beta}{R_{soil,\,O3}} \right] \right)} \quad (63)$$

the deposition of O_3 on external plant surfaces $F_{c,\,ext}(O_3)$ and the soil beneath the canopy $F_{soil}(O_3)$, which are combined to non-stomatal deposition $F_{c,\,non\text{-}stomatal}(O_3)$, from eqs. (64) and (65):

$$F_{c,\,ext}(O_3) = -\frac{\rho_{O3}(z_{ref,\,O3})}{R_{ah} + R_{b,\,O3} + \frac{R_{c,\,ext,\,O3}}{1-\beta} + \left([R_{ah} + R_{b,\,O3}] \cdot \frac{R_{c,\,ext,\,O3}}{1-\beta} \cdot \left[\frac{1-\beta^*}{R_{c,\,stom+mes,\,O3}} + \frac{1-\beta^*}{R_{c,\,cut,\,O3}} + \frac{\beta}{R_{soil,\,O3}} \right] \right)} \quad (64)$$

$$F_{soil}(O_3) = -\frac{\rho_{O3}(z_{ref,\,O3})}{R_{ah} + R_{b,\,O3} + \frac{R_{soil,\,O3}}{\beta} + \left([R_{ah} + R_{b,\,O3}] \cdot \frac{R_{soil,\,O3}}{\beta} \cdot \left[\frac{1-\beta^*}{R_{c,\,stom+mes,\,O3}} + \frac{1-\beta^*}{R_{c,\,cut,\,O3}} + \frac{1-\beta}{R_{c,\,ext,\,O3}} \right] \right)} \quad (65)$$

$F_{c,\,stom}(O_3)$ can further be subdivided into the flux entering the compartment of sunlit leaves, $F_{c,\,stom,\,sunlit}(O_3)$, and the flux taken up by the shaded-leaves compartment, $F_{c,\,stom,\,shaded}(O_3)$:

$$F_{c,\,stom}(O_3) = F_{c,\,stom,\,sunlit}(O_3) + F_{c,\,stom,\,shaded}(O_3) \quad (66)$$

The estimation of $F_{c,\,stom,\,sunlit}(O_3)$ and $F_{c,\,stom,\,shaded}(O_3)$ is controlled by the O_3 bulk resistances assigned to the two compartments and their relation to the bulk canopy resistance $R^*_{c,\,stom,\,O3}$. The latter is proportional to the H_2O bulk canopy resistance $R^*_{c,\,stom,\,O3}$, cf. eq. (37):

$$R^*_{c,\,stom,\,O3} = R^*_{c,\,stom,\,H2O} \cdot \frac{D_{H2O}}{D_{O3}} \tag{67}$$

$R^*_{c,\,stom,\,H2O}$ is obtained from

$$R^*_{c,\,stomatal,\,H2O} = \frac{R_{c,\,stom,\,H2O}}{1-\beta^*} \tag{68}$$

where $R_{c,\,stom,\,H2O}$ is given by eqs. (21) or (22) as the bulk resistance one obtains under neglection of the vertical distribution of within-canopy radiation extinction. In eq. (68), this extinction is accounted for by the correction term $1 - \beta^*$ (eq. (14)).

Similarly the resistances for the two compartments "sunlit leaves" and "shaded leaves", are defined by

$$R^*_{c,\,stom,\,sunlit,\,O3} = \frac{R_{c,\,stom,\,H2O}}{1-\beta^*_{sunlit}} \cdot \frac{D_{H2O}}{D_{O3}} \tag{69}$$

and

$$R^*_{c,\,stom,\,shaded,\,O3} = \frac{R_{c,\,stom,\,H2O}}{1-\beta^*_{shaded}} \cdot \frac{D_{H2O}}{D_{O3}} \tag{70}$$

where $1 - \beta^*_x$ (with x = sunlit, shaded) is given by (cf. Eq. (14)):

$$1-\beta^*_x = \frac{I_{c,x}}{PAR} \tag{71}$$

As the O_3 concentration within the plant can be assumed to be zero, the relations of fluxes are simply given by the inverse ratio of the resistances involved which turns out to be a function of β^*_x and β^*_{sunlit} or β^*_{shaded}, respectively:

$$\frac{F_{c,\,stom,\,sunlit}(O_3)}{F_{c,\,stom}(O_3)} = \frac{R^*_{c,\,stom,\,O3}}{R^*_{c,\,stom,\,sunlit,\,O3}} = \frac{1-\beta^*_{sunlit}}{1-\beta^*} \tag{72}$$

$$\frac{F_{c,\,stom,\,shaded}(O_3)}{F_{c,\,stom}(O_3)} = \frac{R^*_{c,\,stom,\,O3}}{R^*_{c,\,stom,\,shaded,\,O3}} = \frac{1-\beta^*_{shaded}}{1-\beta^*} \tag{73}$$

Dividing $F_{c,\,stom,\,sunlit}(O_3)$ by LAI_{sunlit} (see Appendix B) yields the flux of O_3 through the stomatal pores per unit projected leaf area (*PLA*)

$$F_{leaf,\,stom,\,sunlit}(O_3) = \frac{F_{c,\,stom,\,sunlit}(O_3)}{LAI_{sunlit}} \tag{74}$$

as required by the UNECE Mapping Manual 2004 (UNECE, 2004, 2007). The re-calculation of stomatal conductance of sunlit leaves $g_{leaf,\,stom,\,sunlit,\,O3}$ from bulk stomatal resistance $R_{c,\,stom,\,O3}$ according to eq. (75)

$$g_{leaf,\,stom,\,sunlit,\,O3} = \frac{1-\beta^*_{sunlit}}{R_{c,\,stom,\,O3}} \cdot \frac{1}{LAI_{sunlit}} \tag{75}$$

provides a direct interface between canopy scale and leaf scale measurements as well as between micromet and impact research. Besides verification of the parameterization of stomatal conductance via measurements of canopy level water vapour exchange, *big leaf* stomatal conductance parameterization and water vapour fluxes can now be compared directly with porometer measurements on the leaf level. Upscaling algorithms from leaf to canopy level can be verified or adjusted.

4 Biosphere/atmosphere exchange of fine-particle constituents

The transport of fine-particle constituents to the surface is usually described as proportional to a dry deposition velocity $v_D(z_{ref})$ [m·s^{-1}]. According to Erisman et al. (1994) deposition velocities for fine-particle constituents can be obtained from parameterizations in terms of Monin-Obukhov length L and friction velocity u_* [m·s^{-1}]. For low vegetation v_D is parameterized according to Wesely et al. (1985)

$$v_D = \frac{u_*}{500}, \quad L \geq 0\,\mathrm{m} \tag{76}$$

$$v_D = \frac{u_*}{500} \cdot \left[1 + \left(\frac{300}{-L}\right)^{2/3}\right], \quad L < 0\,\mathrm{m} \tag{77}$$

and for forests according to Erisman et al. (1997):

$$v_D = \frac{1}{\frac{1}{v_{Ds}} + R_{ah}(50)} \tag{78}$$

where v_{Ds} is estimated from:

$$v_{Ds} = \frac{u_*}{u_h} \cdot E(u_*) \tag{79}$$

with $R_{ah}(50)$ turbulent atmospheric resistance between canopy height h and z_{ref} = 50 m [s·m^{-1}]
u_h horizontal wind velocity at canopy height h [m·s^{-1}]
$E(u_*)$ u_*-dependent value for fine-particle constituents [m·s^{-1}] as summarized in Table 4

Table 4
Parameterizations of $E(u_*)$ values for different components and conditions (Erisman et al., 1997)

Species	Wet surface Relative humidity		Dry surface Relative humidity	
	$rH \leq 80$ %	$rH > 80$ %	$rH \leq 80$ %	$rH > 80$ %
	$E(u_*) = a \cdot u_*^b \cdot c$			
NH_4^+	$a = 0.066$	$a = 0.066$	$a = 0.05$	$a = 0.05$
	$b = 0.41$	$b = 0.41$	$b = 0.23$	$b = 0.23$
	$c = 1$	$c = \left[1 + 0.37 \cdot \exp\left(\frac{rH - 80}{20}\right)\right]$	$c = 1$	$c = \left[1 + 0.18 \cdot \exp\left(\frac{rH - 80}{20}\right)\right]$

Table 4 (continued)
Parameterizations of $E(u_*)$ values for different components and conditions (Erisman et al., 1997)

Species	Wet surface Relative humidity $rH \leq 80$ %	Wet surface Relative humidity $rH > 80$ %	Dry surface Relative humidity $rH \leq 80$ %	Dry surface Relative humidity $rH > 80$ %
	$E(u_*) = a \cdot u_*^b \cdot c$			
SO_4^{2-}	$a = 0.08$ $b = 0.45$ $c = 1$	$a = 0.08$ $b = 0.45$ $c = \left[1 + 0.37 \cdot \exp\left(\frac{rH - 80}{20}\right)\right]$	$a = 0.05$ $b = 0.28$ $c = 1$	$a = 0.05$ $b = 0.28$ $c = \left[1 + 0.18 \cdot \exp\left(\frac{rH - 80}{20}\right)\right]$
NO_3^-	$a = 0.10$ $b = 0.43$ $c = 1$	$a = 0.10$ $b = 0.43$ $c = \left[1 + 0.37 \cdot \exp\left(\frac{rH - 80}{20}\right)\right]$	$a = 0.063$ $b = 0.25$ $c = 1$	$a = 0.063$ $b = 0.25$ $c = \left[1 + 0.18 \cdot \exp\left(\frac{rH - 80}{20}\right)\right]$

5 Input parameters needed

To run PLATIN, the following data are needed depending on what is to be calculated by the model. First of all, informations on site location and site characteristics must be defined:

- latitude φ_{geo} [degree]
- longitude λ_{geo} [degree]
- height above sea level [m]; required for site comparisons only
- vegetation type: short vegetation or forest (selector switch)
- soil moisture: site-specific field capacity SM_C [$m^3 \cdot m^{-3}$]
- soil moisture: site-specific wilting point SM_W [$m^3 \cdot m^{-3}$]

Additionally,

- vegetation type-specific minimum bulk stomatal resistance for water vapour $R_{c,\,stom,\,min,\,H2O}$ [$s \cdot m^{-1}$]; cf. Chapter 2.3
- vegetation type-specific attenuation coefficient at solar elevation of 90° $k_{b,90°}$; cf. Chapter 2.3

must be given. The vegetation type-specific values of $R_{c,\,stom,\,min,\,H2O}$ and $k_{b,90°}$ must be adjusted via comparisons of measured and modelled latent heat flux densities. Furthermore, the following informations are needed:

- number of days in the respective year (365 or 366)
- difference between Local Standard Time and Greenwich Mean Time [h]
- duration of measurement interval [h]

This data set provides the framework to operate the various modules and submodules constituting PLATIN, cf. Figure 8.

As mentioned earlier (see Chapter 1), the PLATIN core module solves the canopy energy balance including all the resistances also relevant for trace gas exchange. The solution of the energy balance requires auxiliary modules (radiation, soil moisture, etc.). Results are passed over to modules which calculate the exchange of trace gases (especially O_3) and fine-particle constituents. Finally, a special submodule estimates the stomatal O_3 uptake of the sunlit leaf fraction yielding the leaf area-related

stomatal conductance for sunlit parts of the plant stand and thus providing an interface to measurements of gas exchange on leaf level.

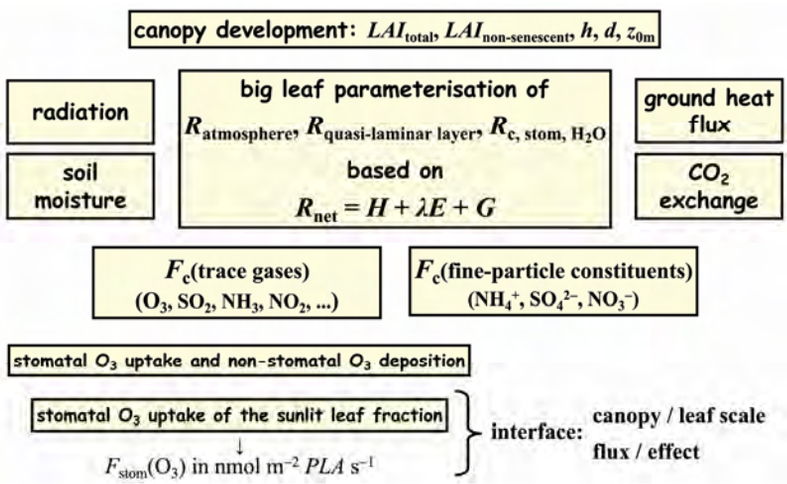

Fig. 8
Modular structure of the PLant-ATmosphere INteraction (PLATIN) model

To estimate the fluxes mentioned in Figure 8, the following data set is indispensably needed

on a half-hourly or hourly base:

- canopy net radiation balance R_{net} [W·m^{-2}]; cf. Appendix A if R_{net} cannot be measured
- global radiation [W·m^{-2}]
- photosynthetically active radiation *PAR* [µmol·m^{2}·s^{-1}]; if *PAR* is not available see Appendix L
- horizontal wind speed u [m·s^{-1}] at a reference height $z_{ref,\ u}$ above the canopy
- air temperature t_a [°C] at a reference height $z_{ref,\ T}$ above the canopy
- relative air humidity *rH* [%] at a reference height $z_{ref,\ rH} = z_{ref,\ T}$ above the canopy
- air pressure p [hPa] at a reference height $z_{ref,\ p}$ (default value: 1013.25 hPa) above the canopy
- precipitation *Precip* [mm $H_2O \equiv 10^{-3}$ m^3·m^{-2}]

and on (at least) a daily base:

- soil moisture *SM* in the uppermost soil layer (e.g. 0 - 16 cm) [m^3·m^{-3}]
- roughness length for momentum z_{0m} [m] or at least canopy height h [m]
- displacement height d [m] or at least canopy height h [m]
- leaf area index of non-senescent leaves $LAI_{non\text{-}senescent}$ [m^2·m^{-2}]
- total surface area of the vegetation *SAI* [m^2·m^{-2}]

The estimation of vertical flux densities of trace gas or fine-particle constituents requires additional data to be provided on half-hourly or hourly base:

- concentrations ρ_A of trace gases or fine-particle constituents [ppb or µg·m^{-3}] at a reference height $z_{ref,\ A}$ above the canopy
- vegetation type-specific ratio of ammonium to protons in the apoplast Γ [mol·mol^{-1}] if NH_3 exchange is to be modelled; for default values see Chapter 3.4

While all the data mentioned above serve to *drive* one or more modules of PLATIN, *calibration* of PLATIN requires the following flux densities to be known (i.e. to be measured) on half-hourly or hourly base:

- sensible heat H [W·m^{-2}]
- latent heat λE [W·m^{-2}]
- total flux of trace gas species A, e.g. ozone, F_c(A) [µg·m^{-2}·s^{-1}]

In some cases, missing data can be substituted by calculated values.

To calculate canopy net radiation balance R_{net}, PLATIN provides parameterizations to estimate global radiation from astronomically maximum possible solar irradiation (depending on cloud-cover degree), the amount of short wave radiation reflected by the big-leaf surface (making use of short-wave albedo α), the long wave downward radiation (depending on readily available data of air temperature and relative humidity at screen height 2 m), and finally the longwave radiation sent out from the big-leaf surface. Details are given in Appendix A. Note that in case of modelling R_{net} short-wave albedo α is required as additional input parameter.

In order to calculate soil moisture *SM*, PLATIN makes use of a refined and extended force-restore model of soil water content, see Appendix H. This submodel needs additional input parameters:

- depth of soil layer under consideration *SLD* [m]
- maximum possible vertical water flow from groundwater into rooted soil layer due to soil capillarity C_{cap} [kg·m^{-2}·s^{-1}]
- RLD_{90} which is the depth of the soil layer containing 90 % of total root mass [m]

Note that, if concentrations of CO_2 are given, PLATIN is able to account for the influence of photosynthesis on the canopy energy balance. In general, photosynthesis is equivalent to an additional sink in the energy balance up to approx. 20 W·m^{-2}. To estimate the CO_2 exchange between canopy and near-surface atmosphere additional data are needed:

- CO_2 concentration [ppm] at a reference height $z_{ref, CO2}$ on half-hourly or hourly base
- soil temperature t_{soil} on half-hourly or hourly base [°C]
- residual (irreducible) soil moisture [m^3·m^{-3}]
- soil moisture content at saturation [m^3·m^{-3}]
- nitrogen content of the aboveground sapwood biomass [g·m^{-2}]

Calibration of the CO_2 exchange submodule requires measured data of

- carbon dioxide exchange $F_c(CO_2)$ [µmol·m^{-2}·s^{-1}]

on a half-hourly or hourly base.

If PLATIN for Excel is to be applied to forest ecosystems, information on the state of the air above the forest canopy is required (wind speed, temperature, humidity, concentrations). If data are not available they have to be estimated from measurements above short vegetation near the forest (cf. Appendix K).

References

Allen RG, Pereira LS, Raes D, Smith M (2002) Crop evapotranspiration: guidelines for computing crop water requirements. FAO irrigation and drainage paper 56. Rome: Food and Agricultural Organization of the United Nations, 300 p, ISBN 92-5-104219-5

Altimir N, Kolari P, Tuovinen J-P, Vesala T, Bäck J, Suni T, Kulmala M, Hari P (2006) Foliage surface ozone deposition: a role for surface moisture? Biogeosciences 3: 209-228.

Altimir N, Tuovinen J-P, Vesala T, Kulmala M, Hari P (2004) Measurements of ozone removal by Scots pine shoots: calibration of a stomatal uptake model including the non-stomatal component. Atmos Environ 38: 2387-2398

Ball JT, Berry JA (1982) The C_i/C_s ratio: A basis for predicting stomatal control of photosynthesis. Carnegie Institution of Washington Yearbook 81: 88-92

Basu S, Porté-Agel F, Foufoula-Georgiou E, Vinuesa J-F, Pahlow M (2006) Revisiting the local scaling hypothesis in stably stratified atmospheric boundary-layer turbulence: an integration of field and laboratory measurements with large-eddy simulations. Bound-Lay Meteorol 119: 473-500

Benner CL, Eatough NL, Lewis EA, Eatough DJ, Huang AA, Ellis EC (1988) Diffusion coefficients for ambient nitric and nitrous acids from denuder experiments in the 1985 nitrogen species methods comparison study. Atmos Environ 22: 1669-1672

Bowden R, Nadelhoffer KJ, Boone RD, Melillo JM, Garrison J.B (1992) Contributions of aboveground litter, belowground litter, and root respiration to total soil respiration in a temperate mixed hardwood forest. Can J For Res 23: 1402–1407

Braden H (1995) The model AMBETI. A detailed description of a Soil-Plant-Atmosphere model. Berichte des deutschen Wetterdienstes 195: 1-117

Brutsaert W (1984) Evaporation into the atmosphere: theory, history, and applications. 2nd edition. Dordrecht: Reidel, 299 p, ISBN 90-277-1247-6

Cannell MGR (1985) Dry matter partitioning in tree crops. In: Cannell MGR, Jackson JE (eds) Attributes of Trees as Crop Plants. Abbots Ripton: Institute of Terrestrial Ecology, Natural Environment Research Council, pp 160-193, ISBN 090428283X

Cellier P, Brunet Y (1992) Flux-gradient relationships above tall plant canopies. Agr Forest Meteorol 58: 93-117

Choudhury BJ, Idso SB, Reginato RJ (1987) Analysis of an empirical model for soil heat flux under a growing wheat crop for estimating evaporation by an infrared-temperature based energy balnce equation. Agr Forest Meteorol 39: 283-297

Collatz GJ, Ball JT, Grivet C, Berry JA (1991) Physiological and environmental regulation of stomatal conductance, photosynthesis and transpiration: a model that includes a laminar boundary layer. Agr Forest Meteorol 54: 107-136

Daamen CC, Simmonds LP (1996) Measurement of evaporation from bare soil and its estimation using surface resistance. Water Resour Res 32: 1393-1402

Dämmgen U, Grünhage L (1998) Response of a grassland ecosystem to air pollutants. V. A toxicological model for the assessment of dose-response relationships for air pollutants and ecosystems. Environ Pollut 101: 375-380

Dämmgen U, Sutton MA (2001) Die Umwelt-Wirkungen von Ammoniak-Emissionen. KTBL-Schr 401: 14-25

Dämmgen U, Grünhage L, Jäger H-J (1997) Description, assessment and meaning of vertical fluxes of matter within ecotopes: a systematic consideration. Environ Pollut 96: 249-260

Dämmgen U, Erisman JW, Cape JN, Grünhage L, Fowler D (2005) Practical considerations for addressing uncertainties in monitoring bulk deposition. Environ Pollut 134: 535-548

de Pury DGG, Farquhar GD (1997) Simple scaling of photosynthesis from leaves to canopies without the errors of big-leaf models. Plant Cell Environ 20: 537-557

Deardorff JW (1978) Efficient prediction of ground surface temperature and moisture, with inclusion of a layer of vegetation. J Geophys Res 83: 1889-1903

Dickinson RE (1984) Modeling evapotranspiration for three-dimensional global climate models. Geophysical Monograph Series, American Geophysical Union 29: 58-72

Drake BG, Gonzàlez-Meler MA, Long SP (1997) More efficient plants: A consequence of rising atmospheric CO_2? Annu Rev Plant Physiol Plant Mol Biol 48: 609-639

Dyer AJ (1974) A review of flux-profile relationships. Bound-Lay Meteorol 7: 363-372

EMEP/CORINAIR (2007) Emission Inventory Guidebook. Group 10: Agriculture. http://reports.eea.europa.eu/EMEPCORINAIR5/en/page019.html

Erisman JW, Versluis AH, Verplanke TAJW, de Haan D, Anink D, van Elzakker BG, Mennen MG, van Aalst RM (1993) Monitoring the dry deposition of SO_2 in the Netherlands: results for grassland and heather vegetation. Atmos Environ A 27: 1153-1161

Erisman JW, van Pul A, Wyers P (1994) Parameterization of surface resistance for the quantification of atmospheric deposition of acidifying pollutants and ozone. Atmos Environ 28: 2595-2607

Erisman JW, Draaijers G, Duyzer J, Hofschreuder P, van Leeuwen N, Römer F, Ruijgrok W, Wyers P, Gallagher M (1997) Particle deposition to forests - summary of results and application. Atmos Environ 31: 321-332

Erisman JW, Draaijers GPJ, Steingröver E, van Dijk H, Boxman A, de Vries W (1998) Assessment of the exposure and loads of acidifying and eutrophying pollutants and ozone, as well as their harmful influence on the vitality of the trees and the Speulder forest ecosystem as a whole. Water Air Soil Pollut 105: 539-571

Erisman JW, Vermeulen A, Hensen A, Flechard C, Dämmgen U, Fowler D, Sutton M, Grünhage L, Tuovinen J-P (2005) Monitoring and modelling of biosphere/atmosphere exchange of gases and aerosols in Europe. Environ Pollut 133: 403-413

Farquhar GD, von Caemmerer S, Berry JA (1980) A biochemical model of photosynthetic CO_2 assimilation in leaves of C_3 species. Planta 149: 178-190

Finlayson-Pitts BJ, Pitts JN (1986) Atmospheric chemistry: fundamentals and experimental techniques. New York: Wiley, 1098 p, ISBN 1-3214-5026-0

Flechard CR, Fowler D (1998) Atmospheric ammonia at a moorland site. I: The meteorological control of ambient ammonia concentrations and the influence of local sources. Q J Roy Meteor Soc 124: 733-757

Flechard CR, Fowler D, Sutton MA, Cape JN (1999) A dynamic chemical model of bi-directional ammonia exchange between semi-natural vegetation and the atmosphere. Q J Roy Meteor Soc 125: 2611-2641

Foken T (2003) Angewandte Meteorologie. Berlin: Springer, 289 p, ISBN 3-540-00322-3

Foken Th, Wichura B (1996) Tools for quality assessment of surface-based flux measurements. Agr. Forest Meteorol. 78: 83-105

Fowler D, Cape JN (1982) Air pollutants in agriculture and horticulture. In: Unsworth MH, Ormrod DP (eds) Effects of gaseous air pollution in agriculture and horticulture. London: Butterworth Scientific, pp 3-26, ISBN 0-408-10705-7

Fowler D, Flechard C, Cape JN, Storeton-West RL, Coyle M (2001) Measurements of ozone deposition to vegetation quantifying the flux, the stomatal and non-stomatal components. Water Air Soil Pollut 130: 63-74

Frühauf C (1998) Verdunstungsbestimmungen von Wäldern am Beispiel eines Fichtenbestandes im Tharandter Wald. Tharandter Klimaprotokolle 1, 185 p, ISBN 3-86005-212-8

Gallagher M, Fontan J, Wyers P, Ruijgrok W, Duyzer J, Hummelshøj P, Pilegaard K, Fowler D (1997) Atmospheric particles and their interactions with natural surfaces. In: Slanina J (ed) Biosphere-atmosphere exchange of pollutants and trace substances. Berlin: Springer, pp 45-83, ISBN 3-540-61711-6

Ganzeveld L, Lelieveld J (1995) Dry deposition parameterization in a chemistry general circulation model and its influence on the distribution of reactive trace gases. J Geophys Res Atmos 100: 20999-21012

Gao W, Wesely ML, Doskey PV (1993) Numerical modeling of the turbulent diffusion and chemistry of NO_x, O_3, isoprene, and other reactive trace gases in and above a forest canopy. J Geophys Res Atmos 98: 18339-18353

Gerosa G, Cieslik S, Ballarin-Denti A (2003) Micrometeorological determination of time-integrated stomatal ozone fluxes over wheat: a case study in Northern Italy. Atmos Environ 37: 777-788

Gerosa G, Marzuoli R, Cieslik S, Ballarin-Denti A (2004) Stomatal ozone fluxes over a barley field in Italy. "Effective exposure" as a possible link between exposure- and flux-based approaches. Atmos Environ 38: 2421-2432

Goumenaki E, Fernandez IG, Papanikolaou A, Papadopoulou D, Askianakis C, Kouvarakis G, Barnes J (2007) Derivation of ozone flux-yield relationships for lettuce: A key horticultural crop. Environ Pollut 146: 699-706

Graedel TE, Crutzen PJ (1995) Atmosphere, climate and change. New York: Freeman, IX, 196 p, ISBN 1-3214-5026-0

Granier A, Loustau D (1994) Measuring and modelling the transpiration of a maritime pine canopy from sap-flow data. Agr Forest Meteorol 71: 61-81

Grant RF, Rochette P, (1994) Soil microbial respiration at different water potentials and temperatures: Theory and mathematical modeling. Soil Sci Soc Am J 58: 1681–1690

Grünhage L, Haenel H-D (1997) PLATIN (PLant-ATmosphere INteraction) I: a model of plant-atmosphere interaction for estimating absorbed doses of gaseous air pollutants. Environ Pollut 98: 37-50

Grünhage L, Haenel H-D (2000) WINDEP - Worksheet-INtegrated Deposition Estimation Programme. In: KRdL - Kommission Reinhaltung der Luft im VDI und DIN (ed.) Troposphärisches Ozon. Eine kritische Bestandsaufnahme über Ursache, Wirkung und Abhilfemaßnahmen. Düsseldorf: Schriftenreihe der KRdL 32, pp 157-173

Grünhage L, Gerosa G (2008) Ozone flux measurement and modelling on leaf/shoot and canopy scale. Ital J Agron / Riv Agron: in press

Grünhage L, Dämmgen U, Hertstein U, Jäger H-J (1993) Response of grassland ecosystem to air pollutants: I - Experimental concept and site of the Braunschweig Grassland Investigation Program. Environ Pollut 81: 163-171

Grünhage L, Hanewald K, Jäger H-J, Ott W (1996) Auswirkungen dynamischer Veränderungen der Luftzusammensetzung und des Klimas auf terrestrische Ökosysteme in Hessen. II. Umweltbeobachtungs- und Klimafolgenforschungsstation Linden: Jahresbericht 1995. Umweltplanung, Arbeits- und Umweltschutz (Schriftenreihe der Hessischen Landesanstalt für Umwelt) 220: 1-191

Grünhage L, Dämmgen U, Haenel H-D, Jäger H-J (1998) Response of a grassland ecosystem to air pollutants. VI. The chemical climate: concentrations and potential flux densities of relevant criteria pollutants. Environ Pollut 101: 215-220

Grünhage L, Jäger H-J, Haenel H-D, Löpmeier F-J, Hanewald K (1999) The European critical levels for ozone: improving their usage. Environ Pollut 105: 163-173

Grünhage L, Haenel H-D, Jäger H-J (2000) The exchange of ozone between vegetation and atmosphere: micrometeorological measurement techniques and models. Environ Pollut 109: 373-392

Grünhage L, Krause GHM, Köllner B, Bender J, Weigel H-J, Jäger H-J, Guderian R (2001) A new flux-orientated concept to derive critical levels for ozone to protect vegetation. Environ Pollut 111: 355-362

Grünhage L, Krupa SV, Legge AH, Jäger H-J (2003) Ambient flux-based critical values of ozone for protecting vegetation: differing spatial scales and uncertainties in risk assessment. In: Karlsson PE, Selldén G, Pleijel H (eds.) Establishing Ozone Critical Levels II. UNECE Workshop Report. IVL report B 1523. Gothenburg, Sweden: IVL Swedish Environmental Research Institute, pp 51-65

Grünhage L, Krupa SV, Legge AH, Jäger H-J (2004) Ambient flux-based critical values of ozone for protecting vegetation: differing spatial scales and uncertainties in risk assessment. Atmos Environ 38: 2433-2437

Haenel H-D, Siebers J (1995) Lindane volatilization under field conditions: estimation from residue disappearance and concentration measurements in air. Agr Forest Meteorol 76: 237-257

Handorf D, Foken T, Kottmeier C (1999) The stable atmospheric boundary layer over an Antarctic ice sheet. Bound-Lay Meteorol 91: 165-189

Hicks BB, Baldocchi DD, Meyers TP Hosker RP, Matt DR (1987) A preliminary multiple resistance routine for deriving dry deposition velocities from measured quantities. Water Air Soil Pollut 36: 311-330

IUPAC - International Union of Pure and Applied Chemistry (1993): Quantities, units and symbols in physical chemistry. 2nd ed. London: Blackwell, 166 p, ISBN 0-632-03583-8

Jäger H-J, Schmidt SW, Kammann C, Grünhage L, Müller C, Hanewald K (2003) The University of Giessen free-air carbon dioxide enrichment study: description of the experimental site and of a new enrichment system. J Appl Bot 77: 117-127

Jarvis PG (1976) The interpretation of the variations in leaf water potential and stomatal conductance found in canopies in the field. Philos T Roy Soc B 273: 593-610

Kasten F, Czeplak G (1980) Solar and terrestrial radiation dependent on the amount and type of cloud. Sol Energy 24: 177-189

Kerstiens G, Federholzner R, Lendzian KJ (1992) Dry deposition and cuticular uptake of pollutant gases. Agr Ecosyst Environ 42: 239-253

Kerstiens G, Lendzian KJ (1989a) Interactions between ozone and plant cuticles. I. Ozone deposition and permeability. New Phytol 112: 13-19

Kerstiens G, Lendzian KJ (1989b) Interactions between ozone and plant cuticles. II. Water permeability. New Phytol 112: 21-27

Kim J, Verma SB (1991) Modeling canopy photosynthesis: scaling up from a leaf to canopy in a temperate grassland ecosystem. Agr Forest Meteorol 57: 187-208

Kirschbaum MUF (1995) The temperature dependence of soil organic matter decomposition, and the effect of global warming on soil organic storage. Soil Biol Biochem 27: 753–760

Kjaersgaard JH, Plauborg FL, Hansen S (2007) Comparison of models for calculating daytime longwave irradiance using long term data set. Agr Forest Meteorol 143: 49-63

Klemm O, Milford C, Sutton MA, Spindler G, van Putton E (2002) A climatology of leaf surface wetness. Theor Appl Climatol 71:107-117

Körner Ch (1994) Leaf diffusive conductances in major vegetation types of the globe. In: Schulze E-D, Caldwell MM (ed.) Ecophysiology of photosynthesis. Berlin: Springer, pp 463-490, ISBN 3-540-55952-3

Körner Ch, Perterer J, Altrichter C, Meusburger A, Slovik S, Zöschg M (1995) Ein einfaches empirisches Modell zur Berechnung der jährlichen Schadgasaufnahme von Fichten- und Kiefernadeln. Allg Forst Jagdztg 166: 1-9

Krupa SV (2002) Sampling and physico-chemical analysis of precipitation: a review. Environ Pollut 120: 565-594

Lendzian KJ, Kerstiens G (1991) Sorption and transport of gases and vapors in plant cuticles. Rev Environ Contam Tox 121: 65-128

Lenoble J (1993) Atmospheric radiative transfer. Hampton, Virginia: Deepak Publishing, 532 p, ISBN 0-937194-21-2

Leuning R (1990) Modelling stomatal behaviour and photosynthesis of Eucalyptus grandis. Aust J Plant Physiol 17: 159-175

Liljequist, G.H. & Cehak, K. (1979): *Allgemeine Meteorologie*. Braunschweig/Wiesbaden: Vieweg, 385 p, ISBN 3-528-13555-7

Lindström G, Gardelin M (1992) Hydrological modelling. In: Sandén P, Warfinger P (eds.) Modelling groundwater response to acidification: Report form the Swedish integrated groundwater acidification project, Vol. 5 of SMHI reports. Hydrology, SMHI, Norrköping

Mahrt L, Vickers, D (2003) Formulation of turbulent fluxes in the stable boundary layer. J Atmos Sci 60: 2538-2548

Massman WJ (1998) A review of the molecular diffusivities of H_2O, CO_2, CH_4, CO, O_3, SO_2, NH_3, N_2O, NO, and NO_2 in air, O_2 and N_2 near STP. Atmos Environ 32: 1111-1127

Massman WJ (2004) Toward an ozone standard to protect vegetation based on effective dose: a review of deposition resistances and a possible metric. Atmos Environ 38: 2323-2337

McArthur AJ (1990) An accurate solution to the Penman Equation. Agr Forest Meteorol 51: 87-92

Midgley P, Builtjes P, Fowler D, Harrison R, Hewitt N, Moussiopoulos N, Noone K, Tørseth K, Volz-Thomas A (2003) Towards cleaner air for Europe - science, tools and application. Part 1. Results from the EUROTRAC-2 synthesis and integration project. Weikersheim: Margraf Publishers, 246 p, ISBN 3-8236-1390-1

Monin AS, Obukhov AM (1954) Basic laws of turbulent mixing in the atmosphere near the ground (Translation in Aerophysics of air pollution edited by Fay JA and Hoult DP, American Institute of Aeronautics and Astronautics, New York, pp. 90-119, 1969). Akademiia Nauk SSSR, Leningrad, Trudy Geofizicheskowo Instituta 151 (No. 24): 163-187

Monteith JL (1965) Evaporation and environment. In: Fogg GE (ed.) The state and movement of water in living organisms. Symposia Society for Experimental Biology, no. 19. Cambridge: Cambridge University Press, pp 205-234, ISSN 0081-1386

Monteith JL, Unsworth MH (1990) Principles of environmental physics, second edition. London: Edward Arnold, 291 p, ISBN 0-7131-2931-X

Nadelhoffer KJ, Raich JW (1992) Fine root production estimates and belowground carbon allocation in forest ecosystems. Ecology 73: 1139–1147

Nemitz E, Sutton MA, Schjoerring JK, Husted S, Wyers GP (2000) Resistance modelling of ammonia exchange over oilseed rape. Agr Forest Meteorol 105: 405-425

Nemitz E, Milford C, Sutton MA (2001) A two-layer canopy compensation point model for describing bi-directional biosphere-atmosphere exchange of ammonia. Q J Roy Meteor Soc 127: 815-833

Nikolov N, Zeller KF (2003) Modeling coupled interactions of carbon, water, and ozone exchange between terrestrial ecosystems and the atmosphere. I: Model description. Environ Pollut 124: 231-246

Oke TR (1978) Boundary layer climates. London: Methuen, 372 p, ISBN 0-470-99381-2

Oltchev A, Ibrom A, Constantin J, Falk M, Richter I, Morgenstern K, Joo Y, Kreilein H, Gravenhorst G (1998) Stomatal and surface conductance of a spruce forest: model simulation and field measurements. Phys Chem Earth 23: 453-458

PORG (1997) Ozone in the United Kingdom. Fourth report of the Photochemical Oxidants Review Group 1997. London: Department of the Environment, Transport and the Regions, 234 p, ISBN 1-870393-30-9

Ritchie JT (1972) Model for predicting evaporation from a row crop with incomplete cover. Water Resour Res 8: 1204-1213

Ross J. (1981) Radiation regime and architecture of plant stands. Series: Tasks for Vegetation Sciences, Vol. 3. Berlin: Springer, p 420, ISBN 90-6193-607-1

Schaaf S, Meesenburg H (2005) Modellierung der Stoffflüsse in Waldbeständen im ANSWER-Projekt. Landbauforsch Völkenrode Sonderheft 279: 45-55

Scheffer F, Schachtschabel P (1982) Lehrbuch der Bodenkunde. Stuttgart (11., von P. Schachtschabel et al. neubearb. Aufl.): Enke, 442 p, ISBN 3-432-84771-8

Schlentner RE, van Cleve K (1984) Relationships between CO_2 evolution from soil, substrate temperature, and substrate moisture in four mature forest types in interior Alaska. Can J For Res 15: 97–106

Schrödter H (1985) Verdunstung - Anwendungsorientierte Mebverfahren und Bestimmungsmethoden. Berlin: Springer, 186 p, ISBN 3-540-15355-1

Sellers PJ (1985) Canopy reflectance, photosynthesis and transpiration. Int J Remote Sens 6: 1335-1372

Sellers PJ, Mintz Y, Sud YC, Dalcher A (1986) A simple biosphere model (SiB) for use in general circulation models. J Atmos Sci 43: 505-531

Simpson D, Fagerli H, Jonson JE, Tsyro S, Wind P, Tuovinen J-P (2003) Transboundary acidification, eutrophication and ground level ozone in Europe. EMEP Status Report 1, Part I: Unified EMEP model description. Oslo: Norwegian Meteorological Institute, p 104, ISSN 0806-4520 (http://www.emep.int/publ/reports/2003/emep_report_1_part1_2003.pdf)

Slinn WGN (1982) Predictions for particle deposition to vegetative canopies. Atmos Environ 16: 1785-1794

Sorteberg A, Hov Ø (1996) Two parametrizations of the dry deposition exchange for SO_2 and NH_3 in a numerical model. Atmos Environ 30: 1823-1840

Spindler G, Teichmann U, Sutton MA (2001) Ammonia dry deposition over grassland - micrometeorological flux-gradient measurements and bidirectional flux calculations using an inferential model. Q J Roy Meteor Soc 127: 795-814

Stewart JB (1988) Modelling surface conductance of pine forest. Agr Forest Meteorol 43: 19-35

Stull RB (1988) An introduction to boundary layer meteorology. Dordrecht: Kluwer, 666 p, ISBN 90-277-2768-6

Sutton MA, Fowler D (1993) A model for inferring bi-directional fluxes of ammonia over plant canopies. In: Proceedings of the WMO conference on the measurement and modelling of atmospheric composition changes including pollutant transport (Sofia, Oct. 1993). GAW-91. Geneva: WMO, 179-182

Sutton MA, Asman WAH, Schjørring JK (1994) Dry deposition of reduced nitrogen. Tellus 46B: 255-273

Sutton MA, Burkhardt JK, Guerin D, Nemitz E, Fowler D (1998) Development of resistance models to describe measurements of bi-directional ammonia surface-atmosphere exchange. Atmos Environ 32: 473-480

Thomas C, Foken T (2002) Re-evaluation of integral turbulence characteristics and their parameterisations. In: 15th Conference on Boundary Layer and Turbulence, 15-19 July 2002, Wageningen, The Netherlands. Boston: American Meteorological Society, pp 129-132

Tuovinen J-P, Ashmore MR, Emberson LD, Simpson D (2004) Testing and improving the EMEP ozone deposition module. Atmos Environ 38: 2373-2385

Uddling J, Pleijel H, Karlsson PE (2004) Measuring and modelling leaf diffusive conductance in juvenile silver birch, *Betula pendula*. Trees-Struct Funct 18: 686-695

UNECE (1979) Convention on Long-Range Transboundary Air Pollution. Geneva, thirteen day of November. Available from www.unece.org/env/lrtap

UNECE (1999) Protocol to the 1979 Convention on Long-Range Transboundary Air Pollution to Abate Acidification, Eutrophication and Ground-Level Ozone. Gothenburg, thirthieth day of November. Available from www.unece.org/env/lrtap

UNECE (2004) Manual on methodologies and criteria for Modelling and Mapping Critical Loads & Levels and Air Pollution Effects, Risks and trends. Available from www.icpmapping.org

UNECE (2007) Mapping Manual 2004. Manual on methodologies and criteria for medelling and mapping critical loads & levels and air pollution effects, risks and trends. 2007 revision. Available from www.icpmapping.org

VDI 3786 sheet 13 (1993) Meteorological measurements. Meteorological measuring station for agricultural purposes with computerized data handling. Berlin: Beuth

von Caemmerer S (2000) Biochemical models of leaf photosynthesis. Collingwood: CSIRO, 165 p, ISBN 0-643-06379-X

Weiss A, Norman JM (1985) Partitioning solar radiation into direct and diffuse, visible and near-infrared components. Agr Forest Meteorol 34 205-213

Wesely ML (1989) Parameterization of surface resistances to gaseous dry deposition in regional-scale numerical models. Atmos Environ 23: 1293-1304

Wesely ML, Cook DR, Hart RL, Speer RE (1985) Measurements and parameterization of particulate sulfur dry deposition over grass. J Geophys Res 90: 2131-2143

Wong SC, Cowan IR, Farquhar GD (1979) Stomatal conductance correlates with photosynthetic capacity. Nature 282: 424-426

Zhang L, Brook JR, Vet R (2002) On ozone dry deposition - with emphasis on non-stomatal uptake and wet canopies. Atmos Environ 36: 4787-4799

Zhang L, Lemeur R (1995) Evaluation of daily evapotranspiration estimates from instantaneous measurements. Agr Forest Meteorol 74: 139-154

Appendix A

Parameterization of net radiation

In cases where net radiation balance R_{net} [W·m^{-2}] is not measured it can be estimated according to:

$$R_{net} = S_t \cdot (1-\alpha) + \varepsilon \cdot L_d - L_u \quad \text{(A1)}$$

with
- S_t global radiation [W·m^{-2}]
- α short-wave albedo
- ε effective long-wave emissivity of the canopy (default value: ε = 0.97)
- L_d flux density of downward long-wave radiation of the atmosphere [W·m^{-2}]
- L_u flux density of upward long-wave radiation of the atmosphere [W·m^{-2}]

Thermal radiation emitted by the canopy L_u is determined by surface temperature T_s [K] at $z = d + z_{0h}$ and its effective longwave emissivity ε:

$$L_u = \varepsilon \cdot \sigma \cdot T_s^4 \quad \text{(A2)}$$

with
- σ Stefan-Boltzmann constant (= 5.669·10^{-8} W·m^{-2}·K^{-4})

If no measured data are available for L_d, it can be approximated, e.g. by parameterisations given in the literature (e.g. Brutsaert, 1984). In general, such parameterisations are based on a clear-sky approach combined with a function of cloud cover degree, cf. eqs. (6.18) and (6.24) in Brutsaert (1984) which adopted for the first version of PLATIN (Grünhage and Haenel, 1997). However, as it is not an easy task to provide cloud cover data routinely, we included an approximation of daytime cloud cover based on the relation of actual global radiation to the maximum possible global radiation, while the nighttime cloud cover was simply assumed to be equal to the latest daytime cloud cover.

During the vegetation periods 1998 and 1999 at the Linden field site at 50.53°N 8.69°E, this approach lead to daytime L_d values considerably different from measured L_d values as is demonstrated by some statistics shown in Table A1.

Table A1: Results of regression analysis of simulated (by former model) vs. observed L_d

	N	R^2	bias (W·m^{-2})	standard deviation (W·m^{-2})
MAY - SEPTEMBER 1998				
daylight hours ($S_t \geq$ 50 W·m^{-2})	3735	0.457	27.61	46.0
nighttime	2820	0.539	−20.75	39.2
MAY - SEPTEMBER 1999				
daylight hours ($S_t \geq$ 50 W·m^{-2})	3830	0.474	38.05	53.1
nighttime	2804	0.532	−17.86	39.4

For regression analysis during daylight hours only data sets with $S_t \geq$ 50 W·m^{-2} were selected to avoid uncertainties during transition times.

Although the nighttime L_d simulation is based on a comparably rough cloud cover estimate, the standard deviation and R^2 were still better than the respective values for the daytime parameterisation. Thus we decided to modify the cloud cover influence while we kept the clear-sky approach of Brutsaert (1984; eq. (6.18)) because of its high physical content (the validity of which was confirmed again only recently by Kjaersgaard et al., 2007). Our improved correction for cloud cover effect should not try to simulate cloud cover degree but should be directly based on screen-height data of global radiation and relative humidity for daytime estimates of L_d, and on relative humidity and air temperature for nighttime estimates of L_d. All input data were routinely recorded at the Linden field site at 50.53°N 8.69°E within BIATEX-2, a subproject of EUROTRAC-2 (cf. Midgley et al., 2003). The new approach and its prelimi-

nary calibration by L_d-measurements of one single month (May 1999) were published in Grünhage and Haenel (2000). Subsequently the new L_d model has been calibrated and tested for the vegetation periods 1998 and 1999 (unpublished), which lead to some minor adjustments of the constants but left unchanged the structure of the L_d model which is given below by eqs. (A3) through (A14). It should be kept in mind that our parameterisation is locally calibrated for Linden and its application to other sites should be accompanied by some sufficient measurements of L_d (cf. discussion of a model similar to ours in Kjaersgaard et al., 2007).

Table A2 gives some statistics of the results obtained with our new parameterisation. Comparison with Table A1 reveals that nighttime simulation of L_d could slightly be improved by the new approximation, but great progress was achieved in daytime L_d estimates.

Table A2: Results of regression analysis of simulated (new parameterisation) vs. observed L_d

	N	R^2	bias ($W \cdot m^{-2}$)	standard deviation ($W \cdot m^{-2}$)
MAY - SEPTEMBER 1998				
daylight hours ($S_t \geq 50$ $W \cdot m^{-2}$)	3735	0.721	−0.91	22.3
nighttime	2820	0.580	−5.51	24.0
MAY - SEPTEMBER 1999				
daylight hours ($S_t \geq 50$ $W \cdot m^{-2}$)	3830	0.734	0.89	21.6
nighttime	2804	0.617	5.60	25.1

The new L_d parameterisation is given by the subsequent equations:

- *daytime L_d* (global radiation $S_t \geq 50$ $W \cdot m^{-2}$):

$$L_{d,\,S_t > 0\ W \cdot m^{-2}} = 1.24 \cdot \left(\frac{e_{2m}}{T_{2m}} \right)^{1/7} \cdot \sigma \cdot T_{2m}{}^4 + A_{dd} + B_{dd} + C_{dd} \qquad \text{(A3)}$$

where e_{2m} is the actual water vapour pressure [hPa] and T_{2m} is the absolute air temperature [K] at z = 2 m above ground

and

$$A_{dd} = 16.9 - 70 \cdot \frac{S_t}{S_{t,\,ref}} \qquad \text{for } S_t \leq S_{t,\,ref} \qquad \text{(A4)}$$

$$A_{dd} = -53.1 \qquad \text{for } S_t > S_{t,\,ref} \qquad \text{(A5)}$$

$$B_{dd} = 2.3 + 1.33 \cdot (rH - 40) \qquad \text{for } rH \geq 40\ \% \qquad \text{(A6)}$$

$$B_{dd} = 2.3 \qquad \text{for } rH < 40\ \% \qquad \text{(A7)}$$

and

$$C_{dd} = -12.3 + 1.1 \cdot (rH - 70) \qquad \text{for } rH \geq 70\ \% \qquad \text{(A8)}$$

$$C_{dd} = -12.3 + 0.6 \cdot (70 - rH) \qquad \text{for } rH < 70\ \% \qquad \text{(A9)}$$

where $S_{t,ref}$ is the maximum possible global radiation according to eq. (A15) and rH is the relative humidity [%] at z = 2 m above ground.

The main contribution to daylight L_d is given by the first term on the right hand side of eq. (A3). It is semi-empirical, but with a firm physical background (see derivation of eq. (6.18) in Brutsaert, 1984).

Term A_{dd} represents a linear ad-hoc approach to estimate cloud cover influence by making use of the ratio of actual solar radiation to maximum possible solar irradiation. Term B_{dd} was derived formally (with the help of some minor simplifications) from the definition of the lifting condensation level (cf. Stull 1988). Other than for A_{dd} and B_{dd}, no direct physical explanation seems possible for the third term, C_{dd}, the contribution of which to the variance, however, is much smaller than that of the other terms. The constants in A_{dd}, B_{dd}, and C_{dd} were separately adjusted to minimise the bias resulting from the variable part in each of these three terms.

• *nighttime L_d* (S_t < 50 W·m^{-2}):

$$L_{\mathrm{d},\,S_t = 0\ \mathrm{W\cdot m^{-2}}} = 1.24 \cdot \left(\frac{e_{2\mathrm{m}}}{T_{2\mathrm{m}}} \right)^{1/7} \cdot \sigma \cdot {T_{2\mathrm{m}}}^4 + A_{\mathrm{dn}} + B_{\mathrm{dn}} \qquad \text{(A10)}$$

with

$$A_{\mathrm{dn}} = 14 + 10.7 \cdot (rH - 92.5) \qquad \text{for } rH \geq 92.5\ \% \qquad \text{(A11)}$$

$$A_{\mathrm{dn}} = 14 \qquad \text{for } rH < 92.5\ \% \qquad \text{(A12)}$$

and

$$B_{\mathrm{dn}} = 11 - 20 \cdot \sqrt{T_{2\mathrm{m,\,n\text{-}1}} - T_{2\mathrm{m,\,n}}} \qquad \text{for } (T_{2\mathrm{m,\,n\text{-}1}} - T_{2\mathrm{m,\,n}}) > 0 \text{ (n: actual data set)} \qquad \text{(A13)}$$

$$B_{\mathrm{dn}} = 11 \qquad \text{for } (T_{2\mathrm{m,\,n\text{-}1}} - T_{2\mathrm{m,\,n}}) \leq 0 \qquad \text{(A14)}$$

where e_{2m} is the actual water vapour pressure (hPa) and T_{2m} is the absolute air temperature (K) at z = 2 m above ground.

The main contribution to nighttime L_d is given by the first term on the right hand side of eq. (A10) which is known already from eq. (A3). Using a plot of the residual of the parameterised clear sky L_d against measured L_d, term A_{dn} was derived as a function of relative humidity. No other meteorological variable measured at Linden investigation site (like wind speed or air temperature) could significantly contribute to further improvement of the parameterisation. Term B_{dn} takes into account that the decrease of nocturnal air temperature is well correlated with fractional cloud cover (depending of course on local surface conditions). The constants in A_{dn} and B_{dn} were separately adjusted to minimise the bias resulting from the introduction of the variable parts of A_{dn} and B_{dn}.

• *maximum possible global radiation $S_{t,\,ref}$*

$S_{t,\,ref}$ is the astronomic maximum possible global radiation at cloudless sky parameterised according to Kasten and Czeplak (1980)

$$S_{\mathrm{t,\,ref}} = S_{\mathrm{t,\,cloudless\,sky}} = a_{\mathrm{Stref,\,1}} \cdot \sin\phi + a_{\mathrm{Stref,\,2}} \qquad \text{(A15)}$$

where $a_{Stref,\,1}$ and $a_{Stref,\,2}$ are empirical coefficients describing the average atmospheric attenuation of short-wave radiation by water vapour and dust at a given site, and ϕ is solar elevation. For the Linden field site at 50.53°N 8.69°E a_1 and a_2 were adjusted to a_1 = 1097 W·m^{-2} and a_2 = –54 W·m^{-2}.

Solar elevation ϕ is calculated depending on latitude, longitude and time according to Lenoble (1993):

$$\sin\phi = \sin\varphi_{\mathrm{geo}} \cdot \sin\Delta_{\mathrm{sun}} + \cos\varphi_{\mathrm{geo}} \cdot \cos\Delta_{\mathrm{sun}} \cdot \cos\varphi_{\mathrm{h}} \qquad \text{(A16)}$$

with

φ_{geo}	latitude [radians]
Δ_{sun}	sun declination [radians]
φ_h	hour angle [radians]

Sun declination Δ_{sun} is given by:

$$\Delta_{sun} = 0.006918 - 0.399912 \cdot \cos\varphi_d + 0.070257 \cdot \sin\varphi_d - 0.006758 \cdot \cos 2\varphi_d + 0.000907 \cdot \sin 2\varphi_d \quad \text{(A17)}$$

where the day angle φ_d [radians] is:

$$\varphi_d = 2 \cdot \pi \cdot \frac{\text{day of the year} - 1}{\text{number of days in the year}} \quad \text{(A18)}$$

The hour angle φ_h is given by

$$\varphi_h = \pi \cdot \left(1 - \frac{TST}{12}\right) \quad \text{(A19)}$$

where TST is the True Solar Time [h; decimal system] for the center of the time interval under consideration:

$$TST = GMT + \frac{\lambda_{geo}}{15} + ET - \frac{DT}{2} \quad \text{(A20)}$$

with
- GMT Greenwich Mean Time (for Germany: CET – 1) [h]
- CET Central European Time [h]
- λ_{geo} longitude [degree]
- DT duration of time interval [h]

and the equation of time ET [h]:

$$ET = 3.819667 \cdot (0.000075 + 0.001868 \cdot \cos\varphi_d - 0.032077 \cdot \sin\varphi_d - 0.014615 \cdot \cos 2\varphi_d - 0.040849 \cdot \sin 2\varphi_d) \quad \text{(A21)}$$

Appendix B

Radiation model

The sunlit and shaded leaf area indices of the canopy as well as the irradiance absorbed by the sunlit and shaded leaf fractions are parameterised according to de Pury and Farquhar (1997).

- *Sunlit and shaded leaf area index*

The sunlit leaf area index of the non-senescent leaves of the canopy [$m^2 \cdot m^{-2}$] is

$$LAI_{\text{sunlit}} = \frac{1 - e^{-k_b \cdot LAI_{\text{non-senescent}}}}{k_b} \quad \text{(B1)}$$

where k_b is a canopy-typical light attenuation coefficient:

$$k_b = \frac{k_{b,90°}}{\sin \phi} \quad \text{(B2)}$$

with $k_{b,90°}$ k_b value for solar elevation of 90° (cf. Chapter 2.3)
ϕ solar elevation (see eq. (A16) in Appendix A)

The shaded leaf area index of the canopy [$m^2 \cdot m^{-2}$] is then calculated from:

$$LAI_{\text{shaded}} = LAI_{\text{non-senescent}} - LAI_{\text{sunlit}} \quad \text{(B3)}$$

- *Irradiance absorbed by the sunlit and shaded leaf fractions of the canopy*

The irradiance absorbed by the canopy is calculated as the sum of direct-beam, diffusive and scattered-beam components of photosynthetically active radiation *PAR* measured above the canopy [$\mu mol \cdot m^{-2} \cdot s^{-1}$].

Direct beam irradiance I_b [$\mu mol \cdot m^{-2} \cdot s^{-1}$] is given by

$$I_b = PAR \cdot (1 - f_d) \quad \text{(B4)}$$

and diffuse irradiance I_d [$\mu mol \cdot m^{-2} \cdot s^{-1}$] by:

$$I_d = PAR \cdot f_d \quad \text{(B5)}$$

with f_d fraction of diffusive radiation (proportion of total attenuated radiation, beam plus diffuse) for cloudless skies

f_d is obtained by

$$f_d = \frac{1 - a_{PAR}^{\ m}}{1 + a_{PAR}^{\ m} \cdot (1/f_a - 1)} \quad \text{(B6)}$$

with a_{PAR} atmospheric transmission coefficient of photosynthetically active radiation PAR for clear sky conditions
(default value: a_{PAR} = 0.72 according to de Pury and Farquhar, 1997)

where the optical air mass m is defined as the ratio of the mass of atmosphere traversed per unit cross-sectional area of the solar beam to that traversed for a site at sea level if the sun was directly overhead:

$$\mathrm{m} = \frac{p \cdot p_0^{-1}}{\sin \phi} \tag{B7}$$

with p actual atmospheric pressure [hPa]
p_0 atmospheric pressure at sea level (p_0 = 1013.25 hPa)

and f_a is the proportion of attenuated radiation that reach the surface as diffuse radiation. Under cloudless skies it has been observed to range from 40 to 45 % (Weiss and Norman, 1985). In accordance with de Pury and Farquhar (1997) f_a = 0.426 is chosen as a default value.

The total irradiance absorbed by the sunlit leaf fraction of the canopy $I_{c,\,sunlit}$ [µmol·m^{-2}·s^{-1}] is given as the sum of direct-beam, diffusive and scattered-beam components:

$$I_{c,\,sunlit} = I_{c,\,direct\text{-}beam,\,sunlit} + I_{c,\,diffuse,\,sunlit} + I_{c,\,scattered\text{-}beam,\,sunlit} \tag{B8}$$

Direct-beam irradiance absorbed by sunlit leaves $I_{c,\,direct\text{-}beam,\,sunlit}$ is given by

$$I_{c,\,direct\text{-}beam,\,sunlit} = I_b \cdot (1-\sigma_{PAR}) \cdot \{1-\exp(-k_b \cdot LAI_{non\text{-}senescent})\} \tag{B9}$$

with σ_{PAR} leaf scattering coefficient of PAR
(default value: σ_{PAR} = 0.15 according to de Pury and Farquhar, 1997)

Diffuse irradiance absorbed by sunlit leaves $I_{c,\,diffuse,\,sunlit}$ can be calculated from:

$$I_{c,\,diffuse,\,sunlit} = I_d \cdot (1-\rho_{cd}) \cdot \{1-\exp[-(k'_d + k_b) \cdot LAI_{non\text{-}senescent}]\} \cdot \frac{k'_d}{k'_d + k_b} \tag{B10}$$

with ρ_{cd} canopy reflection coefficient for diffuse PAR
(default value: ρ_{cd} = 0.036 according to de Pury and Farquhar, 1997)

k'_d diffuse and scattered diffuse PAR extinction coefficient

The extinction coefficient k'_d is given by

$$k'_d = k_d \cdot \sqrt{1-\sigma_{PAR}} = 0.78 \cdot \sqrt{1-\sigma_{PAR}} \tag{B11}$$

with k_d diffuse PAR extinction coefficient
(default value: k_d = 0.78 according to de Pury and Farquhar, 1997)

The scattered-beam irradiance absorbed by sunlit leaves $I_{c,\,scattered\text{-}beam,\,sunlit}$ results from:

$$I_{c,\,scattered\text{-}beam,\,sunlit} = I_b \cdot \left[\begin{array}{l} (1-\rho_{cb}) \cdot \{1 - \exp[-(k'_b + k_b) \cdot LAI_{non\text{-}senescent}]\} \cdot \dfrac{k'_b}{k'_b + k_b} \\ - (1-\sigma_{PAR}) \cdot \dfrac{1 - \exp(-2 \cdot k_b \cdot LAI_{non\text{-}senescent})}{2} \end{array} \right] \tag{B12}$$

with k'_b beam and scattered beam PAR extinction coefficient

$$k'_b = k_b \cdot \sqrt{1-\sigma_{PAR}} \tag{B13}$$

ρ_{cb} canopy reflection coefficient for beam PAR

The reflection coefficient ρ_{cb} is defined as

$$\rho_{cb} = 1 - \exp\left[\frac{-2 \cdot \rho_h \cdot k_b}{1 + k_b}\right] \quad \text{(B14)}$$

with ρ_h reflection coefficient for beam PAR of a canopy with horizontal leaves

$$\rho_h = \frac{1 - \sqrt{1 - \sigma_{PAR}}}{1 + \sqrt{1 - \sigma_{PAR}}} \quad \text{(B15)}$$

The total irradiance absorbed by the shaded leaf area $I_{c,\,shaded}$ [µmol·m^{-2}·s^{-1}] is the sum of diffuse and scattered diffuse irradiance $I_{c,\,diffuse,\,shaded}$ and of scattered beam irradiance $I_{c,\,scattered\text{-}beam,\,shaded}$ absorbed by the shaded leaves:

$$I_{c,\,shaded} = I_{c,\,diffuse\ and\ scattered\ diffuse,\,shaded} + I_{c,\,scattered\text{-}beam,\,shaded} \quad \text{(B16)}$$

with

$$I_{c,\,diffuse\ and\ scattered\ diffuse,\,shaded} = I_d \cdot (1 - \rho_{cd}) \cdot \left[\begin{array}{l} \{1 - \exp[-k'_d \cdot LAI_{non\text{-}senescent}]\} \\ - \{1 - \exp[-(k'_d + k_b) \cdot LAI_{non\text{-}senescent}]\} \cdot \dfrac{k'_d}{k'_d + k_b} \end{array}\right] \quad \text{(B17)}$$

and

$$I_{c,\,scattered\text{-}beam,\,shaded} = I_b \cdot \left[\begin{array}{l} (1 - \rho_{cb}) \cdot \left(\begin{array}{l} \{1 - \exp[-k'_b \cdot LAI_{non\text{-}senescent}]\} \\ - \{1 - \exp[-(k'_b + k_b) \cdot LAI_{non\text{-}senescent}]\} \cdot \dfrac{k'_b}{k'_b + k_b} \end{array} \right) \\ - (1 - \sigma_{PAR}) \cdot \left\{ 1 - \exp[-k_b \cdot LAI_{non\text{-}senescent}] - \dfrac{1 - \exp(-2 \cdot k_b \cdot LAI_{non\text{-}senescent})}{2} \right\} \end{array}\right] \quad \text{(B18)}$$

Appendix C

Parameterization of the atmospheric stability functions

The atmospheric stability functions for momentum Ψ_m and sensible heat Ψ_h are calculated as described in Haenel and Siebers (1995). Adopting the set of empirical coefficients given by Dyer (1974), i.e. $a_u = a_s = 1$, $b_u = -16$, and $b_s = 5$ in context with $\kappa = 0.41$, one obtains for Ψ_m and Ψ_h:

• *unstable atmospheric stratification* ($L < 0$ m)

$$\Psi_m(\zeta) = 2 \cdot \ln\left[\frac{1}{\phi_m(\zeta)} + 1\right] + \ln\left[\frac{1}{\phi_m{}^2(\zeta)} + 1\right] - 2 \cdot \arctan\left[\frac{1}{\phi_m(\zeta)}\right] \quad \text{(C1)}$$

with

$$\phi_m(\zeta) = a_u \cdot (1 + b_u \cdot \zeta)^{-0.25} = (1 - 16 \cdot \zeta)^{-0.25} \quad \text{(C2)}$$

$$\zeta = \frac{z - d}{L} \quad \text{with e.g.} \quad z = z_1 = d + z_{0m} \quad \text{and} \quad z = z_2' = z_{ref,\,u} \quad \text{(C3)}$$

and

$$\Psi_h(\zeta) = 2 \cdot \ln\left[\frac{1}{\phi_h(\zeta)} + 1\right] \quad \text{(C4)}$$

with

$$\phi_h(\zeta) = a_u \cdot (1 + b_u \cdot \zeta)^{-0.5} = (1 - 16 \cdot \zeta)^{-0.5} \quad \text{(C5)}$$

$$\zeta = \frac{z - d}{L} \quad \text{with e.g.} \quad z = z_1 = d + z_{0m} \quad \text{and} \quad z = z_2 = z_{ref,\,T} \quad \text{(C6)}$$

• *stable atmospheric stratification* ($L > 0$ m)

$$\Psi_m(\zeta) = \Psi_h(\zeta) = (1 - a_s) \cdot \ln \zeta - a_s \cdot b_s \cdot \zeta = -5 \cdot \zeta \quad \text{(C7)}$$

with

$$\zeta = \frac{z - d}{L} \quad \text{and e.g.} \quad z = z_1 = d + z_{0m}\ , \quad z = z_2 = z_{ref,\,T}\ , \quad z = z_2' = z_{ref,\,u} \quad \text{(C8)}$$

Note that for stable conditions with ζ approaching unity, stability functions of the type of eq. (C7) are not valid as briefly reviewed by Foken (2003). Ψ_m and Ψ_h should then attain a constant value in order to account for the fact that, for more and more increasing stability, the magnitude of turbulence elements is no longer determined by the height z but by the Monin-Obukhov length (so-called z-less scaling). Therefore, according to Handorf et al. (1999), for $\zeta > 0.8$ the atmospheric stability functions (C7) are restricted in order not to fall below the value of –4.

• *neutral atmospheric stratification* ($|L| \to \infty$)

$$\Psi_m = \Psi_h = 0 \quad \text{(C9)}$$

In the case of the estimation of flux densities of ozone, sulphur dioxide, nitrogen dioxide, carbon dioxide or fine-particle constituents, the height $z = z_2$ represents the concentration measurement height of these species.

Appendix D

Parameterization of ground heat flux density and energy exchange due to photosynthesis

The ground heat flux G at $z = d + z_{0h}$ in the big-leaf approach is the total of three physical heat storage flux densities $G_{\text{physical heat storage}}$ and the energy exchange due to photosynthesis:

$$\begin{aligned} G &= G_{\text{soil}} + S_{\text{in-canopy air}} + S_{\text{vegetation}} + Ph \\ &= G_{\text{physical heat storage}} + Ph \end{aligned} \quad \text{(D1)}$$

with
- G_{soil} soil heat flux density [W·m^{-2}]
- $S_{\text{in-canopy air}}$ flux of energy due to changes in temperature and humidity of the air in the canopy [W·m^{-2}]
- $S_{\text{vegetation}}$ flux of energy due to changes in temperature of the aboveground biomass [W·m^{-2}]
- Ph energy exchange due to photosynthesis and respiration of the aboveground biomass [W·m^{-2}]

For low vegetation (e.g. grass, agricultural crops) G_{soil} is the dominant part of $G_{\text{physical heat storage}}$, allowing to neglect other storage fluxes in eq. (D1), while this is not possible for forests (cf. Frühauf, 1998).

• *physical heat storage flux density [W·m^{-2}]*

In PLATIN, $G_{\text{physical heat storage}}$ is parameterised as proportional to the net radiative flux density R_{net} (cf. Brutsaert, 1984).

$$G_{\text{physical heat storage}} = a_{1,\text{Gphs}} \cdot e^{-k_{b,\max} \cdot SAI} \cdot R_{\text{net}} \quad \text{if} \quad R_{\text{net}} \geq 0 \text{ W·m}^{-2} \quad \text{(D2)}$$

$$G_{\text{physical heat storage}} = a_{2,\text{Gphs}} \cdot R_{\text{net}} \quad \text{if} \quad R_{\text{net}} < 0 \text{ W·m}^{-2} \quad \text{(D3)}$$

with
- $k_{b,\max}$ attenuation coefficient of the canopy at 12 h TST (true solar time)
- SAI total surface area of the vegetation [m^2·m^{-2}]

This parameterisation is based on the fact that, beneath a plant stand, $G_{\text{physical heat storage}}$ represents only a relatively small fraction of the energy balance and that it follows more or less the time course of net radiation R_{net} as the most important fraction of the energy balance. During daylight hours, R_{net} is driven by incoming solar radiation and therefore the parameterisation of G_{soil} must account for shortwave radiation extinction within the plant stand. This can simply be parameterised by $\exp(-k_{b,\max} \cdot SAI)$ as discussed in Chapter 2.3. During nighttime, on the other hand, R_{net} only consists of the longwave radiation balance so that there is no need to consider the plant stand architecture when parameterising nocturnal G.

The empirical coefficients $a_{1,\text{Gphs}}$ and $a_{2,\text{Gphs}}$ should be determined from energy balance measurements for each specific vegetation type separately. However, considering the subordinate contribution of G to the energy balance as well as the simplicity of the approach given above for G, we restrict ourselves to find reasonable values of $a_{1,\text{Gphs}}$ and $a_{2,\text{Gphs}}$ for low vegetation like or grassland and agricultural crops (including the asymptotic limit of bare soil) and forests.

Neglecting the fact that measured energy balances do never close completely due to measurement errors and different footprints of the contributing components (cf. Foken, 2003), we calculated the energy balance residual EB_{residual} which is assumed to be identical with G:

$$EB_{\text{residual}} = G = R_{\text{net}} - H - \lambda E \quad \text{(D4)}$$

From modelled *G* according to eqs. (D2) and (D3), for the Linden semi-natural grassland $a_{1,\,Gphs}$ can be approximated by 0.55 and $a_{2,\,Gphs}$ by 0.9. These values are used in PLATIN as default values for low vegetation (e.g. grassland, crops).

From ratios of $G_{physical\ heat\ storage}/R_{net}$ published in the literature (cf. Fig. 4.21 in Oke, 1978) default values $a_{1,\,Gphs} = a_{2,\,Gphs} \approx 1$ are deduced for forest ecosystems.

• *energy exchange due to photosynthesis [W·m^{-2}]*

The energy needed to fix one mole of CO_2 is $477 \cdot 10^3$ J. Hence *Ph* is approximated as:

$$Ph = 477 \cdot 10^3\ \mathrm{J \cdot mol^{-1}} \cdot A_{net,\,canopy} \qquad \text{(D5)}$$

with $A_{net,\,canopy}$ net rate of canopy photosynthesis in μmol·m^{-2}·s^{-1}

which results in an energy quantity needed to fix 1 μmol·m^{-2}·s^{-1} CO_2 in plant photosynthesis of approximately 0.5 W·m^{-2}.

$A_{net,\,canopy}$ is calculated according to de Pury and Farquhar (1997) taking into account the sunlit and shaded leaf fractions of the canopy as described in Appendix G.

Appendix E

Jarvis functions for radiation, temperature, water vapour pressure deficit of the atmosphere, soil moisture, phenology, ozone and carbon dioxide

- *Jarvis-Stewart function for radiation*

$$f_1(S_t) = \frac{S_t}{S_1}\left(\frac{S_1 + S_2}{S_t + S_2}\right) \quad \text{(E1)}$$

with S_t actual global radiation [W·m^{-2}]
S_1 maximum global radiation (default value: S_1 = 1000 W·m^{-2})
S_2 empirical coefficient governing the shape of the function (default value: S_2 = 100 W·m^{-2})

- *Jarvis-Stewart function for temperature*

$$f_2(t_a) = \left(\frac{t_a - t_1}{t_2 - t_1}\right)\left(\frac{t_3 - t_a}{t_3 - t_2}\right)^{\frac{t_3 - t_2}{t_2 - t_1}} \quad \text{(E2)}$$

with t_a actual temperature [°C]
t_1 vegetation-type dependent minimum temperature (default value: t_1 = 0 °C)
t_2 vegetation-type dependent optimum temperature (default value: t_2 = 20 °C)
t_3 vegetation-type maximum temperature at which stomata no longer remain open (default value: t_3 = 40 °C)

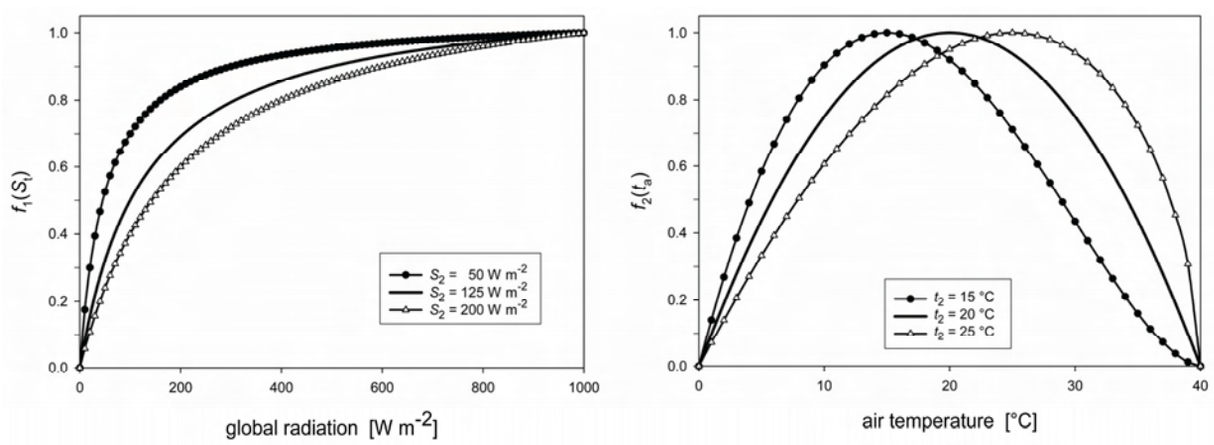

Fig. E1
Dependence of the relative stomatal resistance on solar radiation for various coefficients S_2 (left) and on air temperature for various coefficients t_2 (right)

• *Jarvis-Stewart function for water vapour pressure deficit in the atmosphere*

$$f_3(VPD) = \min\left[1, \max\left(\frac{VPD - V_1}{V_2 - V_1}, \mathrm{V}_3\right)\right] \quad \text{(E3)}$$

with
- VPD actual water vapour pressure deficit of the air [hPa] (see Appendix F, eq. (F1 - F4))
- V_1 maximum value for VPD (default value: V_1 = 40 hPa)
- V_2 threshold value for VPD (default value: V_2 = 10 hPa)
- V_3 minimum threshold (default value: V_3 = 0.15)

• *Jarvis-Stewart function for soil moisture*

$$f_4(SM) = \min\left[1, \max\left(\frac{SM - SM_{\mathrm{W}}}{(SM_{\mathrm{C}} - \mathrm{W}_1) - SM_{\mathrm{W}}}, \mathrm{W}_2\right)\right] \quad \text{(E4)}$$

with
- SM actual soil water content [$m^3 \cdot m^{-3}$] for a specific soil layer
- SM_W site-specific wilting point [$m^3 \cdot m^{-3}$]
- SM_C site-specific field capacity [$m^3 \cdot m^{-3}$]
- W_1 site-specific threshold level [$m^3 \cdot m^{-3}$] (default value: $W_1 = 0.25 \cdot SM_C$)
- W_2 minimum threshold (default value: W_2 = 0.15)

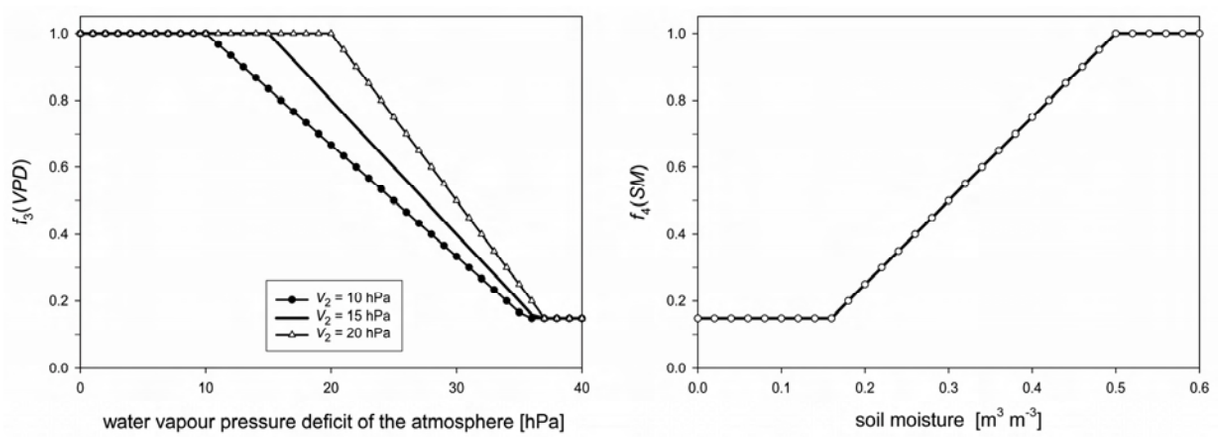

Fig. E2
Dependence of the relative stomatal resistance on water vapour pressure deficit of the atmosphere for different coefficients V_2 (left) and on soil moisture (right)

• *Jarvis-Stewart function for VPD and soil moisture*

In general, the Jarvis-Stewart functions for water vapour pressure deficit in the atmosphere and soil moisture are combined multiplicatively. However, as plants under water stress react more sensitive to *VPD*, in PLATIN a combined function $f_{3/4}(VPD, SM)$ is used which accounts for the interaction effect:

$$f_{3/4}(VPD, SM) = \min\left[1, \max\left(\frac{VPD - (V_1 \cdot \mathrm{V}_5)}{(V_2 \cdot \mathrm{V}_5) - (V_1 \cdot \mathrm{V}_5)}, \mathrm{V}_3\right)\right] \quad \text{(E5)}$$

with $$\mathrm{V}_5 = \mathrm{V}_4 \cdot \frac{SM - SM_{\mathrm{W}}}{(SM_{\mathrm{C}} - W_1) - SM_{\mathrm{W}}} \quad \text{(E6)}$$

and V_4 empirical weighting coefficient (default value: $\mathrm{V}_4 = 1$)

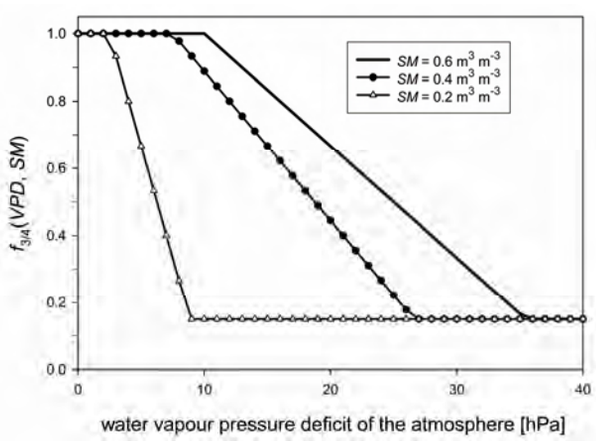

Fig. E3
Dependence of the relative stomatal resistance on water vapour pressure deficit of the atmosphere and soil moisture

• *Jarvis-Stewart function for time of day*

A time dependent impact on stomatal resistance has been often reported in the literature (e.g. Körner, 1994; Uddling et al., 2004; Goumenaki et al., 2007). After Körner (1994), the same set of climatic conditions (e.g. light, temperature, *VPD*, soil moisture) could result in lower stomatal resistances during the morning than in the afternoon. This afternoon increase of $R_{\mathrm{stom,\ H2O}}$ compared to the morning values is in the order of 20 %.

For daylight hours after 2 pm the following relation, derived from the factors given in Körner et al. (1995) for *Picea abies* and *Pinus sylvestris* and in Goumenaki et al. (2007) for *Lactuca sativa*, can serve as a first approximation:

$$f_5(\mathrm{time}) = -0.66 + 0.279 \cdot \mathrm{time} - 0.01147 \cdot \mathrm{time}^2 \quad \text{(E7)}$$

with time time of day [h; decimal fraction]

During daylight hours till 2 pm, f_5(time) is set unity. During night f_5(time) is of no practical use, but is set unity in order to avoid mathematical problems during a 24 hours model run.

• *Jarvis-Stewart functions for phenology, ozone and carbon dioxide*

f_6(PHEN) and $f_7(O_3)$ allow for the modifying influence of phenology and ozone on stomatal resistance: both senescence due to normal aging and premature senescence induced by ozone limit stomatal aperture.

With $f_8(CO_2)$ the influence of elevated CO_2 on stomatal aperture is multiplicatively taken into account (cf. Oltchev et al., 1998):

$$f_8(\mathrm{CO_2}) = \left(\frac{c_1 \cdot \chi_{CO2}}{c_2 + \chi_{CO2}} \right) \cdot \left(\frac{\chi_{CO2,\,base}}{\chi_{CO2}} \right) \qquad \text{(E8)}$$

with

χ_{CO2}	actual mole fraction of CO_2 at reference height [ppm]
$\chi_{CO2,\,base}$	base CO_2 mole fraction (default value: $\chi_{CO2,\,base}$ = 350 ppm)
c_1, c_2	empirical constants describing dependence of photosynthesis rate on ambient CO_2 concentration (c_1: dimensionless, c_2 in ppm)

f_6(PHEN) and $f_8(CO_2)$ must be derived for the respective vegetation by comparison of modelled and measured latent heat fluxes (default value: f_6(PHEN) = 1) and CO_2 fluxes respectively (default value: $f_8(CO_2)$ = 1). $f_7(O_3)$ depends on stomatal uptake of O_3 and must be derived experimentally (default value: $f_7(O_3)$ = 1).

Appendix F

Equations for water vapour pressure deficit of the atmosphere, slope of the water vapour pressure saturation curve and density and specific heat of moist air

- *water vapour pressure deficit of the atmosphere [hPa]*

$$VPD = e_{\text{saturation water vapour pressure}} - e_{\text{water vapour pressure}} \quad \text{(F1)}$$

with the saturation water vapour pressure of the atmosphere [hPa; after Magnus]:

$$e_{\text{saturation water vapour pressure}} = 6.1078 \cdot \mathrm{e}^{\frac{17.08085 \cdot t_a}{234.175 + t_a}} \quad \text{if} \quad \text{actual air temperature } t_a \geq 0°C \quad \text{(F2)}$$

$$e_{\text{saturation water vapour pressure}} = 6.1078 \cdot \mathrm{e}^{\frac{22.44294 \cdot t_a}{272.44 + t_a}} \quad \text{if} \quad \text{actual air temperature } t_a < 0°C \quad \text{(F3)}$$

and the water vapour pressure [hPa]:

$$e_{\text{water vapour pressure}} = e_{\text{saturation water vapour pressure}} \cdot \frac{rH}{100} \quad \text{(F4)}$$

where *rH* [%] is the relative humidity measured at air temperature reference height $z_{\text{ref, } T}$

- *slope of the water vapour saturation pressure curve [hPa·K^{-1}]*

$$\frac{\mathrm{d}e_{\text{saturation water vapour pressure}}}{\mathrm{d}t_a} = e_{\text{saturation water vapour pressure}} \cdot \frac{17.08085 \cdot 234.175}{(234.175 + t_a)^2} \quad \text{if} \quad t_a \geq 0°C \quad \text{(F5)}$$

$$\frac{\mathrm{d}e_{\text{saturation water vapour pressure}}}{\mathrm{d}t_a} = e_{\text{saturation water vapour pressure}} \cdot \frac{22.44294 \cdot 272.44}{(272.44 + t_a)^2} \quad \text{if} \quad t_a < 0°C \quad \text{(F6)}$$

Note that, under certain circumstances, (F5) or (F6) may serve as an approximation of s_c in the Penman-Monteith equation mentioned in Chapter 2.4.

- *density of moist air at absolute temperature T [kg·m^{-3}]*

$$\rho_{\text{moist air}} = \rho_{\text{dry air}} \cdot \left(1 - 0.378 \cdot \frac{e_{\text{water vapor pressure}}}{p}\right) \quad \text{(F7)}$$

with $$\rho_{\text{dry air}} = \frac{p}{R_{\text{dry air}} \cdot (273.15 + t_a)} \cdot 100 \quad \text{(F8)}$$

and p air pressure [hPa]
$R_{\text{dry air}}$ gas constant for dry air ($R_{\text{dry air}}$ = 287.04 J·kg^{-1}·K^{-1})

- *specific heat of moist air at constant pressure [m^2·s^{-2}·K^{-1}]*

$$c_{\text{p, moist air}} = c_{\text{p, dry air}} \cdot (1 + 0.84 \cdot q) \quad \text{(F9)}$$

with $c_{\text{p, dry air}}$ = 1004.67 m^2·s^{-2}·K^{-1}

and q specific air humidity [g·g^{-1}] $$q = \frac{0.622 \cdot e_{\text{water vapor pressure}}}{p - 0.378 \cdot e_{\text{water vapor pressure}}} \quad \text{(F10)}$$

Appendix G

Biosphere/atmosphere exchange of carbon dioxide

The exchange of carbon dioxide between the reference height above the canopy and the phytosphere $F_c(CO_2)$ [µmol·m^{-2}·s^{-1}] arises as the effect of canopy photosynthesis A_{net} (positive towards the canopy, µmol·m^{-2}·s^{-1}) and ecosystem respiration *Resp** (positive upwards, µmol·m^{-2}·s^{-1}).

G1 - Canopy photosynthesis

The net rate of canopy photosynthesis A_{net} is parameterized according to de Pury and Farquhar (1997). The so-called single layered sun/shade model described by the author's is a scaled version of a leaf photosynthesis model (cf. e.g. Farquhar et al., 1980; von Caemmerer 2000) integrating separately the sunlit and shaded leaf fractions of the canopy:

$$A_{\text{net}} = A_{\text{net, sunlit}} + A_{\text{net, shaded}} = (A_{\text{sunlit}} + A_{\text{shaded}}) - (Resp_{\text{d, sunlit}} + Resp_{\text{d, shaded}}) \quad \text{(G1)}$$

with
- $A_{\text{net, x}}$ net rate of photosynthesis of the sunlit (x = sunlit) or shaded (x = shaded) leaf fraction of the canopy [µmol·m^{-2}·s^{-1}]
- $Resp_{\text{d, x}}$ mitochondrial respiration rate (leaf dark respiration) of the sunlit (x = sunlit) or shaded (x = shaded) leaf fraction of the canopy [µmol·m^{-2}·s^{-1}]

• *parameterisation of net rate of photosynthesis of sunlit and shaded leaf fraction of the canopy*

The net rate of photosynthesis of the sunlit and shaded leaf fraction of the canopy, $A_{\text{net, sunlit}}$ and $A_{\text{net, shaded}}$, is calculated based on a biochemical model of photosynthesis according to Farquhar et al. (1980):

$$A_{\text{net, x}} = \min\{A_{\text{c, x}}, A_{\text{j, x}}, A_{\text{p, x}}\} - Resp_{\text{d, x}} \quad \text{(G2)}$$

with
- $A_{\text{net, x}}$ net rate of photosynthesis of the sunlit (x = sunlit) or shaded (x = shaded) leaf fraction of the canopy [µmol·m^{-2}·s^{-1}]
- $A_{\text{c, x}}$ Rubisco-limited rate of CO_2 assimilation of the sunlit (x = sunlit) or shaded (x = shaded) leaf fraction of the canopy [µmol·m^{-2}·s^{-1}]
- $A_{\text{j, x}}$ electron-transport limited rate of CO_2 assimilation of the sunlit (x = sunlit) or shaded (x = shaded) leaf fraction of the canopy [µmol·m^{-2}·s^{-1}], i.e. rate of photosynthesis limited by Rubisco regeneration
- $A_{\text{p, x}}$ triose phosphate utilization-limited rate of CO_2 assimilation of the sunlit (x = sunlit) or shaded (x = shaded) leaf fraction of the canopy [µmol·m^{-2}·s^{-1}]
- $Resp_{\text{d, x}}$ daytime mitochondrial respiration rate of the sunlit (x = sunlit) or shaded (x = shaded) leaf fraction of the canopy [µmol·m^{-2}·s^{-1}] (default value see Table G1)

The Rubisco-limited CO_2 assimilation rate of sunlit $A_{\text{c, sunlit}}$ or shaded leaf fractions $A_{\text{c, shaded}}$ of the canopy is:

$$A_{\text{c, x}} = V_{\text{c, x}} \cdot \frac{p_{\text{i, x}} - \Gamma_*}{p_{\text{i, x}} + K_{\text{c}} \cdot (1 + \frac{O_{\text{i}}}{K_{\text{o}}})} \quad \text{(G3)}$$

with
- $V_{\text{c, x}}$ photosynthetic Rubisco capacity of the sunlit (x = sunlit) or shaded (x = shaded) leaf fraction of the canopy [µmol·m^{-2}·s^{-1}]
- $p_{\text{i, x}}$ intercellular CO_2 partial pressure of the sunlit (x = sunlit) or shaded (x = shaded) leaf fraction of the canopy [Pa]

Γ_* CO_2 compensation point of photosynthesis in the absence of mitochondrial respiration [Pa]
(default value see Table G1)

K_c Michaelis-Menten constant of Rubisco for CO_2 [Pa]
(default value see Table G1)

K_o Michaelis-Menten constant of Rubisco for O_2 [Pa]
(default value see Table G1)

O_i intercellular O_2 partial pressure (= $20.5 \cdot 10^3$ Pa)

Table G1
Photosynthetic parameters for wheat at 25°C according to de Pury and Farquhar (1997)

Parameter	Value	Unit	activation energy E_a [J mol^{-1}]
K_c	40.4	Pa	59400
K_o	$24.8 \cdot 10^3$	Pa	36000
Γ_*	3.69	Pa	29000
k_n	0.713	---	
$V_{\text{leaf at top of canopy}}$ [1)]	110	µmol·m^{-2}·s^{-1}	64800
$Resp_d$ [2)]	$0.0089 \cdot V_c$	µmol·m^{-2}·s^{-1}	66400
J_{max} [2)]	$2.1 \cdot V_c$	µmol·m^{-2}·s^{-1}	37000

[1)] photosynthetic Rubisco capacity per unit leaf area at top of canopy
[2)] $Resp_d$: $0.01 \cdot V_c$ - $0.02 \cdot V_c$ (cf. von Caemmerer, 2000)
J_{max}: $1.5 \cdot V_c$ - $2 \cdot V_c$ (cf. von Caemmerer, 2000)

The photosynthetic capacities of the sunlit and shaded leaf fractions of the canopy $V_{c,\,sunlit}$ and $V_{c,\,shaded}$ are calculated by integrating the leaf photosynthetic capacity $V_{leaf,\,x}$ and the respective leaf area fraction taking into account the leaf nitrogen content (cf. de Pury and Farquhar, 1997).

$V_{c,\,sunlit}$ is approximated as given in eq. (G4) and $V_{c,\,shaded}$ as given in eq. (G5).

$$V_{c,\,sunlit} = LAI_{\text{non-senescent}} \cdot V_{\text{leaf at top of canopy}} \cdot \frac{1 - \exp[-k_n - (k_b \cdot LAI_{\text{non-senescent}})]}{k_n + (k_b \cdot LAI_{\text{non-senescent}})} \quad \text{(G4)}$$

with $V_{\text{leaf at top of canopy}}$ photosynthetic Rubisco capacity per unit leaf area at top of canopy [µmol·m^{-2}·s^{-1}]; (default value: see Table G1)

k_n coefficient of leaf-nitrogen allocation in a canopy (default value: see Table G1)

$$V_{c,\,shaded} = V_c - V_{c,\,sunlit} \quad \text{(G5)}$$

with V_c canopy photosynthetic capacity [µmol·m^{-2}·s^{-1}]

$$V_c = LAI_{\text{non-senescent}} \cdot V_{\text{leaf at top of canopy}} \cdot \frac{1 - \exp[-k_n]}{k_n} \quad \text{(G6)}$$

The Rubisco regeneration-limited or electron-transport-limited rate of the sunlit, $A_{j,\,sunlit}$, or shaded, $A_{j,\,shaded}$, leaf fraction of the canopy is:

$$A_{j,x} = J_x \cdot \frac{p_{i,x} - \Gamma_*}{4 \cdot p_{i,x} + 8 \cdot \Gamma_*} \qquad \text{(G7)}$$

with J_x electron transport rate per unit leaf area of the sunlit (x = sunlit) or shaded (x = shaded) leaf fraction of the canopy [µmol·m^{-2}·s^{-1}]

$$J_x = \frac{I_{2,x} + J_{max,x} - \sqrt{(I_{2,x} + J_{max,x})^2 - 4 \cdot \theta \cdot I_{2,x} \cdot J_{max,x}}}{2 \cdot \theta} \qquad \text{(G8)}$$

with $J_{max,\,x}$ light-saturated (maximum) electron transport rate per unit leaf area of the sunlit (x = sunlit) or shaded (x = shaded) leaf fraction of the canopy [µmol·m^{-2}·s^{-1}] (default value see Table G1)

θ empirical curvature factor (default value: θ = 0.7)

and

$$I_{2,x} = I_{c,x} \cdot \frac{1-f}{2} \qquad \text{(G9)}$$

with $I_{2,\,x}$ photosynthetically active irradiation absorbed by PS II of the sunlit (x = sunlit) or shaded (x = shaded) leaf fraction of the canopy [µmol·m^{-2}·s^{-1}]

$I_{c,\,x}$ photosynthetic active radiation absorbed by the sunlit (x = sunlit) or shaded (x = shaded) leaf fraction of the canopy [µmol·m^{-2}·s^{-1}]

f corrects for spectral quality of light (default value: f ~ 0.15)

The export-limited or phosphate-limited canopy CO_2 assimilation rate $A_{p,\,x}$ of the sunlit (x = sunlit) or shaded (x = shaded) leaf fraction of the canopy is:

$$A_{p,x} = (3 \cdot T_p) \cdot \frac{p_{i,x} - \Gamma_*}{p_{i,x} - \left(1 + 3\frac{\alpha_c}{2}\right) \cdot \Gamma_*} \quad \text{according to von Caemmerer (2000)} \qquad \text{(G10)}$$

with T_p rate of triose phosphate export from the chloroplast [µmol·m^{-2}·s^{-1}]

α_c fraction of glycolate carbon not returned to the chloroplast ($0 < \alpha < 1$)

or

$$A_{p,x} = \frac{V_{c,x}}{2} \quad \text{according to Collatz et al. (1991)} \qquad \text{(G11)}$$

IN PLATIN, eq. (G11) is implemented as a first guess. The phosphate limitation is relevant under conditions where plants are grown under elevated ambient CO_2 concentrations.

De Pury and Farquhar (1997) scaled daytime mitochondrial respiration rate (leaf dark respiration) $Resp_{d,\,x}$ of the sunlit (x = sunlit) or shaded (x = shaded) leaf fraction of the canopy to $V_{c,\,x}$ as:

$$Resp_{d,x} = 0.0089 \cdot V_{c,x} \qquad \text{(G12)}$$

Additionally, in PLATIN daytime canopy leaf respiration rate $Resp_{d,\,c}$ is parameterized by:

$$Resp_{\mathrm{d,\,c}} = LAI_{\text{non-senescent}} \cdot Resp_{\mathrm{d,\,ref}} \cdot \sqrt{\frac{273 + t_{\mathrm{s}}}{298}} \tag{G13}$$

with $Resp_{\mathrm{d,\,ref}}$ reference canopy leaf respiration rate (µmol·m^{-2}·s^{-1})
t_{s} leaf temperature [°C]

$Resp_{\mathrm{d,\,ref}}$ is adjusted by multiple regression analysis to the sum of $Resp_{\mathrm{d,\,sunlit}}$ and $Resp_{\mathrm{d,\,shaded}}$. Taking into account the temperature dependency as described by eq. (G15), nighttime canopy mitochondrial respiration rate $Resp_{\mathrm{c,\,nighttime}}$ is estimated.

The temperature dependence of Γ_* is described by:

$$\Gamma_* = \Gamma_*(25°\mathrm{C}) + 0.188 \cdot (t_{\mathrm{s}} - 25) + 0.0036 \cdot (t_{\mathrm{s}} - 25)^2 \tag{G14}$$

The temperature dependence of $Resp_{\mathrm{d}}$, $Resp_{\mathrm{n}}$ and the kinetic constants k_{c}, k_{o} and $V_{\mathrm{c,\,x}}$ is described by an Arrhenius function of the form:

$$Parameter(t_{\mathrm{S}}) = Parameter(25°\mathrm{C}) \cdot \exp\left(\frac{(t_{\mathrm{s}} - 25) \cdot E_{\mathrm{a}}}{298 \cdot R \cdot (273 + t_{\mathrm{s}})}\right) \tag{G15}$$

with t_{s} leaf temperature [°C]
R universal gas constant (R = 8.314 J K^{-1}·mol^{-1})
E_{a} activation energy [J mol^{-1}], listed in Table G1

The temperature dependency of J_{max} is taken into account by the function:

$$J_{\mathrm{max}}(t_{\mathrm{s}}) = J_{\mathrm{max}}(25°\mathrm{C}) \cdot \frac{((273 + t_{\mathrm{S}}) - 298) \cdot E_{\mathrm{a}}}{298 \cdot R \cdot (273 + t_{\mathrm{S}})} \cdot \frac{1 + \exp\left(\frac{298 \cdot S_{\mathrm{J}} - H_{\mathrm{J}}}{298 \cdot R}\right)}{1 + \exp\left(\frac{(273 + t_{\mathrm{S}}) \cdot S_{\mathrm{J}} - H_{\mathrm{J}}}{R \cdot (273 + t_{\mathrm{S}})}\right)} \tag{G16}$$

with t_{s} leaf temperature [°C]; T = 273 + t_{s} [K]
R universal gas constant (= 8.314 J K^{-1}·mol^{-1})
S_{J} 710 J K^{-1}·mol^{-1}
H_{J} 220000 J·mol^{-1}

G2 - Approximation of belowground respiration and respiration rate of aboveground woody plant parts

An estimation of belowground respiration $Resp_{\mathrm{belowground}}$ as well as of the respiration rate of the aboveground woody plant parts $Resp_{\mathrm{w}}$ are necessary for the computation of canopy net ecosystem exchange, with:

$$Resp^* = Resp_{\mathrm{w}} + Resp_{\mathrm{belowground}} \tag{G17}$$

• *belowground respiration*

In PLATIN, the simple bulk parameterization approach to predict soil CO_2 efflux $Resp_{\mathrm{belowground}}$ described by Nikolov and Zeller (2003) is implemented. The approach considers the effect of soil moisture at 14 cm depth (SM_{14cm}), soil temperature at 10 cm depth $t_{\mathrm{soil,\,10cm}}$ and clay content (Cl) on the net CO_2 release only. The CO_2 evolution from the soil is estimated as:

$$Resp_{\text{belowground}} = Resp_{\text{belowground, max}} \cdot \frac{f_T + f_M - \sqrt{(f_T + f_M)^2 - 4 \cdot \omega \cdot f_T \cdot f_M}}{2\,\omega} \cdot (1 - 0.0065 \cdot Cl) \quad \text{(G18)}$$

with

$Resp_{\text{belowground, max}}$	rate of soil respiration under optimum temperature and moisture conditions [µmol·m^{-2}·s^{-1}]
f_T	non-dimensional factor quantifying the limitations of soil temperature on CO_2 efflux
f_M	non-dimensional factor quantifying the limitations of soil moisture on CO_2 efflux
ω	convexity coefficient defining the smoothness of the transition between f_T and f_M (ω = 0.985)
Cl	clay content [%]

A $Resp_{\text{belowground, max}}$ of 17 µmol·m^{-2}·s^{-1}, derived from respiration rates from hardwood forests around the world, is suggested in Nikolov and Zeller (2003). The temperature factor is computed after Kirschbaum (1995):

$$f_T = \exp\left[-3.764 + 0.204 \cdot t_{\text{soil,10cm}} \cdot \left(1 - 0.5 \cdot \frac{t_{\text{soil,10cm}}}{t_{\text{opt}}}\right)\right] \quad \text{(G19)}$$

with t_{opt} optimum temperature for CO_2 evolution (default value: t_{opt} = 36.9 °C)

Eq. (G19) is based on soil respiration data from 11 studies worldwide (cf. Kirschbaum, 1995) and implies a variable Q_{10}. The effect of actual volumetric moisture on soil respiration is based on measurements and models by Schlentner and van Cleve (1984) and Grant and Rochette (1994):

$$f_M = \frac{1}{1 + \exp[3 - 14 \cdot SM^*]} \quad \text{if} \quad 0 \le SM^* \le 0.74 \quad \text{(G20)}$$

$$f_M = \frac{1}{1 + \exp[3 - 76 \cdot (1 - SM^*)]} \quad \text{if} \quad 0.74 < SM^* \le 1.0 \quad \text{(G21)}$$

where SM^* is the relative moisture saturation at 14 cm depth:

$$SM^* = \frac{SM - SM_{\text{res}}}{SM_{\text{sat}} - SM_{\text{res}}} \quad \text{(G22)}$$

with

SM	actual soil water content [m^3·m^{-3}]
SM_{res}	residual (irreducible) soil moisture [m^3·m^{-3}]
SM_{sat}	soil moisture content at saturation [m^3·m^{-3}]

Nocturnal eddy covariance measurements provide information on the respiratory release of aboveground and belowground processes. Plant respiration $Resp_{\text{c, nighttime}}$ is substracted from the nocturnal atmospheric CO_2 flux to obtain the nocturnal belowground CO_2 flux.

For crops and grassland systems $Resp^*$ equals $Resp_{\text{belowground}}$.

• *aboveground woody respiration*

For ecosystems other than crops and grassland, aboveground woody respiration $Resp_w$ is parameterized according to Nikolov and Zeller (2003). As described by the author's, this total respiratory flux is partitioned into a maintenance $Resp_{w, m}$ and growth $Resp_{w, g}$ component.

Aboveground woody maintenance respiration $Resp_{w,m}$ is assumed to be linearly related to the nitrogen content of living tissue and varies exponentially with air temperature:

$$Resp_{w,m} = 0.2103 \cdot N_s \cdot Q_{10}^{\frac{t_{lag3h} - 20}{10}} \quad \text{(G23)}$$

with
- $Resp_{w,m}$ aboveground woody maintenance respiration [µmol·m^{-2}·s^{-1}]
- N_s nitrogen content of the aboveground sapwood biomass [g·m^{-2}]
- Q_{10} relative change of the respiration rate per 10 K temperature increase
- t_{lag3h} ambient air temperature lagged by three hours [°C]

As reported in the description of the FORFLUX model (Nikolov and Zeller, 2003) N_s typically ranges between 1 and 13 g·m^{-2}. Q_{10} is approximated as follows, taking into account an acclimation response:

$$Q_{10} = 3.25 - 0.077 \cdot t_{7days} \quad \text{if} \quad t_{7days} \geq 0\ °C \quad \text{(G24)}$$

$$Q_{10} = 3.25 \quad \text{if} \quad t_{7days} < 0\ °C \quad \text{(G25)}$$

with
- t_{7days} mean daily air temperature of the past 7 days [°C]

Both, t_{7days} and Q_{10} must be updated daily in the model.

The respiration rate from aboveground woody biomass due to construction of new tissue $Resp_{w,g}$ is assumed to be constant during a day and proportional to the net carbon gain of vegetation in the previous day (cf. Nikolov and Zeller, 2003):

$$Resp_{w,g} = f_g \cdot \delta_a \cdot \frac{A'_{net} - Resp'_{w,m} - Resp'_{r,m}}{86.4} \quad \text{(G26)}$$

with
- $Resp_{w,g}$ aboveground woody maintenance respiration due to construction of new tissue [µmol·m^{-2}·s^{-1}]
- f_g construction cost (f_g = 0.2 mol·mol^{-1})
- δ_a carbon allocation coefficient
- A'_{net} 24-h integrated canopy net photosynthesis of the previous day [mmol·m^{-2}·d^{-1}]
- $Resp'_{w,m}$ cumulative daily maintenance respiratory flux from aboveground woody biomass [mmol·m^{-2}·d^{-1}]
- $Resp'_{r,m}$ cumulative daily maintenance respiratory flux from roots [mmol·m^{-2}·d^{-1}]

The factor 86.4 converts flux units mmol·m^{-2}·d^{-1} to µmol·m^{-2}·s^{-1}. As summarized by Nikolov and Zeller (2003) the carbon allocation coefficient δ_a depends on species physiology, tree age and growth conditions. Typically it varies between 0.34 and 0.8 (cf. Cannell, 1985). Root maintenance respiration $Resp'_{r,m}$ is estimated from the daily integral of root total respiration $Resp'_{r,t}$ assuming roots have the same construction cost as the aboveground biomass:

$$Resp'_{r,m} = f_g \cdot \delta_a \cdot \frac{Resp'_{r,t} - f_g \cdot (1 - \delta_a) \cdot (A'_{net} - Resp'_{w,m})}{1 - f_g \cdot (1 - \delta_a)} \quad \text{(G27)}$$

where $Resp'_{r,t}$ must be computed as a site-specific fraction of the total CO_2 efflux from soil $Resp_{belowground}$ (cf. Bowden et al., 1992; Nadelhoffer and Raich, 1992).

The total aboveground woody respiration $Resp_w$ is:

$$Resp_w = Resp_{w,m} + Resp_{w,g} \quad \text{(G28)}$$

G3 - Coupling of biochemical and diffusion equations for biosphere/atmosphere CO_2 exchange

The net rate of canopy photosynthesis A_{net} is related to the net ecosystem CO_2 exchange, i.e. the vertical above-canopy CO_2 flux $F_c(CO_2)$ [µmol·m^{-2}·s^{-1}] by:

$$\begin{aligned} F_c(CO_2) &= -\frac{c_{CO2}(z_{ref}) - c_{CO2}(d+z_{0CO2})}{R_{ah} + R_{b,CO2}} \\ &= -(A_{net} - Resp_w - Resp_{belowground}) \\ &= -A_{net} + Resp^* \end{aligned} \quad \text{(G29)}$$

with
- $c_{CO2}(z_{ref})$ concentration (amount concentration) of CO_2 at reference height [µmol·m^{-3}]
- $c_{CO2}(d+z_{0CO2})$ CO_2 concentration at conceptual height $z = d + z_{0CO2}$ [µmol·m^{-3}]
- R_{ah} atmospheric resistance [s·m^{-1}]; c.f. chapter 2.1
- $R_{b,CO2}$ quasi-laminar layer resistance for CO_2 [s·m^{-1}]; c.f. chapter 2.2

$$R_{b,CO2} = R_{b,heat} \cdot 1.23 \quad \text{(G30)}$$

- $Resp_w$ respiration rate of aboveground woody plant parts [µmol·m^{-2}·s^{-1}]
- $Resp_{belowground}$ belowground respiration rate (roots, microbes) [µmol·m^{-2}·s^{-1}]
- $Resp^*$ $Resp_w$ + $Resp_{belowground}$

In order to obtain A_{net} as function of the reference-height concentration $c_{CO2}(z_{ref})$ some additional considerations and approximations are needed. First of all, A_{net} is rewritten as an analogue to Ohm's law:

$$\begin{aligned} A_{net} &= A_{net,sunlit} + A_{net,shaded} \\ &= \frac{c_{CO2}(d+z_{0CO2}) - c_{i,sunlit}}{R^*_{c,stom,sunlit,CO2}} + \frac{c_{CO2}(d+z_{0CO2}) - c_{i,shaded}}{R^*_{c,stom,shaded,CO2}} \end{aligned} \quad \text{(G31)}$$

with
- $c_{i,x}$ intercellular CO_2 concentration of the sunlit or shaded leaf fraction of the canopy [µmol·m^{-3}]

The bulk stomatal resistance for CO_2 exchange via stomata of the sunlit and shaded leaf fraction at a specific canopy development stage $R^*_{c,stom,CO2}$ [s·m^{-1}] is given by

$$R^*_{c,stom,sunlit,CO2} = \frac{R_{c,stom,H2O}}{(1-\beta^*_{sunlit})} \cdot \frac{D_{H2O}}{D_{CO2}} = \frac{R_{c,stom,H2O}}{(1-\beta^*_{sunlit})} \cdot 1.6 \quad \text{(G32)}$$

$$R^*_{c,stom,shaded,CO2} = \frac{R_{c,stom,H2O}}{(1-\beta^*_{shaded})} \cdot \frac{D_{H2O}}{D_{CO2}} = \frac{R_{c,stom,H2O}}{(1-\beta^*_{shaded})} \cdot 1.6 \quad \text{(G33)}$$

taking into account the differences between the molecular diffusivity for water vapour D_{H2O} and molecular diffusivity of the CO_2 in air (cf. Table 2) and the actual canopy development stage (cf. chapter 2.3).

Algebraic rearrangements of eqs. (G31) with (G29) yield an expression for $c_{i,sunlit}$ and $c_{i,sunlit}$:

$$\begin{aligned} c_{i,sunlit} &= c_{CO2}(d+z_{0CO2}) - (A_{net,sunlit} \cdot R^*_{c,stom,sunlit,CO2}) \\ &= c_{CO2}(z_{ref}) - [(A_{net} - Resp^*) \cdot (R_{ah} + R_{b,CO2})] - (A_{net,sunlit} \cdot R^*_{c,stom,sunlit,CO2}) \end{aligned} \quad \text{(G34)}$$

$$\begin{aligned} c_{i,shaded} &= c_{CO2}(d+z_{0CO2}) - (A_{net,shaded} \cdot R^*_{c,stom,shaded,CO2}) \\ &= c_{CO2}(z_{ref}) - [(A_{net} - Resp^*) \cdot (R_{ah} + R_{b,CO2})] - (A_{net,sunlit} \cdot R^*_{c,stom,shaded,CO2}) \end{aligned} \quad \text{(G35)}$$

Conversion of CO_2 concentration [µmol·m^{-3}] in partial pressure [Pa] yields for p_i (cf. Appendix M):

$$p_{\mathrm{i,\,sunlit}} = (\phi_{\mathrm{cf}} \cdot p) \cdot \left[c_{\mathrm{CO2}}(d + z_{0\mathrm{CO2}}) - (A_{\mathrm{net,\,sunlit}} \cdot R*_{\mathrm{c,\,stom,\,sunlit,\,CO2}})\right] \quad \text{(G36)}$$
$$= (\phi_{\mathrm{cf}} \cdot p) \cdot \left[c_{\mathrm{CO2}}(z_{\mathrm{ref}}) - [(A_{\mathrm{net}} - Resp*) \cdot (R_{\mathrm{ah}} + R_{\mathrm{b,\,CO2}})] - (A_{\mathrm{net,\,sunlit}} \cdot R*_{\mathrm{c,\,stom,\,sunlit,\,CO2}})\right]$$

$$p_{\mathrm{i,\,shaded}} = (\phi_{\mathrm{cf}} \cdot p) \cdot \left[c_{\mathrm{CO2}}(d + z_{0\mathrm{CO2}}) - (A_{\mathrm{net,\,shaded}} \cdot R*_{\mathrm{c,\,stom,\,shaded,\,CO2}})\right] \quad \text{(G37)}$$
$$= (\phi_{\mathrm{cf}} \cdot p) \cdot \left[c_{\mathrm{CO2}}(z_{\mathrm{ref}}) - [(A_{\mathrm{net}} - Resp*) \cdot (R_{\mathrm{ah}} + R_{\mathrm{b,\,CO2}})] - (A_{\mathrm{net,\,sunlit}} \cdot R*_{\mathrm{c,\,stom,\,shaded,\,CO2}})\right]$$

with p atmospheric pressure [Pa]
ϕ_{cf} combined conversion factor ($\phi_{\mathrm{cf}} = 22.4 \cdot 10^{-9}$ m^3·µmol^{-1})

The system of eqs. (G1), (G2), (G29), (G31) (G36) and (G37) are solved iteratively. The initial value is chosen as $p_i = 0.7 \cdot p_{CO2}(z_{ref})$. This value is based on the fact that a constant ratio c_i/c_a in the order of magnitude of 0.7 for C_3 plants can be observed under non-limiting conditions even when ambient CO_2 concentration c_a is varied (cf. Ball and Berry, 1982; Drake et al., 1997; Kim and Verma, 1991; Wong et al., 1979). Only when stomata are nearly closed the ratio c_i/c_a deviates from this cardinal values tending towards unity. Note, eq. (G31) applies to steady-state conditions for $R_{\mathrm{c,\,stom,\,x,\,CO2}}$ and $A_{\mathrm{net,\,x}}$, because responses of leaf biochemistry and stomatal resistance to changes in environmental conditions have quite different relaxation times (e.g. Leuning, 1990).

G4 - Calculation of biosphere/atmosphere exchange of carbon dioxide

The exchange of carbon dioxide between the reference height above the canopy and the plant/soil system $F_c(CO_2)$ is calculated during times with solar elevation angle $\phi > 0$ as given in eq. (G38)

$$F_{\mathrm{c}}(\mathrm{CO_2}) = -A_{\mathrm{net}} + Resp^* \quad \text{(G38)}$$

and during times with solar elevation angle $\phi = 0$ as given in eq. (G39):

$$F_{\mathrm{c}}(\mathrm{CO_2}) = Resp_{\mathrm{c,\,nighttime}} + Resp^* \quad \text{(G39)}$$

Appendix H

Soil water model

PLATIN makes use of a so-called force-restore model (cf. Deardorff, 1978) to provide a measure of volumetric soil water content *SM* [$m^3 \cdot m^{-3}$] which is needed to estimate stomatal resistance (cf. Chapter 2.3, Appendix E). Other than more complex modelling concepts, the force-restore approach is limited to predict the average soil water content of only one single layer the top side of which is the soil surface:

$$\frac{\mathrm{d}SM}{\mathrm{d}t} = \frac{1}{\rho_{\mathrm{H2O}} \cdot SLD} \cdot \left[-\frac{\lambda E_{\mathrm{SLD}}}{\lambda} + \frac{W_{\mathrm{in}}}{DTI} + C_{\mathrm{cap}} \cdot \left(1 - \frac{SM - SM_{\mathrm{W}}}{SM_{\mathrm{C}} - SM_{\mathrm{W}}} \right) \right] \qquad \text{(H1)}$$

with

ρ_{H2O}	density of water [$kg \cdot m^{-3}$]
SLD	depth of soil layer under consideration [m]
λE_{SLD}	turbulent vertical flux density of latent heat in case of non-zero evapotranspiration [$W \cdot m^{-2}$] originated from the *SLD*-layer
λ	latent heat of water vaporisation [$J \cdot kg^{-1}$]
W_{in}	precipitation and/or dew reaching the ground [$kg \cdot m^{-2} \equiv$ mm H_2O]
DTI	measurement time interval [s]
C_{cap}	maximum possible vertical water flow from groundwater into rooted soil layer due to soil capillarity [$kg \cdot m^{-2} \cdot s^{-1}$]
SM_{W}	site-specific wilting point [$m^3 \cdot m^{-3}$]
SM_{C}	site-specific field capacity [$m^3 \cdot m^{-3}$]

The value of C_{cap} site-specifically depends on the vertical distance between ground water table and the soil layer under consideration and can reach up to 5 $mm \cdot d^{-1}$ (Scheffer and Schachtschabel, 1982) which is about $5.8 \cdot 10^{-5}$ mm s^{-1}.

Equations like (H1) are often used with $\lambda E_{\mathrm{SLD}} = \lambda E$ and accordingly $SLD = RLD$ where *RLD* is a measure of the depth of the rooted soil layer. The deeper the layer the lower is the amplitude of the diurnal course of soil water content calculated by eq. (H1). This dampening is an undesired result with respect to the influence of soil water content on the modelling of the diurnal variation of stomatal resistance. Therefore another way has been chosen in PLATIN: the soil water content is calculated for a given soil layer depth *SLD* in the order of 0.1 m, because, at least for agricultural crops, the water content in such a thin layer (along with its pronounced diurnal variation) seems to be appropriate for stomatal resistance modelling. In addition, a special parameterization of λE_{SLD} has been developed[2] in order to account for the fact that, especially in case of high evaporative demand, transpiration should be fed not only by the roots in the thin subsurface soil layer but also by roots located below.

The basic idea of this parameterization is that plants tend to minimize the amount of energy needed to supply water for transpiration. The respective modelling concept in PLATIN is based on the assumption that the vertical distribution of soil water content does not influence root water uptake and that roots of deeper soil layers contribute to transpiration the lesser the lesser transpiration rate is itself, and vice versa.

To develop the approach, evapotranspiration λE is separated into bare soil evaporation $\lambda E_{\mathrm{evaporation}}$ (the water for which is assumed to be always completely drawn from the *SLD*-layer) and canopy transpiration $\lambda E_{\mathrm{transpiration}}$,

$$\lambda E = \lambda E_{\mathrm{evaporation}} + \lambda E_{\mathrm{transpiration}} \qquad \text{(H2)}$$

where $\lambda E_{\mathrm{evaporation}}$ and $\lambda E_{\mathrm{transpiration}}$ are given in Chapter 2.4, eqs. (26) and (27).

[2] This parameterization was presented already in Grünhage and Haenel (1997), where some equations had been slightly mistyped.

The fraction of $\lambda E_{\text{transpiration}}$ which is originating from the *SLD*-layer is called $\lambda E_{\text{transpiration, SLD}}$. If the density distribution of the transpiration-relevant roots is assumed to decay exponentially with soil depth and if the water uptake by the roots is directly proportional to the local root density, the ratio of $\lambda E_{\text{transpiration, SLD}}$ to $\lambda E_{\text{transpiration}}$ is given by

$$\frac{\lambda E_{\text{transpiration, SLD}}}{\lambda E_{\text{transpiration}}} = 1 - \exp\left(-2.303 \cdot \frac{SLD}{RLD_{90}}\right) \tag{H3}$$

where RLD_{90} is the depth of the soil layer containing 90 % of total root mass. The vertical distribution of water uptake according to an exponential expression was used for example also by Lindström and Gardelin (1992).

Eq. (H3) does not yet account for the desired influence of evaporative demand on root water uptake. To meet with this requirement, the constant RLD_{90} is replaced by a variable layer depth *VLD*. As a first order guess, *VLD* is assumed to be roughly proportional to the transpiration rate. However, *VLD* should never tend to zero even when the transpiration rate does so, because the depth from which water is extracted by roots will never decline to zero even in case of very low or zero values of λE. In order to keep the resulting ratio of $\lambda E_{\text{transpiration, SLD}}$ to $\lambda E_{\text{transpiration}}$ as simple as possible with respect to its mathematical formulation (see eq. (H5)), the following approach is chosen for *VLD*:

$$\frac{VLD}{VLD_{\max}} = \left[1 - \ln\left(\frac{\lambda E}{\lambda E_{\max}}\right)\right]^{-1} \tag{H4}$$

where $VLD_{\max} = VLD(\lambda E = \lambda E_{\max})$ corresponds to RLD_{90} and $\lambda E_{\max}$ will be specified below. Figure H1 shows $VLD \cdot VLD_{\max}^{-1}$ as function of $\lambda E \cdot \lambda E_{\max}^{-1}$.

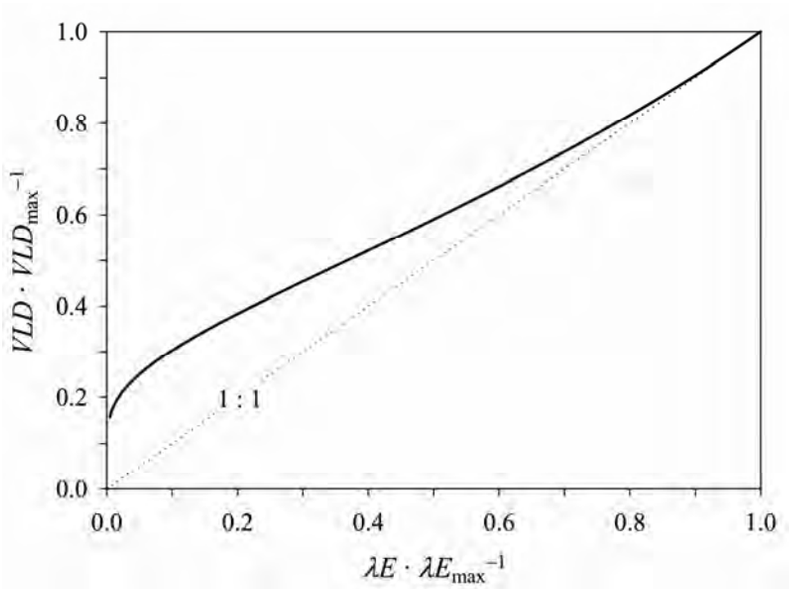

Fig. H1
$VLD \cdot VLD_{\max}^{-1}$ as function of $\lambda E \cdot \lambda E_{\max}^{-1}$ (solid line) and the 1:1 reference line (dotted line)

The obvious deficiency of eq. (H5) in case of $\lambda E = 0$ is cured when combining eqs. (H3) and (H4) and replacing RLD_{90} with *VLD* in order to obtain a modified equation for the ratio of $\lambda E_{\text{transpiration, SLD}}$ to $\lambda E_{\text{transpiration,}}$:

$$\frac{\lambda E_{\text{transpiration, SLD}}}{\lambda E_{\text{transpiration}}} = 1 - \left(\frac{\lambda E}{\lambda E_{\text{ref}}} \right)^{-2.303 \cdot \frac{SLD}{VLD_{\max}}} \tag{H5}$$

where $\lambda E_{ref} = e \cdot \lambda E_{max}$ may roughly be estimated as 10^3 W·m^{-2} implying λE_{max} to be about 370 W·m^{-2}. The latter seems to be a reasonable value under central European climate conditions. This can be concluded e.g. from the approach of Zhang and Lemeur (1995) who approximate the daily average of λE, λE_{day}, by $\lambda E_{day} = (2/\pi) \cdot \lambda E_{max} \cdot (n_h/24)$, where n_h is the number of daylight hours. Then for a clear day in June in the mid-latitudes with $n_h = 16$, $\lambda E_{max} = 370$ W·m^{-2} corresponds to $\lambda E_{day} = 157$ W·m^{-2} or 5.5 mm H_2O, which is only slightly less than typical observed maximum values of about 6 mm (Schrödter, 1985). Figure H2 shows some results of eq. (H5) for $SLD = 0.1$ m and different values of VLD_{max}.

Finally, the entity λE_{SLD} required to apply equation (H1) is obtained from:

$$\lambda E_{\text{SLD}} = \lambda E_{\text{soil}} + \lambda E_{\text{transpiration, SLD}} \tag{H6}$$

Application of the soil water model presented above requires proper selection of the site-specific parameters SLD, $VLD_{max} = RLD_{90}$, and C_{cap}. In context with model calibration it may also be necessary to adjust the value of λE_{ref} (or the fraction $\lambda E_{max} = \lambda E_{ref} \cdot e^{-1}$).

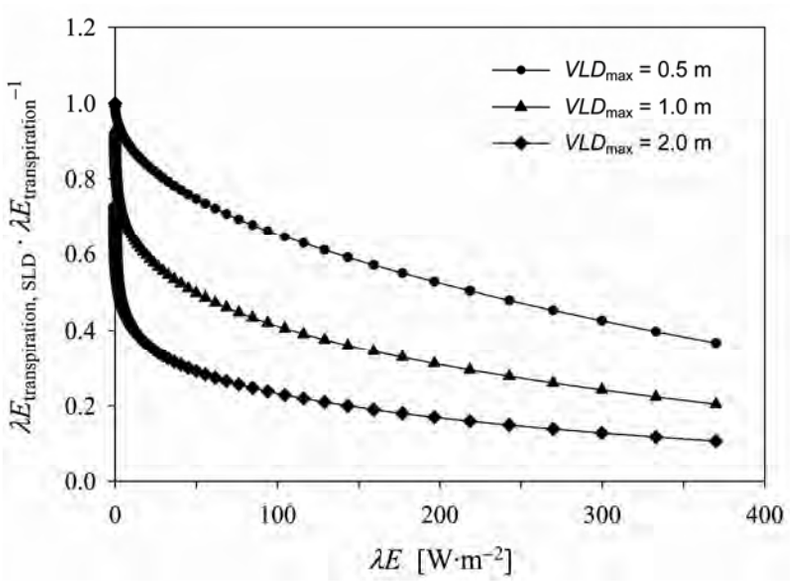

Fig. H2
Results of eq. (H6) for $SLD = 0.1$ m and different values of VLD_{max}

Appendix I

Estimation of displacement height and momentum roughness length from measured data

Friction velocity u_* from eddy covariance measurements at height z_* above ground, horizontal wind velocity u measured at two heights z_1 and z_2 above ground (with $z_1 < z_* < z_2$), and Monin-Obukhov length L based on eddy covariance data (for definition of L see eq. (5)), can be used to estimate displacement height d and momentum roughness length z_{0m}. All measurements are expected as half-hourly or hourly samplings. We recommend to apply the procedure described below on data sets measured during well established turbulence only: unstable atmospheric stratification, global radiation $S_t > 200$ W·m^{-2}, horizontal wind velocity $u(z_1) > 1.5$ m·s^{-1}.

Starting point to derive a calculation procedure is the profile equation for horizontal wind velocity according to Monin-Obukhov theory:

$$u(z) = \frac{u_*}{\kappa} \cdot \left\{ \ln\left(\frac{z - d}{z_{0m}} \right) - \Psi_m\left(\frac{z - d}{L} \right) + \Psi_m\left(\frac{z_{0m}}{L} \right) \right\} \tag{I1}$$

Eq. (I1) which contains both unknowns, d and z_{0m}, applies to both wind velocity measurement heights. However, the roughness length can easily be eliminated by subtracting one equation from the other:

$$u(z_2) - u(z_1) = \frac{u_*}{\kappa} \cdot \left\{ \ln\left(\frac{z_2 - d}{z_1 - d} \right) - \Psi_m\left(\frac{z_2 - d}{L} \right) + \Psi_m\left(\frac{z_1 - d}{L} \right) \right\} \tag{I2}$$

As eq. (I2) does not allow a closed mathematical solution for d, iteration is required. An iteration rule is obtained by simple re-arrangement of eq. (I2):

$$d_{i+1} = z_1 - \frac{z_2 - d_i}{\exp\left\{ \frac{\kappa \cdot [u(z_2) - u(z_1)]}{u_*} + \Psi_m\left(\frac{z_2 - d_i}{L} \right) - \Psi_m\left(\frac{z_1 - d_i}{L} \right) \right\}} \tag{I3}$$

Neglecting the atmospheric stability functions Ψ_m in eq. (I3) and setting $d_{i+1} = d_i = d_0$ delivers an equation for the initial value of d:

$$d_0 = \frac{z_2 - z_1 \cdot \exp\left\{ \frac{\kappa \cdot [u(z_2) - u(z_1)]}{u_*} \right\}}{1 - \exp\left\{ \frac{\kappa \cdot [u(z_2) - u(z_1)]}{u_*} \right\}} \tag{I4}$$

In case of negative d_0 resulting from (I4), set $d_0 = 0$.

Convergence of iteration by (I3) depends on u, u_*, and L. We found by trial and error that for many cases convergence can be accelerated by using a modified iteration equation:

$$d_{i+1} = d_i \cdot (1 - r) + r \cdot \left[z_1 - \frac{z_2 - d_i}{\exp\left\{ \frac{\kappa \cdot [u(z_2) - u(z_1)]}{u_*} + \Psi_m\left(\frac{z_2 - d_i}{L} \right) - \Psi_m\left(\frac{z_1 - d_i}{L} \right) \right\}} \right] \tag{I5}$$

with

$$\mathrm{r} = 1 + \frac{u_*}{u(z_2) - u(z_1)} \tag{I6}$$

Eq. (I5) mostly converges over about ten or less iteration steps. For PLATIN, we use 15 steps to make sure the solution obtained to be stable. However, as Monin-Obukhov theory is not always met by real micrometeorological conditions, iteration sometimes fails yielding a non-convergent series of *d* or even negative *d*. But experience shows that, in general, there are still enough successful iteration results to provide a daily average of *d* which is adequate to run PLATIN.

Once *d* is known, z_{0m} is the only unknown left in the profile equation (I1). But again, there is no way to get a closed mathematical solution from (I1). Thus, z_{0m} must be iterated, too. Appropriate rearrangement of eq. (I1) provides the following iteration rule where *z* represents one of the two measurement heights for *u,* z_1 and z_2:

$$z_{0\mathrm{m},\,\mathrm{i+1}} = \frac{z - d}{\exp\left\{\frac{\kappa \cdot u(z)}{u_*} + \Psi_{\mathrm{m}}\left(\frac{z-d}{L}\right) - \Psi_{\mathrm{m}}\left(\frac{z_{0\mathrm{m},\,\mathrm{i}}}{L}\right)\right\}} \tag{I7}$$

Iteration is initialized by

$$z_{0\mathrm{m},\,0} = \frac{z - d}{\exp\left\{\frac{\kappa \cdot u(z)}{u_*}\right\}} \tag{I8}$$

which can be derived from eq. (I7) by neglecting the stability functions. Usually the iteration takes less than ten steps (a number we generally use for PLATIN).

As there are two heights with wind velocity measurements, eq. (I7) may be applied twice offering the chance for intercomparison of the results which ideally should coincide.

Appendix J

Estimation of bulk canopy resistance for water vapour from measured data

Eddy covariance measurements of sensible heat H, latent heat λE, and friction velocity u_* together with measurements of air temperature t_a and relative humidity rH can be used to estimate bulk canopy resistance for water vapour $R_{c,\,H2O}$ according to:

$$R_{c,\,H2O} = \frac{0.622 \cdot \rho_{moist\ air}}{p} \cdot \frac{e_{sat}(d+z_{0h}) - e(d+z_{0h})}{(\lambda E \cdot \lambda^{-1})} \qquad \text{(J1)}$$

with
- $\rho_{moist\ air}$ density of moist air at absolute temperature T [kg·m^{-3}]; cf. (F7) and (F8)
- p air pressure [hPa]
- $e_{sat}(d+z_{0h})$ saturation water vapour pressure at $z = d + z_{0h}$ [hPa]; cf. eqs. (F2) and (F3)
- $e(d+z_{0h})$ actual water vapour pressure at $z = d + z_{0h}$ [hPa]
- λ latent heat of water vaporisation at $z = d + z_{0h}$ [J·kg^{-1}]; cf. eq. (28)

Canopy surface temperature T_s needed for e calculations is related to potential canopy surface temperature as described by eq. (25). Actual water vapour pressure $e(d+z_{0h})$ is given by:

$$e(d+z_{0h}) = e(z_{ref,\,T}) + \frac{(\lambda E \cdot \lambda^{-1}) \cdot p}{0.622 \cdot \rho_{moist\ air}} \cdot \left(R_{ah}(d+z_{0m}, z_{ref,\,T}) + R_{b,\,heat}\right) \qquad \text{(J2)}$$

with
- $e(z_{ref,\,T})$ actual water vapour pressure at $z = z_{ref,\,T}$ [hPa]; cf. eq. (F4)
- $R_{ah}(d+z_{0m}, z_{ref,\,T})$ atmospheric resistance [s·m^{-1}]; cf. eqs. (2) and (3)
- $R_{b,\,heat}$ quasi-laminar resistance for sensible heat [s·m^{-1}]; cf. eq. (7)

Atmospheric resistance $R_{ah}(d+z_{0m}, z_{ref,\,T})$, quasi-laminar resistance for sensible heat $R_{b,\,heat}$, and Monin-Obukhov length L (cf. eq. (5)), needed for the resistance estimations, are calculated using measured friction velocity u_* and sensible heat flux H.

As described in Chapter 2.3, bulk canopy resistance $R_{c,\,H2O}$ is a composite resistance describing stomatal and cuticular transpiration and evaporation. In PLATIN, $R_{c,\,H2O}$ is approximated by a weighted combination of soil resistance $R_{soil,\,H2O}$, bulk stomatal resistance $R_{c,\,stom,\,H2O}$ and bulk cuticle resistance $R_{c,\,cut,\,H2O}$ known for a fully developed canopy (without senescent leaves) under optimum conditions for maximal transpiration. The weights β^* and β depend on the actual canopy development stage taking into account the transition from a dense canopy to a sparse canopy as given by eq. (8).

Consequently, for a given canopy development stage bulk stomatal resistance $R_{c,\,stom,\,H2O}$ or bulk stomatal conductance for water vapour $g_{c,\,stom,\,H2O}$ can be calculated by:

$$g_{c,\,stom,\,H2O} = \frac{1-\beta^*}{R_{c,\,stom,\,H2O}} = \frac{1}{R_{c,\,H2O}} - \frac{1-\beta^*}{R_{c,\,cut,\,H2O}} - \frac{\beta}{R_{soil,\,H2O}} \qquad \text{(J3)}$$

For a dense canopy, which may be assumed when evaporation from soil is below 5 % of total evapotranspiration, $R_{c,\,H2O}$ is often used as a first estimate of $R_{c,\,stom,\,H2O}$. We found that this assumption is associated with a mean error of approx. 10 %. Therefore, eq. (J3) represents a useful tool to derive stomatal resistance directly from measurement-based latent and sensible heat flux, friction velocity, Monin-Obukhov length and canopy resistance for water vapour. These measurement-based entities can serve for calibration of PLATIN during daylight hours with global radiation $S_t \geq 100$ W·m^{-2} if the subsequent quality criteria are met:

- consistency of measured data set indicated by: $e_{sat}(d+z_{0h}) - e(d+z_{0h}) > 0$ hPa
- consistency of measured λE as indicated by positive values during daylight hours
- no rainfall
- interception reservoir empty for current and previous data set (cf. eqs. (17) and (18))

- relative air humidity rH < 75 %
- integral turbulence characteristic (ITC) test according to Thomas and Foken (2002)
- stationarity tests for friction velocity, latent and sensible heat according to Foken and Wichura (1996)

Additionally, as PLATIN is based on the canopy energy balance, data sets to be used for model calibration are required to closely approach the energy balance closure. Therefore, the following criteria must be satisfied:

- closure of energy balance: ABS($R_{net} - G - \lambda E - H$) < 25 W·m^{-2}

This holds also for nighttime, where only measured sensible heat fluxes can be used for model calibration.

Appendix K

Upscaling of meteorological data measured above short vegetation to a height of 50 m

If PLATIN for Excel is to be applied to forest ecosystems, information on the state of the air above the forest canopy is required (wind speed, temperature, humidity, concentrations). If data are not available they have to be estimated from measurements above short vegetation near the forest. While this does not impose serious problems for daylight hours with well established turbulence, transition times with growing internal boundary layers near the surface and especially the night with vertically high reaching, sometimes strongly stable stratification allow only for a rough estimation procedure.

• *daytime with unstable atmospheric stratification regime*

Once unstable stratification is established on daylight hours (MO length $L < 0$ m), vertical exchange leads to effective coupling between surface fluxes and fluxes in heights well above the surface. Neglecting occasional horizontal advection (which, as a matter of fact, can never be accounted for in one-dimensional models like PLATIN), it seems reasonable to extend the concept of height-constant fluxes up to heights of some tens of metres. Monin-Obukhov theory can then be used to predict wind speed, temperature, and humidity above the forest canopy from data measured at a nearby short-vegetation location. For the height up to which profiles are to be extended we arbitrarily select 50 m above ground in the field, making sure to be well above the canopy even in case of tall forests. The calculation procedure, which we shortly call upscaling procedure, will be described in the following.

The horizontal wind velocity u at $z = 50$ m can be obtained from the vertical profile equation based on Monin-Obukhov theory:

$$u(z) = \frac{u_*}{\kappa} \cdot \left[\ln\left(\frac{z - d}{z_{0\mathrm{m}}} \right) - \Psi_{\mathrm{m}}\left(\frac{z - d}{L} \right) + \Psi_{\mathrm{m}}\left(\frac{z_{0\mathrm{m}}}{L} \right) \right] \qquad \text{(K1)}$$

The parameterisations for the atmospheric stability functions for momentum Ψ_{m} and sensible heat Ψ_{h} are described in Appendix C. The calculation friction velocity is computed from eq. (4).

Estimation of air temperature at $z = 50$ m above ground is based on the calculation of the potential temperature θ [K]:

$$\theta(z) = \theta(d + z_{0\mathrm{m}}) - \frac{H \cdot R_{\mathrm{ah}}(z, d + z_{0\mathrm{m}})}{\rho_{\mathrm{moist\ air}} \cdot c_{\mathrm{p,\,moist\ air}}} \qquad \text{(K2)}$$

from which the absolute air temperature T can easily be derived using the relation given in eq. (6):

$$\theta(z) = T(z) + (z \cdot \Gamma_{\mathrm{d}}) \qquad \text{(K3)}$$

with $\Gamma_{\mathrm{d}} = -9.76$ K·km^{-1}

assuming $\rho_{\mathrm{moist\ air}}(z) \approx \rho_{\mathrm{moist\ air}}(z_{\mathrm{ref\ T}}) \cong \rho_{\mathrm{moist\ air}}(d+z_{0\mathrm{m}})$

and $c_{\mathrm{p,\,moist\ air}}(z) \approx c_{\mathrm{p,\,moist\ air}}(z_{\mathrm{ref\ T}}) \cong c_{\mathrm{p,\,moist\ air}}(d+z_{0\mathrm{m}})$.

The turbulent atmospheric resistance R_{ah} between the heights $z = 50$ m and $z = d+z_{0\mathrm{m}}$ is given by:

$$R_{\mathrm{ah}}(z, d + z_{0\mathrm{m}}) = \frac{\ln\left(\frac{z - d}{z_{0\mathrm{m}}} \right) - \Psi_{\mathrm{h}}\left(\frac{z - d}{L} \right) + \Psi_{\mathrm{h}}\left(\frac{z_{0\mathrm{m}}}{L} \right)}{\kappa \cdot u_*} \qquad \text{(K4)}$$

The potential air temperature θ at $z = d + z_{0m}$ follows from:

$$H = \rho_{\text{moist air}} \cdot c_{\text{p, moist air}} \cdot \frac{\theta(d + z_{0m}) - \theta(z_{\text{ref, T}})}{R_{\text{ah}}(z_{\text{ref, T}}, d + z_{0m})} \approx \rho_{\text{moist air}} \cdot c_{\text{p, moist air}} \cdot \frac{T(d + z_{0m}) - T(z_{\text{ref, T}})}{R_{\text{ah}}(z_{\text{ref, T}}, d + z_{0m})} \quad \text{(K5)}$$

with $z_{\text{ref, T}} \approx 2$ m above ground

The relative humidity *rH* at $z = 50$ m above ground is defined by:

$$rH(z) = \frac{e_{\text{water vapour pressure}}(z)}{e_{\text{saturation water vapour pressure}}(z)} \cdot 100 \quad \text{(K6)}$$

The water vapour pressure *e* at $z = 50$ m is calculated from modelled latent heat flux λE and the specific humidity of air *q* at $z = 50$ m, which in turn is estimated from *q* at $z = d + z_{0m}$ making use of the turbulent atmospheric resistance R_{ah} between the two heights:

$$e_{\text{water vapour pressure}}(z) = \frac{p \cdot q(z)}{0.622 + 0.378 \cdot q(z)} \quad \text{(K7)}$$

with *p* the air pressure [hPa] neglecting the relatively weak height dependence of *p* which is about 1/8 hPa·m^{-1} in the lower 100 m of the atmosphere (e.g. Liljequist and Cehak, 1979).

The specific humidity of air at $z = 50$ m above ground is given by:

$$q(z) = q(d + z_{0m}) - \frac{\lambda E \cdot R_{\text{ah}}(z, d + z_{0m})}{\lambda \cdot \rho_{\text{moist air}}} \quad \text{(K8)}$$

with λ latent heat of water vaporisation (eq. (28))
and

$$q(d + z_{0m}) = q(z_{\text{ref, T}}) + \frac{\lambda E \cdot R_{\text{ah}}(z_{\text{ref, T}}, d + z_{0m})}{\lambda \cdot \rho_{\text{moist air}}} \quad \text{(K9)}$$

assuming $\rho_{\text{moist air}}(z) \approx \rho_{\text{moist air}}(z_{\text{ref T}}) \cong \rho_{\text{moist air}}(d+z_{0m})$.

The saturation water vapour pressure of the atmosphere at $z = 50$ m is calculated according to eqs. (F2) and (F3) in Appendix F.

The ozone concentration ρ_{O3} at $z = 50$ m above ground is approximated by:

$$\rho_{O3}(z) = -\left[F_{\text{total}}(O_3) \cdot R_{\text{ah}}(z, d + z_{0m})\right] + \rho_{O3}(d + z_{0m}) \quad \text{(K10)}$$

Like the other profile equations mentioned before, eq. (K10) results from Monin-Obukhov theory which assumes vertically constant fluxes. In case of ozone this means a drastic simplification as it completely neglects the influence of air chemistry. However, chemistry modelling would be far beyond the aim of simply estimating missing data above the forest canopy.

• *nighttime with stable atmospheric stratification regime*

During night, surface cooling leads to increasing atmospheric stability finally restricting the layer of presumably height-constant fluxes to a couple of metres above surface. The air above this shallow layer

is in a so-called z-less state (Mahrt and Vickers, 2003; Basu et al., 2006) which means that fluxes are determined by local physics and, if ever, are only loosely correlated with surface fluxes. As Monin-Obukhov theory is not applicable especially during situations with strong stable atmospheric stratification, i.e. low wind velocities, no equations like that described above for daylight hours can be given for the night. Nevertheless, there should be a way of roughly estimating the desired data at height 50 m.

In the first place, as a special case, we shall deal with very stable atmospheric stratification. We start with the assumption that the air above ten metres height can generally be described by z-less scaling (cf. e.g. Mahrt and Vickers, 2003). Combination of the definition of vertical momentum mixing length *l*,

$$l(z) \equiv \frac{u_*}{\partial u / \partial z} \tag{K11}$$

where z height z above ground [m]
u_* friction velocity [m·s^{-1}]
u wind speed at height z [m·s^{-1}]

and the z-less mixing length approximation according, e. g., to Mahrt and Vickers (2003),

$$l = 0.5 \cdot \frac{u_*}{N} \tag{K12}$$

yields (with gravitational acceleration g = 9.81 m·s^{-2} and potential temperature θ)

$$\frac{\partial u}{\partial z} = 2 \sqrt{\frac{g}{\theta} \cdot \frac{\partial \theta}{\partial z}} \tag{K13}$$

when it is taken into account that the Brunt-Vaisala frequency N is given by (cf. Stull, 1988):

$$N = \sqrt{\frac{g}{\theta} \cdot \frac{\partial \theta}{\partial z}} \tag{K14}$$

As the potential temperature gradient can be assumed vertically constant for the height range considered (cf. e.g. large eddy simulation results in Basu et al., 2006), the partial derivatives in (K13) may be replaced by differential quotients. After additional introduction of an effective mean potential temperature $\bar{\theta}$, (K13) becomes:

$$\frac{\Delta u}{\Delta z} = 2 \sqrt{\frac{g}{\bar{\theta}} \cdot \frac{\Delta \theta}{\Delta z}} \tag{K15}$$

With the potential temperature gradient in the order of 1 K·100 m^{-1} (cf. e.g. Figure 3 in Basu et al., 2006) and a reasonable mean temperature of 280 K, (K15) leads to

$$u(50\,\mathrm{m}) = u(10\,\mathrm{m}) + 1.5\,\mathrm{m} \cdot \mathrm{s}^{-1} \tag{K16}$$

Especially for calm weather conditions it may yield too high a value of u(50 m). As the majority of the nocturnal Linden grassland site wind data is characterized by low winds, we often found (K16) to yield nocturnal u(50 m) considerably exceeding u(50 m) during subsequent daylight hours as calculated by eq. (K1). Because the daily course of u(50 m) should exhibit a certain continuity, we looked for another way to estimate the nocturnal u(50 m). Applying eq. (K1) for nighttime data sets, we found on the average that for u(10 m) > 2 m·s^{-1} the ratio u(50 m)·u(10 m)$^{-1}$ is about 1.5 ± 0.1 while it significantly decays for lower values of u(10 m). We assume that eq. (K1) is applicable in case of nocturnal u(10 m) > 2 m·s^{-1} and suggest to use the factor 1.5 for lower wind speed:

$$u(50\,\mathrm{m}) = u(10\,\mathrm{m}) \cdot 1.5 \qquad \text{(K17)}$$

With the potential temperature gradient in the order of 1 K·100 m^{-1} the potential temperature at 50 m turns out to be:

$$\theta(50\,\mathrm{m}) = \theta(10\,\mathrm{m}) + 0.4\,\mathrm{K} \qquad \text{(K18)}$$

Unless in the very rare case of nocturnal air warming induced by horizontal advection, θ(50 m) should be limited by the last daylight-hour value.

As temperature is measured at the meteorological screen height, i.e. 2 m above ground, the potential temperature difference between 2 and 10 m has still to be estimated. Additionally, potential temperature has to be transformed into actual temperature, as the latter is needed as input to PLATIN. As the nocturnal forest energy balance will not be very sensitive to the exact temperature at 50 m height, we restrict ourselves to a rough order-of-magnitude estimate: The temperature gradient at higher levels above ground is of the order 10^{-2} K·m^{-1}, while it is of the order 1 K·m^{-1} near the ground. Therefore we assume an intermediate lapse rate of 10^{-1} K·m^{-1} for the layer between 2 and 10 m. Combining this with (K18) and taking into account that actual temperature at 50 m height is about 0.4 K higher than potential temperature at this level (cf. eq. (K3)), we arrive at the final rough approximation equation for the actual temperature:

$$T(50\,\mathrm{m}) = T(2\,\mathrm{m}) + 1\,\mathrm{K} \qquad \text{(K19)}$$

It has already been mentioned that, unless there is a temperature increase due to horizontal advection of warmer air, the temperature at 50 m height should not exceed the respective last daylight-hour value. This also holds for the actual temperature as estimated from (K19).

To approximate air humidity at 50 m height, we assume a homogeneous air mass with vertically constant mixing ratio between water vapour and dry air, which is practically the same as to assume vertically constant specific humidity. Therefore we suggest as a rough estimate:

$$q(50\,\mathrm{m}) = q(2\,\mathrm{m}) \qquad \text{(K20)}$$

Especially during night, the O_3 concentration at reference height can be reduced significantly by reaction with NO. The extent of reduction depends on the NO source strength of the ecosystem under consideration or e.g. of exhaust emissions. Taking into account a stable atmospheric stratification regime it can be assumed, that the mean O_3 gradient during night be greater than the mean gradient during unstable stratification. We calculate a mean ratio for $\rho_{O3}(50\,\mathrm{m}) \cdot \rho_{O3}(z_{ref})$ of approx. 1.1 under unstable atmospheric stratification regime and suggest this value as a rough estimate for nighttime where we accept a probable underestimation of the upscaled O_3 concentration at z = 50 m:

$$\rho_{O3}(50\,\mathrm{m}) = \rho_{O3}(z_{ref}) \cdot 1.1 \qquad \text{(K21)}$$

• *transition times*

The micrometeorological processes during transition times would deserve a special treatment, because neither the upscaling procedure for daylight hours nor the one for nighttime can be applied to transition hours. It must be stated that there is no physically based model to describe the interrelation of the meteorological entities at 50 m height and those at the ground. For wind speed this problem is overcome by simply applying the scheme described in context of eq. (K17), i.e. by calculating wind speed at 50 m by eq. (K17) for u(10 m) ≤ 2 m·s^{-1} and by eq. (K1) for u(10 m) > 2 m·s^{-1}. Ozone concentration and air temperature at 50 m during transition times must be calculated by linearly interpolating 50 m data between day and night (in the late afternoon and early evening) and vice versa (in the early morning hours). Data gaps of relative humidity are closed by calculating relative humidity from temporally interpolated data of specific humidity and air temperature.

• *mean diurnal variation of micrometeorological parameters*

The mean diurnal variations of horizontal wind velocity, air temperature, relative humidity and ozone concentration measured at reference height and upscaled to a height of 50 m above ground according to the procedure described above are illustrated in Figure K1.

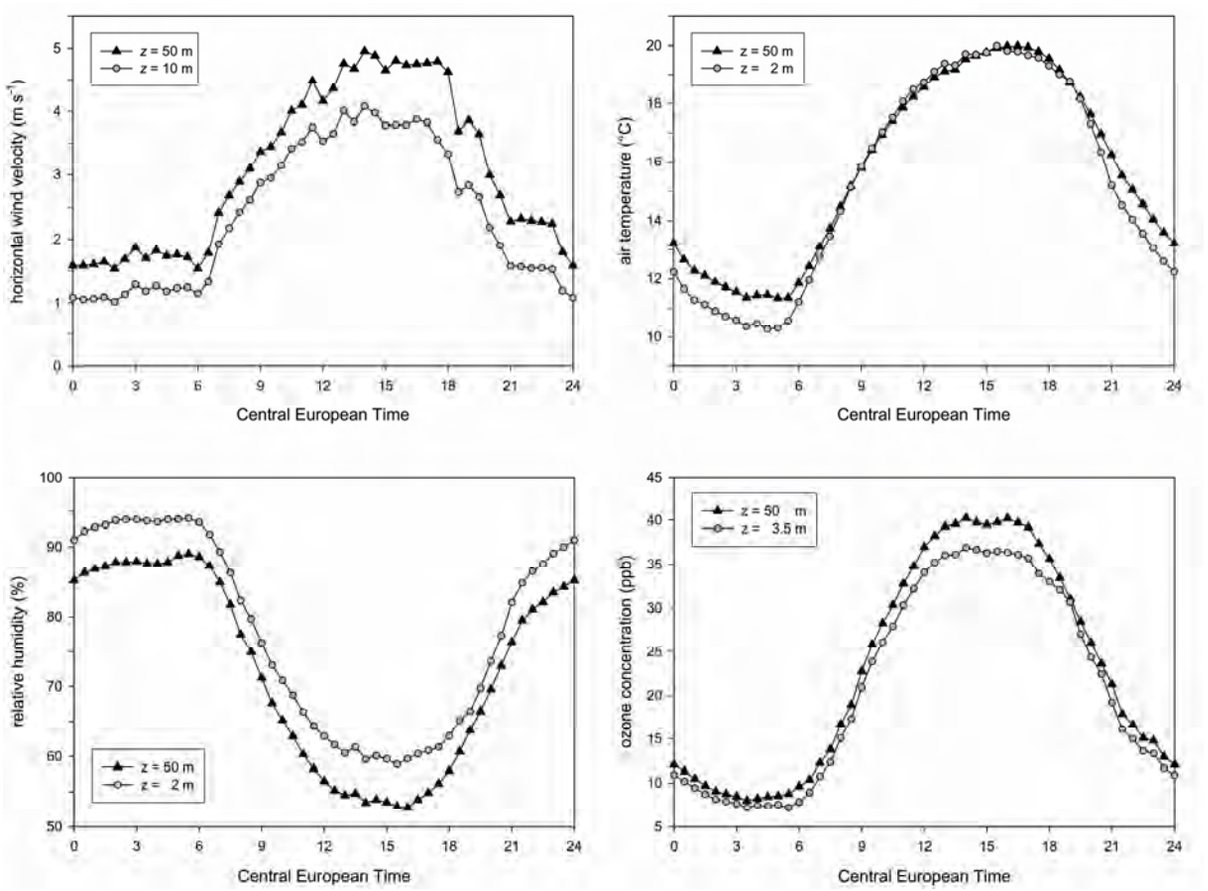

Fig. K1
Mean diurnal variations of horizontal wind velocity, air temperature, relative humidity and ozone concentration measured at reference height in June 2004 and upscaled to a height of 50 m above ground

• *reference surface for upscaling procedure*

In principle, the application of the "daytime" approach presupposes the knowledge of all the canopy characteristics (e.g. $R_{c,\,stom,\,min}$, Jarvis factors, *LAI* development) and input parameters (e.g. soil moisture) as described in this manual. If these informations are not available, a reference surface should be applied. We recommend a grassland with an assumed height *h* of 0.12 m and a short-wave albedo α of 0.23 as described in the FAO guideline for computing crop evapotranspiration (Allen et al., 2002). Soil moisture is assumed to be constant at 70 % of field capacity. Instead of a fixed surface resistance $R_{c,\,H2O}$ we recommend to apply e.g. the canopy characteristics of the Linden grassland site. According to Allen et al. (2002) this "reference surface closely resembles an extensive surface of green, well-watered grass of uniform height, actively growing and completely shading the ground".

At least the following input parameters must be measured at the monitoring station: global radiation, horizontal wind velocity at 10 m above ground, air temperature, relative humidity and ozone concentration.

Note:
Conversion of ozone concentration unit $\mu g \cdot m^{-3}$ into ppb at upscaling height z according to eq. (M1) presuppose an upscaling of atmospheric pressure $p(z_{ref})$:

$$p(z) = p(z_{ref}) \cdot \exp\left(- \frac{g \cdot (z - z_{ref})}{R \cdot T_m} \right) \quad \text{(K22)}$$

with g gravitational acceleration ($\cong 9.81\ m \cdot s^{-2}$)
R gas constant for dry air ($= 287.04\ J \cdot kg^{-1} \cdot K^{-1}$)
T_m average temperature of the air layer under consideration ($\approx [T(z) + T(z_{ref})] \cdot 0.5$)

Appendix L

Calculation of photosynthetic photon flux density from global radiation

According to VDI 3786 sheet 13 (1993) *PPFD* can be calculated from the global radiation with an accuracy sufficient for practical purposes. For countries in the centre of Europe, the following conversion factors can be applied.

$$PPFD = a \cdot S_t \qquad \text{(L1)}$$

with *PPFD* photosynthetic photon flux density [$\mu mol \cdot m^{-2} \cdot s^{-1}$]
S_t global radiation [$W \cdot m^{-2}$]
a conversion factor [$\mu mol\ W^{-1} \cdot s^{-1}$]

The variation of factor *a* with time of year is given in Table L1.

Table L1: Variation of factor *a* with time of year

Month	Means of all days *a* in $\mu mol\ W^{-1} \cdot s^{-1}$
January	2.01
February	1.90
March	1.95
April	1.96
May	2.04
June	2.07
July	2.07
August	2.10
September	2.07
October	2.07
November	2.06
December	2.03
total of year	2.03

Appendix M

Conversion of units

The denotation follows IUPAC (1993).

gas concentration

$$\rho_A = (\chi_A \cdot \alpha_{cf}) \cdot \left(\frac{M_A \cdot \beta_{cf}}{V_m \cdot \gamma_{cf}}\right) \cdot \left(\frac{T_0}{T}\right) \cdot \left(\frac{p}{p_0}\right) \quad \text{(M1)}$$

with
- ρ_A partial mass density (mass concentration) of a gaseous species A [µg·m^{-3}]
- χ_A mixing ratio or mole fraction of a gaseous species A [ppm]
- α_{cf} mixing ratio conversion factor (α_{cf} = 10^{-6} mol·mol^{-1}·ppm^{-1})
- M_A molar mass of a gaseous species A [g·mol^{-1}]
- β_{cf} mass conversion factor (β_{cf} = 10^6 µg·g^{-1})
- V_m molar volume (V_m = 22.4 l·mol^{-1})
- γ_{cf} volume conversion factor (γ_{cf} = 10^{-3} m^3·l^{-1})
- T_0 standard temperature (T_0 = 273.15 K)
- T actual absolute temperature [K]; $\frac{T - T_0}{\mathrm{K}} = \frac{t_a}{°\mathrm{C}}$
- t_a actual air temperature [°C]
- p_0 standard atmospheric pressure (p_0 = 1013.25 hPa)
- p actual atmospheric pressure [hPa]

$$p_A = (\chi_A \cdot \alpha_{cf}) \cdot p = c_A \cdot (V_m \cdot \gamma_{cf}) \cdot p \quad \text{(M2)}$$

with
- p_A partial pressure of a gaseous species A [Pa]
- χ_A mixing ratio or mole fraction of a gaseous species A [ppm]
- α_{cf} mixing ratio conversion factor (α_{cf} = 10^{-6} mol·mol^{-1}·ppm^{-1})
- p atmospheric pressure [Pa]
- c_A concentration (amount concentration) of a gaseous species A [mol·m^{-3}]
- V_m molar volume (V_m = 22.4 l·mol^{-1})
- γ_{cf} volume conversion factor (γ_{cf} = 10^{-3} m^3·l^{-1})

$$\rho_A = c_A \cdot (M_A \cdot \beta_{cf}) \quad \text{(M3)}$$

with
- ρ_A partial mass density (mass concentration) of a gaseous species A [µg·m^{-3}]
- c_A concentration (amount concentration) of a gaseous species A [mol·m^{-3}]
- M_A molar mass of a gaseous species A [g·mol^{-1}]
- β_{cf} mass conversion factor (β_{cf} = 10^6 µg·g^{-1})

$$c_A = (\chi_A \cdot \alpha_{cf}) \cdot \left(\frac{1}{V_m \cdot \gamma_{cf}}\right) \cdot \left(\frac{T_0}{T}\right) \cdot \left(\frac{p}{p_0}\right) \quad \text{(M4)}$$

with
- c_A concentration (amount concentration) of a gaseous species A [mol·m^{-3}]
- χ_A mixing ratio or mole fraction of a gaseous species A [ppm]
- α_{cf} mixing ratio conversion factor (α_{cf} = 10^{-6} mol·mol^{-1}·ppm^{-1})
- V_m molar volume (V_m = 22.4 l·mol^{-1})

γ_{cf} volume conversion factor ($\gamma_{cf} = 10^{-3}$ m^3·l^{-1})
T_0 standard temperature (T_0 = 273.15 K)
T actual absolute temperature [K]; $\frac{T - T_0}{\mathrm{K}} = \frac{t_a}{°\mathrm{C}}$
t_a actual air temperature [°C]
p_0 standard atmospheric pressure (p_0 = 1013.25 hPa)
p actual atmospheric pressure [hPa]

vertical flux density of gaseous species F_A

$$F(\mathrm{A})[\mathrm{g}\cdot\mathrm{m}^{-2}\cdot\mathrm{s}^{-1}] = F(\mathrm{A})[\mathrm{mol}\cdot\mathrm{m}^{-2}\cdot\mathrm{s}^{-1}]\cdot M_A \quad \text{(M5)}$$

with F(A) vertical flux density of a gaseous species A [g·m^{-2}·s^{-1} or mol·m^{-2}·s^{-1}]
M_A molar mass of a gaseous species A [g·mol^{-1}]

conductance for gaseous species g_A

$$g_A[\mathrm{m}\cdot\mathrm{s}^{-1}] = g_A[\mathrm{mol}\cdot\mathrm{m}^{-2}\cdot\mathrm{s}^{-1}]\cdot\left\{\left(\frac{1}{V_m\cdot\gamma_{cf}}\right)\cdot\left(\frac{T_0}{T}\right)\cdot\left(\frac{p}{p_0}\right)\right\}^{-1} \quad \text{(M6)}$$

with g_A conductance for a gaseous species A [mol·m^{-2}·s^{-1} or m·s^{-1}]
V_m molar volume (V_m = 22.4 l·mol^{-1})
γ_{cf} volume conversion factor ($\gamma_{cf} = 10^{-3}$ m^3·l^{-1})
T_0 standard temperature (T_0 = 273.15 K)
T actual absolute temperature [K]; $\frac{T - T_0}{\mathrm{K}} = \frac{t_a}{°\mathrm{C}}$
t_a actual air temperature [°C]
p_0 standard atmospheric pressure (p_0 = 1013.25 hPa)
p actual atmospheric pressure [hPa]

List of symbols

Symbol	Description	Bezeichnung	unit/Einheit
α	short-wave albedo	kurzwellige Albedo der Erd- bzw. Bestandesoberfläche	dimensionless
α_{cf}	mixing ratio conversion factor	Molenbruch-Konversionsfaktor	10^{-6} mol·mol^{-1} ppm^{-1}
α_c	fraction of glycolate carbon not returned to the chloroplast	Fraktion des Glycolat-C, der nicht zurück in die Chloroplasten transloziert wird	dimensionless
β	weighting factor for canopy development stage based on LAI_{total} or SAI	Wichtungsfaktor für den Entwicklungszustand des Bestandes basierend auf LAI_{total} bzw. SAI	dimensionless
β^*	weighting factor for canopy development stage based on $LAI_{non\text{-}senescent}$	Wichtungsfaktor für den Entwicklungszustand des Bestandes basierend auf $LAI_{nicht\text{-}seneszent}$	dimensionless
β^*_{shaded}	weighting factor for canopy development stage based on the shaded $LAI_{non\text{-}senescent}$	Wichtungsfaktor für den Entwicklungszustand des Bestandes basierend auf $LAI_{nicht\text{-}seneszent}$ der Schattenblätter	dimensionless
β^*_{sunlit}	weighting factor for canopy development stage based on the sunlit $LAI_{non\text{-}senescent}$	Wichtungsfaktor für den Entwicklungszustand des Bestandes basierend auf $LAI_{nicht\text{-}seneszent}$ der Sonnenblätter	dimensionless
β_{cf}	mass conversion factor	Molekulargewicht-Konversionsfaktor	10^{6} µg·g^{-1}
Γ	vegetation type-specific ratio of ammonium to protons in the apoplast	vegetationsspezifisches Verhältnis von NH_4^+ und H^+ im Apoplasten	mol·mol^{-1}
Γ_*	CO_2 compensation point in the absence of mitochondrial respiration	CO_2-Kompensationspunkt der Bruttophotosynthese	Pa
Γ_d	dry adiabatic lapse rate	trockenadiabatischer Temperaturänderungsbetrag	K·km^{-1}
γ	psychrometric constant	Psychrometerkonstante	hPa·K^{-1}
γ_{cf}	volume conversion factor	Molvolumen-Konversionsfaktor	10^{-3} m^3·l^{-1}
Δ_{sun}	sun declination	Sonnendeklination	radians, Bogenmaß
Δt	time interval	Zeitintervall	s
Δz	e.g. depth of canopy layer	z.B. Bestandestiefe	m
δ_a	carbon allocation coefficient	C-Allokationskoeffizient	dimensionless
ε	effective long-wave emissivity of the canopy	effektiver langwelliger Emissionsgrad der Erd- bzw. Bestandesoberfläche	dimensionless
ζ	dimensionless height	dimensionslose Höhe	dimensionless
θ	potential air temperature	potentielle Lufttemperatur	K
$\overline{\overline{\theta}}$	average potential air temperature of the layer under consideration	potentielle Luftschicht-Mitteltemperatur	K
θ_s	potential canopy surface temperature	potentielle Bestandesoberflächentemperatur	K
ϑ	empirical curvature factor	empirischer Kurvaturfaktor	dimensionless
κ	von Kármán constant	von-Kármán-Konstante	dimensionless
λ	latent heat of water vaporisation	Verdunstungswärme	J·kg^{-1}
λE	turbulent vertical flux density of latent heat (evapotranspiration)	vertikale turbulente Flussdichte latenter Wärme (Evapotranspiration)	W·m^{-2}
$\lambda E_{evaporation}$	evaporation	Evaporation	W·m^{-2}
$\lambda E_{tranpiration}$	transpiration	Transpiration	W·m^{-2}
λ_{geo}	longitude	geographische Länge	degree, Grad
ν	kinematic viscosity of dry air	molekulare kinematische Viskosität der Luft	m^2·s^{-1}
$\rho_A(d+z_{0c})$	partial mass density of a gaseous species A at height $z = d+z_{0c} = d+z_{0h}$	Partialdichte des Spurengases A in der Höhe $z = d+z_{0c} = d+z_{0h}$	µg·m^{-3}
$\rho_A(d+z_{0m})$	partial mass density of a gaseous species A at height $z = d+z_{0m}$	Partialdichte des Spurengases A in der Höhe $z = d+z_{0m}$	µg·m^{-3}

Symbol	Description	Bezeichnung	unit/Einheit
$\rho_A(z_{ref,A})$, $\rho_A(z_{ref})$	partial mass density of a gaseous species A at height $z = z_{ref,A}$	Partialdichte des Spurengases A in der Messhöhe $z = z_{ref,A}$	$\mu g \cdot m^{-3}$
$\rho_{A,comp}$	canopy compensation concentration of gaseous species A	Bestandeskompensationskonzentration für die Spurengasspezies A	$\mu g \cdot m^{-3}$
$\rho_{A,soil}$	partial mass density of a trace gas A in the soil	Partialdichte des Spurengases A im Boden	$\mu g \cdot m^{-3}$
$\rho_{A,stom}$	partial mass density of a trace gas A in the substomatal cavities	Partialdichte des Spurengases A in den substomatären Räumen	$\mu g \cdot m^{-3}$
ρ_{cd}	canopy reflection coefficient for diffuse PAR	Bestandesreflektionskoeffizient für diffuse photosynthetisch-aktive Strahlung	dimensionless
ρ_{cb}	canopy reflection coefficient for beam PAR	Bestandesreflektionskoeffizient für direkte photosynthetisch-aktive Strahlung	dimensionless
ρ_h	reflection coefficient for beam PAR of a canopy with horizontal leaves	Bestandesreflektionskoeffizient für direkte photosynthetisch-aktive Strahlung für einen Pflanzenbestand mit horizontaler Blattausrichtung	dimensionless
$\rho_{dry\ air}$	density of dry air	Dichte der trockenen Luft	$kg \cdot m^{-3}$
$\rho_{moist\ air}$	density of moist air	Dichte der feuchten Luft	$kg \cdot m^{-3}$
σ	Stefan-Boltzmann constant	Stefan-Boltzmann-Konstante	$W \cdot m^{-2} \cdot K^{-4}$
σ_{PAR}	leaf scattering coefficient of PAR	PAR Blatt-Streuungskoeffizient	dimensionless
ϕ	solar elevation angle	Sonenhöhe	radians
ϕ_{cf}	combined conversion factor	Umrechnungsfaktor	$m^3 \cdot \mu mol^{-3}$
φ_d	day angle	Tageswinkel	radians, Bogenmaß
φ_{geo}	latitude	geographische Breite	radians, Bogenmaß
φ_h	hour angle	Stundenwinkel	radians, Bogenmaß
χ_A	mole fraction of gaseous species A	Mischungsverhältnis bzw. Molenbruch der Spurengasspezies A	ppm, $\mu mol \cdot mol^{-1}$
Ψ_h	atmospheric stability function for sensible heat	integrierte Schichtungsfunktion für fühlbare Wärme	dimensionless
Ψ_m	atmospheric stability function for momentum	integrierte Schichtungsfunktion für Impuls	dimensionless
ω	convexity coefficient defining the smoothness of the transition between f_T and f_M	Faktor, der den Übergang zwischen den f_T und f_M bestimmt	dimensionless
$a_{1,Gphs}$	empirical constant	empirische Konstante	dimensionless
$a_{2,Gphs}$	empirical constant	empirische Konstante	dimensionless
A	canopy assimilation	Bestandesbruttophotosynthese	$\mu mol \cdot m^{-2} \cdot s^{-1}$
A_c	Rubisco-limited rate of CO_2 assimilation	Rubisco-limitierte Bestandesbruttophotosynthese	$\mu mol \cdot m^{-2} \cdot s^{-1}$
A_j	electron-transport limited rate of CO_2 assimilation	Elektronentransport-limitierte Bestandesbruttophotosynthese	$\mu mol \cdot m^{-2} \cdot s^{-1}$
A_{net}, $A_{net,canopy}$	net rate of canopy photosynthesis	Bestandesnettophotosynthese	$\mu mol \cdot m^{-2} \cdot s^{-1}$
A'_{net}	24-h integrated canopy net photosynthesis of the previous day	integrierte Bestandesnettophotosynthese des vergangenen Tages	$\mu mol \cdot m^{-2} \cdot s^{-1}$
A_p	triose phosphate utilization-limited rate of CO_2 assimilation	durch Mangel an anorganischem P limitierte Bestandesbruttophotosynthese	$\mu mol \cdot m^{-2} \cdot s^{-1}$
a_{NH3}	empirical constant	empirische Konstante	dimensionless
a_{PAR}	atmospheric transmission coefficient of PAR for clear sky conditions	atmosphärischer Transmissionskoeffizient für PAR bei wolkenfreiem Himmel	dimensionless
a_{soil}	empirical constant	empirische Konstante	mm^{-1}
$a_{Stref,1}$	empirical coefficient	empirischer Koeffizient	$W \cdot m^{-2}$
$a_{Stref,2}$	empirical coefficient	empirischer Koeffizient	$W \cdot m^{-2}$

Symbol	Description	Bezeichnung	unit/Einheit
b_{INT}	constant of proportionality	Proportionalitätskonstante	mm
c_A	concentration of gaseous species A	Konzentration des Spurengases A	$mol \cdot m^{-3}$
c_i	intercellular CO_2 concentration	CO_2-Konzentration in den Interzellularen	$\mu mol \cdot m^{-3}$
c_{LAI}	mean vegetation type-specific attenuation coefficient	mittlerer Strahlungsextinktionskoeffizient des Pflanzenbestandes	dimensionless
c_{NH3}	dimension adaptation factor	Faktor zur Dimensionsadaptation	$K \cdot \mu g \cdot m^{-3}$
$c_{p,\ dry\ air}$	specific heat of dry air at a constant pressure	spezifische Wärme von trockener Luft bei konstantem Druck	$m^2 \cdot s^{-2} \cdot K^{-1}$
$c_{p,\ moist\ air}$	specific heat of moist air at a constant pressure	spezifische Wärme von feuchter Luft bei konstantem Druck	$m^2 \cdot s^{-2} \cdot K^{-1}$
c_1, c_2	empirical constant of the Jarvis CO_2 function describing dependence of photosynthesis rate on ambient CO_2 concentration	Konstanten, die die Abhängigkeit der Photosyntheserate von der CO_2-Konzentration in der Umgebungsluft in der Jarvis-CO_2-Funktion beschreiben	dimensionless, ppm
CET	Central European Time	mitteleuropäische Zeit	h
Cl	clay content	Tongehalt	%
d	displacement height	Verschiebungshöhe	m
$d+z_{0c}$	sink height of a trace gas	Niveau der Spurengassenke	m
$d+z_{0m}$	momentum sink height	Niveau der Impulssenke	m
D_A	diffusivity of a trace gas A in air	molekularer Diffusionskoeffizient der Spurengasspezies A in Luft	$m^2 \cdot s^{-1}$
d_p	aerodynamic diameter of particles	aerodynamischer Partikeldurchmesser	µm
DT	duration of time interval	Dauer des Messintervalls	h
E	actual evapotranspiration	aktuelle Evapotranspiration	mm
E_{pot}	potential evapotranspiration	potentielle Evapotranspiration	mm
E_a	activation energy	Aktivierungsenergie	$J \cdot mol^{-1}$
$E(u_*)$	u_*-dependent value for fine-particle constituents	schubspannungsgeschwindigkeitsabhängiger Wert für Schwebstaubbestandteile	$m \cdot s^{-1}$
$EB_{residual}$	energy balance residual	Residuum der Energiebilanz	$W \cdot m^{-2}$
$e_{saturation\ water\ vapour\ pressure}$, e_{sat}	saturation water vapour pressure	Sättigungsdampfdruck	hPa
ET	equation of time	Zeitgleichung	h
$e_{water\ vapour\ pressure}$, e	water vapour pressure	Wasserdampfdruck	hPa
f	corrects for spectral quality of light	Lichtqualitätskorrekturfaktor	dimensionless
$f_{0,\ A}$	chemical reactivity factor of trace gas A	chemischer Reaktivitätsfaktor der Spurengasspezies A	dimensionless
f_d	fraction of diffusive radiation for cloudless skies	Anteil diffuser Sonnenstrahlung bei unbewölktem Himmel	dimensionless
f_g	construction cost	"Konstruktions"kosten	$mol \cdot mol^{-1}$
f_T	factor quantifying the limitations of soil temperature on CO_2 evolution	Faktor, der die Limitierung der Bodenatmung durch die Bodentemperatur quantifiziert	dimensionless
f_M	factor quantifying the limitations of soil moisture on CO_2 evolution	Faktor, der die Limitierung der Bodenatmung durch die Bodenfeuchte quantifiziert	dimensionless
F	turbulent vertical flux density	turbulente vertikale Flussdichte	$g \cdot m^{-2} \cdot s^{-1}$, $mol \cdot m^{-2} \cdot s^{-1}$
F_c(A)	flux density of a gaseous species including water vapour or an fine-particle constituent	Flussdichte einer Spurengasspezies einschließlich Wasserdampf oder eines Schwebstaubinhaltsstoffes	$g \cdot m^{-2} \cdot s^{-1}$, $mol \cdot m^{-2} \cdot s^{-1}$
$F_{c,\ absorbed}$	absorbed flux density	absorbierte Flussdichte	$g \cdot m^{-2} \cdot s^{-1}$, $mol \cdot m^{-2} \cdot s^{-1}$
$F_{c,\ cut}$	flux density absorbed through the cuticle	durch die Cuticula absorbierte Flussdichte	$g \cdot m^{-2} \cdot s^{-1}$, $mol \cdot m^{-2} \cdot s^{-1}$

Symbol	Description	Bezeichnung	unit/Einheit
$F_{c,\ external\ plant\ surfaces}$, $F_{c,\ ext}$	flux density on external plant surfaces	Flussdichte auf externe Pflanzenoberflächen	$g \cdot m^{-2} \cdot s^{-1}$, $mol \cdot m^{-2} \cdot s^{-1}$
$F_{c,\ non\text{-}stomatal}$	non-stomatal deposition	nicht-stomatäre Deposition	$g \cdot m^{-2} \cdot s^{-1}$, $mol \cdot m^{-2} \cdot s^{-1}$
$F_{c,\ stom\ \&\ cut}$	flux density absorbed through the stomata and the cuticle	durch Stomata und Cuticula absorbierte Flussdichte	$g \cdot m^{-2} \cdot s^{-1}$, $mol \cdot m^{-2} \cdot s^{-1}$
$F_{c,\ stomatal,\ shaded}$	stomatal uptake by the shaded leaf fraction of the canopy	stomatäre Aufnahme der Schattenblätter des Bestandes	$g \cdot m^{-2} \cdot s^{-1}$, $mol \cdot m^{-2} \cdot s^{-1}$
$F_{c,\ stomatal,\ sunlit}$	stomatal uptake by the sunlit leaf fraction of the canopy	stomatäre Aufnahme der Sonnenblätter des Bestandes	$g \cdot m^{-2} \cdot s^{-1}$, $mol \cdot m^{-2} \cdot s^{-1}$
$F_{c,\ stomatal}$, $F_{c,\ stom}$	stomatal uptake of the canopy	stomatäre Aufnahme des Bestandes	$g \cdot m^{-2} \cdot s^{-1}$, $mol \cdot m^{-2} \cdot s^{-1}$
$F_{c,\ total}$	total flux density	Gesamt-Flussdichte	$g \cdot m^{-2} \cdot s^{-1}$, $mol \cdot m^{-2} \cdot s^{-1}$
$F_{leaf,\ stom,\ sunlit}$	stomatal uptake of the sunlit leaf fraction of the canopy per unit projected leaf area	stomatäre Aufnahme der Sonnenblätter des Bestandes normiert auf eine Blattflächeneinheit	$g \cdot m^{-2} \cdot s^{-1}$, $mol \cdot m^{-2} \cdot s^{-1}$
F_{rH}	humidity factor	Luftfeuchtigkeitsfaktor	dimensionless
F_{soil}	flux density on the soil	Flussdichte auf Bodenoberflächen	$g \cdot m^{-2} \cdot s^{-1}$, $mol \cdot m^{-2} \cdot s^{-1}$
g	gravitational acceleration	Gravitationsbeschleunigung	$m \cdot s^{-2}$
G	ground heat flux density	Energie, die in Bestand und Boden gespeichert bzw. von dort abgegeben wird	$W \cdot m^{-2}$
g_A	conductance for a gaseous species A	Leitwert für Spurengasspezies A	$mol \cdot m^{-2} \cdot s^{-1}$, $m \cdot s^{-1}$
$g_{leaf,\ stom,\ sunlit,\ O3}$	stomatal conductance of sunlit leaves per unit projected leaf area	stomatärer Leitwert der Sonnenblätter des Bestandes normiert auf eine Blattflächeneinheit	$s \cdot m^{-1}$
GMT	Greenwich Mean Time	Mittlere Greenwich-Zeit	h
$G_{physical\ heat\ storage}$	physical heat storage flux density	Energie, die physikalisch in Bestand und Boden gespeichert bzw. von dort abgegeben wird	$W \cdot m^{-2}$
G_{soil}	soil heat flux density	Bodenwärmestrom	$W \cdot m^{-2}$
h	canopy height	Bestandeshöhe	m
H	turbulent flux density of sensible heat	vertikale turbulente Flussdichte fühlbarer Wärme	$W \cdot m^{-2}$
H_A*	effective Henry's law value of a trace gas A	effektiver Henry-Koeffizient der Spurengasspezies A	$M \cdot atm^{-1}$
I_2	photosynthetically active radiation absorbed by PSII of the leaves of the canopy	PAR absorbiert durch PSII derBlätter des Bestandes	$\mu mol \cdot m^{-2}\ s^{-1}$
I_b	direct beam irradiance	direkte PAR	$\mu mol \cdot m^{-2}\ s^{-1}$
$I_{c,\ shaded}$	irradiance absorbed by the shaded fraction of non-senescent leaves of the canopy	PAR absorbiert durch die nichtseneszenten Schattenblätter des Bestandes	$\mu mol \cdot m^{-2}\ s^{-1}$
$I_{c,\ sunlit}$	irradiance absorbed by the sunlit fraction of non-senescent leaves of the canopy	PAR absorbiert durch die nichtseneszenten Sonnenblätter des Bestandes	$\mu mol \cdot m^{-2}\ s^{-1}$
I_d	diffusive irradiance	diffuse PAR	$\mu mol \cdot m^{-2}\ s^{-1}$
INT	interception	Interzeption	mm
INT_{max}	interception reservoir capacity of the canopy	Bestandesinterzeptionskapazität	mm
J	electron transport rate per unit leaf area	Elektronentransportrate pro Blattflächeneinheit	$\mu mol \cdot m^{-2}\ s^{-1}$
J_{max}	light-saturated (maximum) electron transport rate per unit leaf area	maximale Elektronentransportrate pro Blattflächeneinheit	$\mu mol \cdot m^{-2}\ s^{-1}$
k_b	attenuation coefficient of the canopy beam radiation extinction coefficient of the canopy	Strahlungsextinktionskoeffizient des Pflanzenbestandes	dimensionless

Symbol	Description	Bezeichnung	unit/Einheit
k'_b	beam and scattered beam PAR extinction coefficient of the canopy	PAR-Strahlungsextinktionskoeffizient des Pflanzenbestandes	dimensionless
$k_{b,90°}$	attenuation coefficient of the canopy for solar elevation of 90°	Strahlungsextinktionskoeffizient des Pflanzenbestandes bei einer Sonnenhöhe von 90°	dimensionless
$k_{b,max}$	attenuation coefficient of the canopy at 12 h TST	Strahlungsextinktionskoeffizient des Pflanzenbestandes um 12 Uhr wahrer Ortszeit	dimensionless
$k_{b,max,\ summer\ solstice}$	attenuation coefficient of the canopy at 12 h TST on summer solstice	Strahlungsextinktionskoeffizient des Pflanzenbestandes um 12 Uhr wahrer Ortszeit am Tag der Sommersonnenwende	dimensionless
K_c	Michaelis-Menten constant of Rubisco for CO_2	Michaelis-Menten-Konstante der Rubisco für CO_2	Pa
k_d	diffuse PAR extinction coefficient	Extinktionskoeffizient für diffuse photosynthetisch-aktive Strahlung	dimensionless
k'_d	diffuse and scattered diffuse PAR extinction coefficient	Extinktionskoeffizient für diffuse und gestreute photosynthetisch-aktive Strahlung	dimensionless
k_n	coefficient of leaf-nitrogen allocation in a canopy	Blatt-N-Allokationskoeffizient im Bestand	dimensionless
K_o	Michaelis-Menten constant of Rubisco for O_2	Michaelis-Menten-Konstante der Rubisco für O_2	Pa
L	Monin-Obukhov length	Monin-Obukhov-Länge	m
LAI	one-sided leaf area index	einseitiger Blattflächenindex	$m^2 \cdot m^{-2}$
$LAI_{leaf,\ literature}$	leaf area index described in the literature	in der Literatur dokumentierter Blattflächenindex	$m^2 \cdot m^{-2}$
LAI_{max}	maximum leaf area index	maximaler Blattflächenindex	$m^2 \cdot m^{-2}$
$LAI_{non\text{-}senescent}$, LAI_{green}	one-sided leaf area index of non-senescent (green) leaves	einseitiger Blattflächenindex nichtseneszenter (grüner) Blätter	$m^2 \cdot m^{-2}$
LAI_{shaded}	one-sided leaf area index of the shaded leaf fraction of the canopy	einseitiger Blattflächenindex der Schattenblätter des Bestandes	$m^2 \cdot m^{-2}$
LAI_{sunlit}	one-sided leaf area index of the sunlit leaf fraction of the canopy	einseitiger Blattflächenindex der Sonnenblätter des Bestandes	$m^2 \cdot m^{-2}$
LAI_{total}	one-sided leaf area index of non-senescent and senescent leaves	einseitiger Blattflächenindex nichtseneszenter und seneszenter Blätter	$m^2 \cdot m^{-2}$
L_d	flux density of downward long-wave radiation of the atmosphere	Flussdichte der langwelligen Gegenstrahlung der Atmosphäre	$W \cdot m^{-2}$
$L_{neutral}$	Monin-Obukhov length under neutral atmospheric stability conditions	Monin-Obukhov-Länge bei neutral geschichteter Atmosphäre	m
L_u	flux density of upward long-wave radiation of the atmosphere	Flussdichte der langwelligen, "emittierten" Ausstrahlung der Erd- bzw. Bestandesoberfläche	$W \cdot m^{-2}$
M_A	molar mass of gaseous species A	Molekulargewicht des Spurengases A	$g \cdot mol^{-1}$
N_S	nitrogen content of the aboveground sapwood biomass	N-Gehalt des oberirdischen Saftholzes	$g \cdot m^{-2}$
O_i	intercellulat O_2 partial pressure	O_2-Partialdruck in den Interzellularen	PA
p	air pressure	Luftdruck	hPa
p_0	standard atmospheric pressure	Standardluftdruck	hPa
p_{CO2}	CO_2 partial pressure	CO_2-Partialdruck	Pa
p_i	intercellular CO_2 partial pressure	CO_2-Partialdruck in den Interzellularen	Pa
PAD(A)	pollutant absorbed dose of trace gas A	absorbierte Dosis des Spurengases A	$\mu g \cdot m^{-3}$
PAR	photosynthetically active irradiation	photosynthetisch-aktive Strahlung	$\mu mol \cdot m^{-2}\ s^{-1}$
Ph	energy exchange due to photosynthesis and respiration of the aboveground biomass	Energiefluss aufgrund von Photosynthese und Respiration der oberirdischen Bimasse	$W \cdot m^{-2}$
PLA	projected leaf area (≡ LAI)	projezierte Blattfläche(≡ LAI)	$m^2 \cdot m^{-2}$

Symbol	Description	Bezeichnung	unit/Einheit
Pr	Prandtl number	Prandtl-Zahl	dimensionless
Precip	precipitation	Niederschlag	mm
q	specific air humidity	spezifische Luftfeuchte	$g \cdot g^{-1}$
Q_{10}	relative change of a physiological process per 10 K temperature increase	relative Veränderung eines physiologischen Prozesse bei einer Temperaturerhöhung um 10 K	dimensionless
R	universal gas constant	universelle Gaskonstante	$J \cdot K^{-1}\ mol^{-1}$
$R^*_{c,\ stom,\ H2O}$	bulk stomatal resistance for water vapour for a given canopy development stage	Bulk-Stomata-Widerstand für Wasserdampf bei einem gegebenen Entwicklungszustand des Bestandes	$s \cdot m^{-1}$
$R^*_{c,\ stom,\ CO2}$	CO_2 bulk stomatal resistance for a given canopy development stage	CO_2-Bulk-Stomata-Widerstand für ein gegebenes Entwicklungszustand des Bestandes	$s \cdot m^{-1}$
$R^*_{c,\ stom,\ O3}$	O_3 bulk stomatal resistance for a given canopy development stage	O_3-Bulk-Stomata-Widerstand für ein gegebenes Entwicklungszustand des Bestandes	$s \cdot m^{-1}$
$R^*_{c,\ stom,\ shaded,\ CO2}$	CO_2 bulk stomatal resistance of the shaded leaf area fraction for a given canopy development stage	CO_2-Bulk-Stomata-Widerstand der Schattenblätter für ein gegebenes Entwicklungszustand des Bestandes	$s \cdot m^{-1}$
$R^*_{c,\ stom,\ shaded,\ O3}$	O_3 bulk stomatal resistance of the shaded leaf area fraction for a given canopy development stage	O_3-Bulk-Stomata-Widerstand der Schattenblätter für ein gegebenes Entwicklungszustand des Bestandes	$s \cdot m^{-1}$
$R^*_{c,\ stom,\ sunlit,\ CO2}$	CO_2 bulk stomatal resistance of the sunlit leaf area fraction for a given canopy development stage	CO_2-Bulk-Stomata-Widerstand der Sonnenblätter für ein gegebenes Entwicklungszustand des Bestandes	$s \cdot m^{-1}$
$R^*_{c,\ stom,\ sunlit,\ O3}$	O_3 bulk stomatal resistance of the sunlit leaf area fraction for a given canopy development stage	O_3-Bulk-Stomata-Widerstand der Sonnenblätter für ein gegebenes Entwicklungszustand des Bestandes	$s \cdot m^{-1}$
$R_{ah}(z_{ref,\ A},\ d+z_{0m})$	turbulent atmospheric resistance between the reference height $z_{ref,\ A}$ and the momentum sink height $z = d+z_{0m}$	turbulenter atmosphärischer Transportsäulenwiderstand zwischen Messhöhe $z_{ref,\ A}$ und dem Niveau der Impulssenke $z = d+z_{0m}$	$s \cdot m^{-1}$
$R_{ah,\ forest}$	turbulent atmospheric resistance above a forest	turbulenter atmosphärischer Transportsäulenwiderstand über Wald	$s \cdot m^{-1}$
$R_{atmosphere}$ R_{ah}	turbulent atmospheric resistance	turbulenter atmosphärischer Transportsäulenwiderstand	$s \cdot m^{-1}$
$R_{c,\ A}$	bulk canopy or surface resistance for water vapour or other gaseous species	Gesamtheit der Bulk-Transport- und Bulk-Reaktionswiderstände des Systems Vegetation Boden für Wasserdampf oder andere Spurengase	$s \cdot m^{-1}$
$R_{c,\ cut}$	bulk cuticle resistance	Bulk-Cuticular-Widerstand	$s \cdot m^{-1}$
$R_{c,\ cut,\ A}$	bulk cuticle resistance for water vapour or other gaseous species	Bulk-Cuticular-Widerstand für Wasserdampf oder andere Spurengase	$s \cdot m^{-1}$
$R_{c,\ ext}$	bulk external plant surface resistance	Bulk-Widerstand für die Reaktion an Pflanzenoberflächen	$s \cdot m^{-1}$
$R_{c,\ ext,\ A}$	bulk external plant surface resistance for a gaseous species A	Bulk-Widerstand für die Reaktion der Spurengasspezies A an Pflanzenoberflächen	$s \cdot m^{-1}$
$R_{c,\ ext,\ dry,\ A}$	bulk external plant surface resistance for a gaseous species A and dry external plant surfaces	Bulk-Widerstand für die Reaktion der Spurengasspezies A an trockenen Pflanzenoberflächen	$s \cdot m^{-1}$
$R_{c,\ ext,\ wet,\ A}$	bulk external plant surface resistance for a gaseous species A and wet external plant surfaces	Bulk-Widerstand für die Reaktion der Spurengasspezies A an feuchten Pflanzenoberflächen	$s \cdot m^{-1}$
$R_{c,\ mes}$	bulk mesophyll resistance	Bulk-Mesophyllwiderstand	$s \cdot m^{-1}$
$R_{c,\ mes,\ A}$	bulk mesophyll resistance for a gaseous species A	Bulk-Mesophyllwiderstand für Spurengasspezies A	$s \cdot m^{-1}$
$R_{c,\ non\text{-}stomatal,\ dry,\ O3}$	non-stomatal resistance for O_3 and dry external plant surfaces	nicht-stomatärer Widerstand für O_3 an trockenen Pflanzenoberflächen	$s \cdot m^{-1}$

Symbol	Description	Bezeichnung	unit/Einheit
$R_{c,\ stom,}$	bulk stomatal resistance	Bulk-Stomata-Widerstand	$s \cdot m^{-1}$
$R_{c,\ stom,\ A}$	bulk stomatal resistance for water vapour or other gaseous species	Bulk-Stomata-Widerstand für Wasserdampf oder andere Spurengase	$s \cdot m^{-1}$
$R_{c,\ stom,\ min,\ H2O}$	minimum value of bulk stomatal resistance for water vapour	minimaler Bulk-Stomata-Widerstand für Wasserdampf	$s \cdot m^{-1}$
$R_{c,\ stom+mes,\ O3}$	$R_{c,\ stom,\ O3} + R_{c,\ mes,\ O3}$	$R_{c,\ stom,\ O3} + R_{c,\ mes,\ O3}$	$s \cdot m^{-1}$
$R_{c,\ stomatal,\ H2O}$	bulk stomatal resistance for water vapour for a given stage of canopy development	Bulk-Stomata-Widerstand für Wasserdampf für einen bestimmten Entwicklungszustand des Bestandes	$s \cdot m^{-1}$
R_{canopy}, R_c	bulk canopy or surface resistance	Gesamtheit der Bulk-Transport- und Bulk-Reaktionswiderstände des Systems Vegetation Boden	$s \cdot m^{-1}$
$R_{dry\ air}$	gas constant for dry air	Gaskonstante für trockene Luft	$J \cdot kg^{-1}\ K^{-1}$
rH	relative humidity	relative Luftfeuchte	%
R_{leaf}	leaf resistance	Blattwiderstand	$s \cdot m^{-1}$
$R_{leaf,\ cut,\ A}$	leaf cuticle resistance for water vapour or other gaseous species	Blatt-Cuticular-Widerstand für Wasserdampf oder andere Spurengase	$s \cdot m^{-1}$
$R_{leaf,\ ext,\ dry,\ A}$	leaf external plant surface resistance for a gaseous species A and dry external plant surfaces	Blatt-Widerstand für die Reaktion der Spurengasspezies A an trockenen Pflanzenoberflächen	$s \cdot m^{-1}$
$R_{leaf,\ literature}$	resistance derived on leaf basis described in the literatre	in der Literatur dokumentierter Blatt-Widerstand	$s \cdot m^{-1}$
R_{low}	low temperature resistance	Widerstand bei niedriger Temperatur	$s \cdot m^{-1}$
$R_{molecular}$	molecular atmospheric resistance	molekularer atmosphärischer Widerstand	$s \cdot m^{-1}$
R_{net}	net radiation balance	Flussdichte der Gesamtstrahlungsbilanz	$W \cdot m^{-2}$
$R_{quasi\text{-}laminar\ layer,\ A}$ $R_{b,\ A}$	quasi-laminar layer resistance for sensible heat, water vapour or other gaseous species	Transportsäulenwiderstand der quasi-laminaren Schicht für fühlbare Wärme, Wasserdampf oder andere Spurengase	$s \cdot m^{-1}$
R_{soil}	soil resistance	Widerstand der Bodenoberfläche	$s \cdot m^{-1}$
$R_{soil,\ A}$	soil resistance for water vapour or other gaseous species	Widerstand der Bodenoberfläche für Wasserdampf oder andere Spurengase	$s \cdot m^{-1}$
$R_{soil,\ dry,\ A}$	soil resistance for gaseous species A under "dry conditions"	Widerstand der Bodenoberfläche für ein Spurengas A unter "trockenen Bedingungen"	$s \cdot m^{-1}$
$R_{soil,\ H2O,\ min}$	minimum value of soil resistance for water vapour	minimaler Widerstand der Bodenoberfläche für Wasserdampf	$s \cdot m^{-1}$
$R_{soil,\ min}$	minimum value of soil resistance	minimaler Widerstand der Bodenoberfläche	$s \cdot m^{-1}$
$R_{turbulent}$	turbulent atmospheric resistance	turbulenter atmosphärischer Widerstand	$s \cdot m^{-1}$
RX	fraction of $R_{soil,\ H2O,\ min}$	Bruchteil von $R_{soil,\ H2O,\ min}$	dimensionless
$R_{x,\ cut}$	bulk or leaf cuticle resistance	Bulk- oder Blatt-Cuticulawiderstand	$s \cdot m^{-1}$
$R_{x,\ non\text{-}stomatal}$	bulk or leaf non-stomatal resistance	nicht-stomatärer Bulk- oder Blatt-Widerstand	$s \cdot m^{-1}$
$R_{x,\ stom\ \&\ cut}$	combined bulk or leaf stomatal and cuticle resistance	kombinierter Bulk- oder Blatt-Stomata- und Cuticulawiderstand	$s \cdot m^{-1}$
$R_{x,\ stom}$, $R_{x,\ stomatal}$	bulk stomatal resistance	Bulk- oder Blatt-Stomatawiderstand	$s \cdot m^{-1}$
$R_{x,\ y,\ dry}$	resistance of a dry surface	Widerstand trockener Oberflächen	$s \cdot m^{-1}$
$R_{x,\ y,\ wet}$	resistance of a wet surface	Widerstand feuchter Oberflächen	$s \cdot m^{-1}$
*Resp**	sum of belowground respiration and the respiration rate of the aboveground woody plant parts	Summe der Bodenatmung und Atmung der der verholzten oberirdischen Pflanzenteile	$\mu mol \cdot m^{-2} \cdot s^{-1}$
$Resp_{belowground}$	belowground respiration	Bodenatmung	$\mu mol \cdot m^{-2} \cdot s^{-1}$
$Resp_d$	daytime mitochondrial respiration rate of the canopy	mitochondriale Bestandesatmung bei Tage	$\mu mol \cdot m^{-2} \cdot s^{-1}$
$Resp_{c,\ nighttime}$	nightime ecosystem respiration rate	nächtliche ökosystemare Atmung	$\mu mol \cdot m^{-2} \cdot s^{-1}$

Symbol	Description	Bezeichnung	unit/Einheit
$Resp'_{r,m}$	cumulative daily maintance respiratory flux from roots	kumulierte tägliche Erhaltungsatmung der Wurzeln	$\mu mol \cdot m^{-2} \cdot s^{-1}$
$Resp_w$	respiration rate of the aboveground woody plant parts	Atmung der verholzten oberirdischen Pflanzenteile	$\mu mol \cdot m^{-2} \cdot s^{-1}$
$Resp_{w,g}$	aboveground woody maintance respiration due to construction of new tissue	Erhaltungsatmung der verholzten oberirdischen Pflanzenteile aufgrund der Bildung von neuem Gewebe	$\mu mol \cdot m^{-2} \cdot s^{-1}$
$Resp_{w,m}$	aboveground woody maintance respiration	Erhaltungsatmung der verholzten oberirdischen Pflanzenteile	$\mu mol \cdot m^{-2} \cdot s^{-1}$
$Resp'_{w,m}$	cumulative daily maintance respiratory flux from aboveground woody biomass	kumulierte tägliche Erhaltungsatmung der verholzten oberirdischen Pflanzenteile	$\mu mol \cdot m^{-2} \cdot s^{-1}$
RLD_{90}	depth of the soil layer containing 90 % of total root mass	Mächtigkeit der Bodenschicht, die 90 % der Wurzelbiomasse enthält	m
RY	fraction of $R_{soil,\ H2O,\ min}$	Bruchteil von $R_{soil,\ H2O,\ min}$	dimensionless
SAI	total surface area index of the vegetation	Oberflächenindex der Vegetation	$m^2 \cdot m^{-2}$
s_c	difference quotient $\Delta e_{sat}/\Delta T$	Differenzenquotient $\Delta e_{sat}/\Delta T$	$hPa \cdot K^{-1}$
Sc_A	Schmidt number of a trace gas A	Schmidt-Zahl der Spurengasspezies A	dimensionless
$S_{in\text{-}canopy\ air}$	flux of energy due to changes in temperature and humidity of the air in the canopy	fühlbarer Wärmestrom im Bestandesraum	$W \cdot m^{-2}$
SM	soil moisture	volumetrischer Bodenwassergehalt	$m^3 \cdot m^{-3}$
SM_c	field capacity	Feldkapazität	$m^3 \cdot m^{-3}$
SM_{res}	residual (irreducible) soil moisture	absolutes Minimum des Bodenwassergehaltes	$m^3 \cdot m^{-3}$
SM_{sat}	soil moisture at saturation	Bodenwassergehalt bei Sättigung	$m^3 \cdot m^{-3}$
SM_w	wilting point	permanenter Welkepunkt	$m^3 \cdot m^{-3}$
S_t	global radiation	Globalstrahlung	$W \cdot m^{-2}$
$S_{t,ref}$ $S_{t,\ cloudless\ sky}$	astronomical maximum possible global radiation at cloudless sky	astronomisch maximal mögliche Globalstrahlung bei wolkenlosem Himmel	$W \cdot m^{-2}$
S_1	maximum global radiation for the Jarvis radiation function	maximal mögliche Globalstrahlung in der Jarvis-Funktion für Strahlung	$W \cdot m^{-2}$
S_2	empirical coefficient governing the shape of the Jarvis radiation function	Koeffizient, der die Kurvenform der Jarvis-Funktion für Strahlung bestimmt	$W \cdot m^{-2}$
subscript c	canopy	Bestand	---
subscript shaded	shaded leaf fraction of the canopy	Fraktion der Schattenblätter eines Bestandes	---
subscript sunlit	sunlit leaf fraction of the canopy	Fraktion der Sonnenblätter eines Bestandes	---
$S_{vegetation}$	flux of energy due to changes in temperature of the aboveground biomass	Wärmespeicherung in der Biomasse	$W \cdot m^{-2}$
SLD	depth of soil layer	Mächtigkeit der Bodenschicht	m
t	time	Zeit	s, min, h, d, a
T	absolute air temperature	absolute Lufttemperatur	K
T_0	standard temperature	Standardtemperatur	K
t_a	actual air temperature	aktuelle Lufttemperatur	°C
t_1	vegetation-type dependent minimum temperature of the Jarvis temperature function	vegetationsspezifische Minimumtemperatur in der Jarvis-Funktion für Temperatur	°C
t_2	vegetation-type dependent optimum temperature of the Jarvis temperature function	vegetationsspezifische Optimumtemperatur in der Jarvis-Funktion für Temperatur	°C

Symbol	Description	Bezeichnung	unit/Einheit
t_3	vegetation-type dependent maximum temperature of the Jarvis temperature function at which stomata no longer remain open	vegetationsspezifische Maximumtemperatur in der Jarvis-Funktion für Temperatur, bei der die Stomata nicht länger geöffnet sind	°C
t_{7days}	mean daily air temperature of the past 7 days	mittlere Lufttemperatur der letzten 7 Tage	°C
t_{lag3h}	ambient air temperature lagged by three hours	aktuelle Lufttemperatur vor drei Stunden	°C
t_{opt}	optimum soil temperature for CO_2 evolution	optimale Bodentemperatur für die Bodenatmung	°C
T_p	rate of triose phosphate export from the chloroplast	Rate des Triosephosphatexports aus den Chloroplasten	$\mu mol \cdot m^{-2} \cdot s^{-1}$
T_s	absolute canopy surface temperature	absolute Bestandesoberflächentemperatur	K
t_s	surface temperature	aktuelle Oberflächentemperatur	°C
t_{soil}	soil temperature	Bodentemperatur	°C
TST	True Solar time	wahre Sonnenzeit	h
u	horizontal wind velocity	horizontale Windgeschwindigkeit	$m \cdot s^{-1}$
u_h	horizontal wind velocity at canopy height	horizontale Windgeschwindigkeit an der Bestandesoberfläche	$m \cdot s^{-1}$
u_*	friction velocity	Schubspannungsgeschwindigkeit	$m \cdot s^{-1}$
V_c	photosynthetic Rubisco capacity of the canopy	Rubisco-Kapazität des Bestandes	$\mu mol \cdot m^{-2} \cdot s^{-1}$
v_D	dry deposition velocity	Depositionsgeschwindigkeit	$m \cdot s^{-1}$
$V_{leaf\ at\ top\ of\ canopy}$	photosynthetic Rubisco capacity per unit leaf area at top of canopy	Rubisco-Kapazität pro Blattflächeneinheit an der Bestandesoberfläche	$\mu mol \cdot m^{-2} \cdot s^{-1}$
V_m	molar volume	Molvolumen	$l \cdot mol^{-1}$
VPD	water vapour pressure deficit of the atmosphere	Wasserdampfsättigungsdefizit der Atmosphäre	hPa
V_1	maximum value of *VPD* Jarvis function	maximaler Wert für die *VPD*-Jarvis-Funktion	hPa
V_2	threshold value of *VPD* Jarvis function	Schwellenwert für die *VPD*-Jarvis-Funktion	hPa
V_3	minimum threshold of *VPD* Jarvis function	minimaler Schwellenwert für die *VPD*-Jarvis-Funktion	dimensionless
V_4	empirical weighting coefficient of *VPD* Jarvis function	Wichtungsfaktor für die *VPD*-Bodenfeuchte-Jarvis-Funktion	dimensionless
W_1	site-specific threshold level of the Jarvis soil moisture function	standortspezifischer Schwellenwert in der Jarvis-Funktion für Bodenfeuchte	$m^{-3} \cdot m^{-3}$
W_2	minimum threshold of the Jarvis soil moisture function	minimaler Schwellenwert in der Jarvis-Funktion für Bodenfeuchte	dimensionless
W_{in}	precipitation and/or dew reaching the ground	Niederschlag und Tau, der den Boden erreicht	mm
z	height above ground	Höhe über Grund	m
$z_{0,scalar}$	roughness length for a scalar (sensible heat, gases)	Rauhigkeitslänge für Skalar (fühlbare Wärme, Gase)	m
z_{0c}	roughness length for water vapour or other gaseous species	Rauhigkeitslänge für Wasserdampf oder andere Spurengase	m
z_{0h}	roughness length for sensible heat	Rauhigkeitslänge für fühlbare Wärme	m
z_{0m}	roughness length for momentum	Rauhigkeitslänge für Impuls	m
z_{ref}	reference height above the ground	Messhöhe über Grund	m
$z_{ref,\ A}$	reference height for a trace gas A	Messhöhe der Konzentration der Spurengasspezies A	m
$z_{ref,\ p}$	reference height for air pressure	Messhöhe des Luftdrucks	m
$z_{ref,\ rH}$	reference height for relative humidity	Messhöhe der relativen Luftfeuchte	m

Symbol	Description	Bezeichnung	unit/Einheit
$z_{ref,\,T}$	reference height for actual air temperature	Messhöhe der aktuellen Lufttemperatur	m
$z_{ref,\,u}$	reference height for horizontal wind velocity	Messhöhe der horizontalen Windgeschwindigkeit	m

Landbauforschung
vTI Agriculture and Forestry Research

Lieferbare Sonderhefte / Special issues available

287	Maria del Carmen Rivas *(2005)* **Interactions between soil uranium contamination and fertilazation with N, P and S on the uranium content and uptake of corn, sunflower and beans, and soil microbiological parameters**	8,00 €
288	Alexandra Izosimova *(2005)* **Modelling the interaction between Calcium and Nickel in the soil-plant system**	8,00 €
290	Gerold Rahmann (Hrsg.) *(2005)* **Ressortforschung für den Ökologischen Landbau 2005**	9,00 €
292	Franz-Josef Bockisch und Elisabeth Leicht-Eckardt (Hrsg.) *(2006)* **Nachhaltige Herstellung und Vermarktung landwirtschaftlicher Erzeugnisse**	15,00 €
293	Judith Zucker *(2006)* **Analyse der Leistungsfähigkeit und des Nutzens von Evaluationen der Politik zur Entwicklung ländlicher Räume in Deutschland und Großbritannien am Beispiel der einzelbetrieblichen Investitionsförderung**	12,00 €
294	Gerhard Flachowsky (Hrsg.) *(2006)* **Möglichkeiten der Dekontamination von "Unerwünschten Stoffen nach Anlage 5 der Futtermittel-verordnung (2006)"**	15,00 €
295	Hiltrud Nieberg und Heike Kuhnert *(2006)* **Förderung des ökologischen Landbaus in Deutschland – Stand, Entwicklung und internationale Perspektive**	14,00 €
296	Wilfried Brade und Gerhard Flachowsky (Hrsg.) *(2006)* **Schweinezucht und Schweinefleischerzeugung – Empfehlungen für die Praxis**	12,00 €
297	Hazem Abdelnabby *(2006)* **Investigations on possibilities to improve the antiphytopathogenic potential of soils against the cyst nematode Heterodera schachtii and the citrus nematode Tylenchulus semipenetrans**	8,00 €
298	Gerold Rahmann (Hrsg.) *(2006)* **Ressortforschung für den Ökologischen Landbau 2006**	9,00 €
299	Franz-Josef Bockisch und Klaus-Dieter Vorlop (Hrsg.) *(2006)* **Aktuelles zur Milcherzeugung**	8,00 €
300	**Analyse politischer Handlungsoptionen für den Milchmarkt** *(2006)*	12,00 €
301	Hartmut Ramm *(2006)* **Einfluß bodenchemischer Standortfaktoren auf Wachstum und pharmazeutische Qualität von Eichenmisteln (*Viscum album* auf *Quercus robur* und *petraea*)**	11,00 €
302	Ute Knierim, Lars Schrader und Andreas Steiger (Hrsg.) *(2006)* **Alternative Legehennenhaltung in der Praxis: Erfahrungen, Probleme, Lösungsansätze**	12,00 €
303	Claus Mayer, Tanja Thio, Heike Schulze Westerath, Pete Ossent, Lorenz Gygax, Beat Wechsler und Katharina Friedli *(2007)* **Vergleich von Betonspaltenböden, gummimodifizierten Spaltenböden und Buchten mit Einstreu in der Bullenmast unter dem Gesichtspunkt der Tiergerechtheit**	8,00 €
304	Ulrich Dämmgen (Hrsg.) *(2007)* **Calculations of Emissions from German Agriculture – National Emission Inventory Report (NIR) 2007 for 2005** [304] **Introduction, Methods and Data (GAS-EM)** [304A] **Tables** **Berechnungen der Emissionen aus der deutschen Landwirtschaft – Nationaler Emissionsbericht (NIR) 2007 für 2005** [304] **Einführung, Methoden und Daten (GAS-EM)** [304A] **Tabellen**	16,00 €

305	Joachim Brunotte *(2007)* **Konservierende Bedenbearbeitung als Beitrag zur Minderung von Bodenschadverdichtungen, Bodenerosion, Run off und Mykotoxinbildung im Getreide**	14,00 €
306	Uwe Petersen, Sabine Kruse, Sven Dänicke und Gerhard Flachowsky (Hrsg.) *(2007)* **Meilensteine für die Futtermittelsicherheit**	10,00 €
307	Bernhard Osterburg und Tania Runge (Hrsg.) *(2007)* **Maßnahmen zur Reduzierung von Stickstoffeinträgen in Gewässer – eine wasserschutzorientierte Landwirtschaft zur Umsetzung der Wasserrahmenrichtlinie**	15,00 €
308	Torsten Hinz and Karin Tamoschat-Depolt (eds.) *(2007)* **Particulate Matter in and from Agriculture**	12,00 €
309	Hans Marten Paulsen und Martin Schochow (Hrsg.) *(2007)* **Anbau von Mischkulturen mit Ölpflanzen zur Verbesserung der Flächenproduktivität im ökologischen Landbau – Nährstoffaufnahme, Unkrautunterdrückung, Schaderregerbefall und Produktqualitäten**	9,00 €
310	Hans-Joachim Weigel und Stefan Schrader (Hrsg.) *(2007)* **Forschungsarbeiten zum Thema Biodiversität aus den Forschungseinrichtungen des BMELV**	13,00 €
311	Mamdoh Sattouf *(2007)* **Identifying the Origin of Rock Phosphates and Phosphorus Fertilisers Using Isotope Ratio Techniques and Heavy Metal Patterns**	12,00 €
312	Fahmia Aljmli *(2007)* **Classification of oilseed rape visiting insects in relation to the sulphur supply**	15,00 €
313	Wilfried Brade und Gerhard Flachowsky (Hrsg.) *(2007)* **Rinderzucht und Rindfleischerzeugung – Empfehlungen für die Praxis**	10,00 €
314	Gerold Rahmann (Hrsg.) *(2007)* **Ressortforschung für den Ökologischen Landbau, Schwerpunkt: Pflanze**	12,00 €
315	Andreas Tietz (Hrsg.) *(2007)* **Ländliche Entwicklungsprogramme 2007 bis 2013 in Deutschland im Vergleich – Finanzen, Schwerpunkte, Maßnahmen**	12,00 €
316	Michaela Schaller und Hans-Joachim Weigel *(2007)* **Analyse des Sachstands zu Auswirkungen von Klimaveränderungen auf die deutsche Landwirtschaft und Maßnahmen zur Anpassung**	16,00 €
317	Jan-Gerd Krentler *(2008)* **Vermeidung von Boden- und Grundwasserbelastungen beim Bau von Güllelagern Prevention of soil and groundwater contamination from animal waste storage facilities**	12,00 €
318	Yelto Zimmer, Stefan Berenz, Helmut Döhler, Folkhard Isermeyer, Ludwig Leible, Norbert Schmitz, Jörg Schweinle, Thore Toews, Ulrich Tuch, Armin Vetter, Thomas de Witte *(2008)* **Klima- und energiepolitische Analyse ausgewählter Bioenergie-Linien**	14,00 €
319	Ludger Grünhage and Hans-Dieter Haenel *(2008)* **Detailed documentation of the PLATIN (PLant-ATmosphere Interaction) model**	10,00 €

Johann Heinrich
von Thünen-Institut

Landbauforschung
vTI Agriculture and Forestry Research

Sonderheft 319
Special Issue

Preis / Price 10 €

ISBN 978-3-86576-044-9